UNIVERSITY OF AGDER

Development of simulation model for virtual testing and design of a riser tensioner system

By
Servet Haziri
Øystein Dyngvold

Supervisor
Professor Michael Rygaard Hansen

This Master's Thesis is carried out as a part of the education at the University of Agder and is therefore approved as a part of this education. However, this does not imply that the University answers for the methods that are used or the conclusions that are drawn.

University of Agder, 2011

Faculty of technology

Department of engineering

ABSTRACT

This project contains a study of a wireline riser tensioner system provided by TTS Energy. A mathematical model is derived for both the pneumatic-, hydraulic and the mechanical system. The main motivation for this work is the development of a multibody mechanics model in simulationX, together with 1D mechanics and fluid power systems in the shape of both hydraulics and pneumatics.

After the models are verified as sound, several simulations are ran and a number of parameters are varied in order to investigate the response of the system under different load-cases.

The investigation of the system is done for several operation modes. In all of them a vertical total load from the marine riser string together with a constant horizontal load are acting on the tensioner units, while the rig is following a sinus motion with amplitude of 4,8 meter and time of period 18 seconds.

The first scenario is normal operation. The second one is when one or two wires in diametrally opposite positioned cylinders rupture at the same time. The third one is system performance if the marine riser must be decoupled from the BOP, and the anti recoil system have to ensure that the cylinder positions are moved in a controlled way to maximum stroke.

Different values for key parameters of the system will be investigated and the results are summarized on the last pages of these thesis.

ACKNOWLEDGEMENTS

Our sincere gratitude goes to our supervisor at the university, Professor Michael Rygaard Hansen, for his attention, patience and guidance while working on this thesis; it would have been impossible to deliver this work without him. His expertise on modeling and understanding of the physical system has been of invaluable help and inspiration. We would like to thank him for always having his door open for discussions throughout this project.

We also want to thank TTS Energy, especially Mr. Alv Repstad, for his support and guidance throughout this project. In several meetings at TTS Energy in Kristiansand he has been very helpful, and made us understand the system behavior. His expertise in engineering has been a vital asset for us.

Finally, many thanks to the Department of Engineering at the University of Agder for all the help rendered to ensure the success of this thesis.

Table of content

1. INTRODUCTION

Deepwater activities have increased in recent years as the world oil reserves are being depleted. The conventionally moored drilling vessels used in shallow water are being replaced by dynamically positioned rigs at water depths typically greater than 300 m. While the dynamic positioning systems (dp) automatically maintain the position of the vessel or rig, the construction is still submitted to heave motion induced by the waves.

An important component of an off-shore drilling installation is the marine riser tensioner system. The purpose of the riser tensioner system is to hold the marine riser that isolates the drill string and the mudflow from the seawater. It is connected to the wellhead on the sea bed and therefore the tensioner must manage the differential movements between the riser and the rig. If there were no tensioner and the rig moves downward, the riser would buckle; if the rig rises then high forces would be transmitted to the riser and it would stretch and be damaged.

The riser tensioner system must ensure that a certain tension is maintained in the marine riser. Hence, the main performance parameter is the variation in the tension force supplied by the wires/cylinders to the tensioner ring that is connected to the top of the marine riser.

Tensioners have historically been composed of hydraulic actuated cylinders with wire sheaves, but more recently, active electrical motors have been used for compensation purposes [1].

There are two different types of riser tensioner system:

- The wireline riser tensioner system (WRT).

Consists of a hydraulic cylinder with sheaves at both sides. The cylinder is connected to a number of high-pressure gas bottles via a medium separator. A wire rope is rigged in the cylinder; one end is connected to the fixed part of the tensioner, the other end is connected to the riser tensioner ring.

- The direct acting riser tensioner system (DAT).

Compared to the previous system it has a very similar structure. The main different is its direct connection of the cylinders pistons to the tensioner ring. This obvious indicates a less complex construction. The disadvantage is the exposure of seawater on the cylinders since they are located near the sea surface. This means a shorter life expectancy and a higher maintenance interval.

The system of most interest is therefore the WRT, and the analysis done in this project will be on this system.

1.1 HISTORY

Offshore platform concepts are usually classified into two major categories; fixed and compliant. Fixed platforms stand at the seabed and remain in place by a combination of their weight and/or piles driven into the soil. Little or no motions are observed for such structures. The fixed platforms resist the environmental forces like wind, wave and current by generating large internal reaction forces.

The first offshore oil and gas fields were found in shallow waters, and mainly fixed structures were build in the first decades of offshore oil production.

As offshore development moved towards deeper waters, the application of conventional fixed jackets approached its limits principally imposed by the dynamic behavior of the structures. With increasing water depths, fixed platforms become more flexible, and their natural periods started to enter the high energy levels of the ocean waves. To keep the eigenperiods away from this damaging range, fixed structures had to be designed to be stiffer, requiring more steel and exponentially increasing costs.

The obvious alternative to fixed platforms in deep water is to use compliant platforms. The basic idea is to allow for rigid body motions with eigenperiods longer than wave periods. Compliant platforms may be divided into three types; floaters, towers and TLPs.

Each of these structures will experience a heave motion relative to the seabed due to waves, wind and currents.

In order to ensure that the relative distance between the blow out preventer (BOP) and the marine riser tensioner ring remains as constant as possible, the marine riser tensioner system is implemented.

1.2 PROBLEM SPECIFICATION

According to the problem statement outlined in the project content, it is required to analyze the system behavior provided the following scenarios prevail:

Scenario 1: Normal loading conditions.

Marine riser string exerts a high vertical force onto a riser tensioner. In addition, a small constant horizontal load and rig heave motion add up an additional loading on the system.

System component failures:

The failure mode for a WRT system is an unexpected break of one of the wires.

Analysis to be performed:

It is required to study the behavior of the system in response to the assumed system disturbances. The study should reflect the subsequent variations in pressure, volume flow, and mechanical motion in the system components.

Data available:

- Heave sinusoidal motion with amplitude A=4.8 meter and time of period t=18 seconds. Thus, the maximum velocity of the vessel due to heave motion is 1.68 m/s.
- Marine riser string exerts a high vertical force onto the riser tensioner system.
- Horizontal force acting on the marine riser is 350 kN.

Scenario 2: Normal loading condition.

Marine riser string exerts a medium vertical force onto a riser tensioner. At the same time a 350 kN horizontal force is acting on the marine riser.

System component failures:

The same as described under scenario one.

Analysis to be performed:

The same as described under scenario one.

Data available:

- The same data as described under scenario one.

Scenario 3: The same loading conditions as described under scenario one.

System component failures:

It is assumed that respectively one wire, and then two wires, unexpectedly breaks on diametrically opposite positioned cylinders of the WRT system.

Analysis to be performed:

The same as described under scenario one and two.

Data available:

- The same data as described under scenario one and two.

Scenario 4: Riser disconnection from BOP.

When the weather is expected to be going so worse that the wave height might become higher than the ability of heave compensator system to compensate the motion, the riser string is disconnected at its bottom end with LMRP (Lower Marine Riser Package) which is the kind of BOP. In addition, there could be an unexpected storm attack, which could not allow enough time for the vessel to recover the riser string on board. Because of these two unfavorable events, the rig cannot maintain its DP (dynamic positioning) position.

When the marine riser is decoupled, a large amount of energy stored in the gas banks of the tensioner system is released, which will accelerate the cylinder pistons upwards. If this motion is not controlled, the cylinders and the marine riser may be damaged as the cylinders reach their end stop.

In order to ensure that the cylinders move in a controlled manner, and hence prevent the damages, a so-called "anti recoil" system is actuated.

The loading exerted on the system is the same as given under scenario one.

System component failures:

Marine riser string disconnected and hence the drilling operations are halted.

Analysis to be performed:

The same as described under scenario one and two.

Data available:

- The same data as described under scenario one and two.

Sensitivity analysis

Determine the variation in the tensioner force as an output variable by varying of the following model parameters:

- Gas bank volume and pressure
- Friction in the sheaves
- Dynamic parameters of a flow-shut off valve
- System response without a horizontal force

2. LITERATURE REVIEW

The manufacturing of drilling related equipment has for decades been a growing industry, and the demand for knowledge of system behavior has been increasing. As a result of this several articles and books describing the riser tensioner system have been published. In addition there are also master thesis and ph.d thesis which brings up challenges regarding deep water sea drilling.

- Charles Sparks
  Fundamentals of Marine Riser Mechanics
  PennWell Books (2007)

Charles Sparks has written this definitive work on the fundamentals of riser mechanics, with the aim of increasing understanding of many aspects of riser static and dynamic behavior. The primary parameters that influence riser behavior are identified, and their influence is illustrated in a very illustrative way. It gives a very good understanding of the riser behavior.

- Olawale Kolade
  Deepwater drilling problemes.
  University of Stavanger (2009)

In his master thesis he is discussing the effect on the marine riser upon disconnect from the BOP. He is focusing on the axial oscillation of the risers. This can be useful information when modeling the forces. He is also modeling the riser as a spring, finding the eigenfrequency, but ignoring the dampening effect of the surrounding water.

- When_Yen Tein
  Approximate harmonic analysis of marine risers.
  Rice university (1987)

In this master thesis the analyzing of the nonlinearity of the riser through finite element methods is done. He has come up with a simplified model that requires only 1/10 of the computation time of the numerical integration procedure. He is doing a thorough analysis of the riser spring and dampening characteristics.

- Anne Marthine Rustad
  Modeling and Control of Top Tensioned Risers.
  NTNU (2007)

In her ph.d thesis she is discussing modeling and control of top tensioned risers. She is especially focusing on the control system, and the optimization of the riser's top angle. She claims that both riser tensioner systems (WRT and DAT), give a nearly constant tension to the marine risers and compensate for rig motions. She also brings up the fact that if one cylinder fails, both systems are symmetrical, so, the opposite cylinder is set free, and the remaining four will keep on working. She is also emphasizing the importance of having an accurate controller for the heave motion.

- Suzuki H and Tanaka S
  Basic research on an anti-recoil system of a deepsea riser.
  Journal of the Society of Naval Architects of Japan Y. 1999, vol. 186, pages 393-400. (1999)

In their article they are doing a basic research on an anti-recoil system. When disconnected, the riser starts to lift and recoil, and if the tension is not properly reduced the riser hits the floater and destroy both the floater and riser. If the tension is reduced too fast, riser cannot reach the vessel and riser drops on to the sea floor and destroyed. The anti-recoil system is necessary to protect the riser and vessel from destruction and make the catching successful. In their research response prediction system of disconnected riser is developed considering coupled response of riser and dynamic response of internal and external fluid.

Vessel heave motion prediction system is also developed. An algorithm is developed to search catching timing from the both predictions of riser motion and vessel heave motion. To achieve successful catching, the catching timing must satisfy catching condition of no relative displacement, velocity and acceleration.

Once the catching timing is found, riser disconnection timing is determined from the predicted riser motion. Feedback control is employed at the final stage of catching to adjust and absorb modeling errors and prediction errors and secure successful catching. Effectiveness of the developed algorithm is verified by simulation calculation.

- RD. Young, Stress Engineering Services Inc.; C.J. Hock, Sonat Offshore Drilling; Geir Karlsen, BP Exploration; and J.W. Albert, Stress Engineering Services Inc.
  Comparison of Analysis and Full-Scale Testing of Anti-Recoil System for Emergency Disconnect of Deepwater Riser.
  Offshore Technology Conference, 4 May-7 May 1992, Houston, Texas.

This is an 18 years old paper, but its content is still valid. It describes the verification of a procedure for analyzing the emergency disconnect of deepwater drilling risers. The procedure was used to design an anti-recoil system for Sonat's Discoverer 534 drillship. The purpose of this system is to provide control of the riser's ascent velocity and hence to limit its impact with the diverter housing. The system was tested during an actual disconnect in 3700 feet of water. This test was full scale and instrumented to provide riser displacement and pressure drop across the anti-recoil valves in some of the tensioners. The data was used to verify the analysis and design procedure. This procedure is briefly discussed herein.

- American Steel and Wire Company.
  American tiger brand wire rope engineering handbook.
  Revision (2008)

This book has useful information about the behavior of wires in a mechanical system consisting of drums and sheaves. It contains a lot of formulas useful to us when analyzing the forces in the different wire sections. This book was originally written as early as 1946, but has been revised 2 times since then.

- T. J. Kozik, Texas A&M U.; J. Noerager, Exxon Production Research Co.
  Riser Tensioner Force Variations.
  Offshore Technology Conference, Houston, Texas (1976).

Excessive riser force variation on the upper joint in a riser string can lead to buckling and excessive fatigue. This variation is due to two components of the riser support system. These are the riser tensioning system and the telescopic, or slip, joint.

By means of specific examples, the paper reaches two conclusions. The first is that the force variation at the top of the riser string may be much greater than that indicated by monitoring the tensioner system's air tank pressure. The second conclusion is that a major contribution to this variation can be the pressure drop in the air valves.

The paper consists of two main topics. One is emphasizing by numerical examples the strong dependence of the riser tensioner force variations on the character of the assumed losses (pressure drop) in the tensioner system air

valves. The other is the presentation of an analytical expression and numerical results for the tensioner system force variations at the upper ball joint, thereby emphasizing the strong effects of vessel motion on the riser string force.

After doing a literature search we came to the conclusion that the marine riser have been modeled and thoroughly investigated in numerous literatures. Also the anti recoil valve has several articles describing its behavior during a decoupling of the marine riser from the BOP.

Literature about the inner dynamics of the hydraulic and pneumatic systems during the earlier mentioned scenario is not much discussed. It may be because information describing the dynamics in detail often is considered as confidential information and therefore not released for public investigation.

Another reason might well be that there are a lack of information about these phenomena. There have been done mathematical approaches in describing the different elements of the system, but it seems to be a lack of simulation data to get the overall view. This probably is because it is a time consuming task, and companies up to now have been reluctant initiating such an initiative.

3 SYSTEM DESCRIPTION

In figure 1 and figure 2, both spatial and a block diagram of the system interrelationship of the wireline riser tensioner system is shown. Its main function is to ensure a certain tension is maintained in the marine riser and at the same time avoid that the riser is displaced outside the boundaries of the tensioner system.

The system comprises drilling control room, control system, power distribution board, high-pressure air compression unit, working air pressure vessel unit, standby air pressure vessels unit, air control valve unit(2), hydraulic unit(8) and tensioner unit(8).

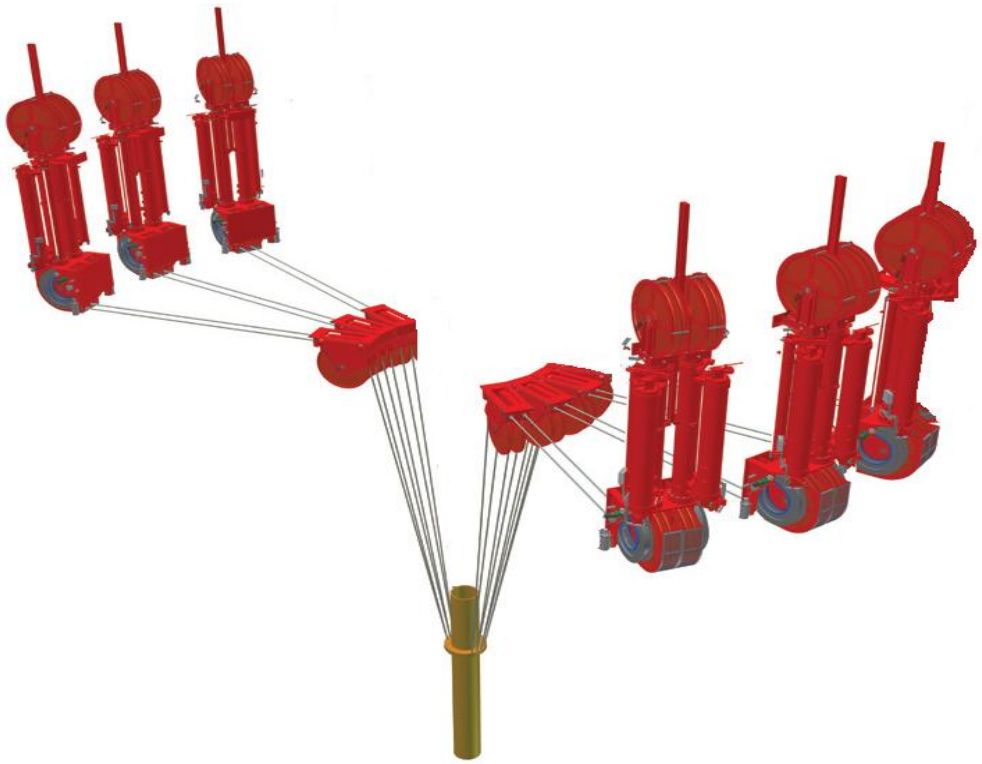

Figure 1: -An illustration of a riser tensioner system with six dual units.

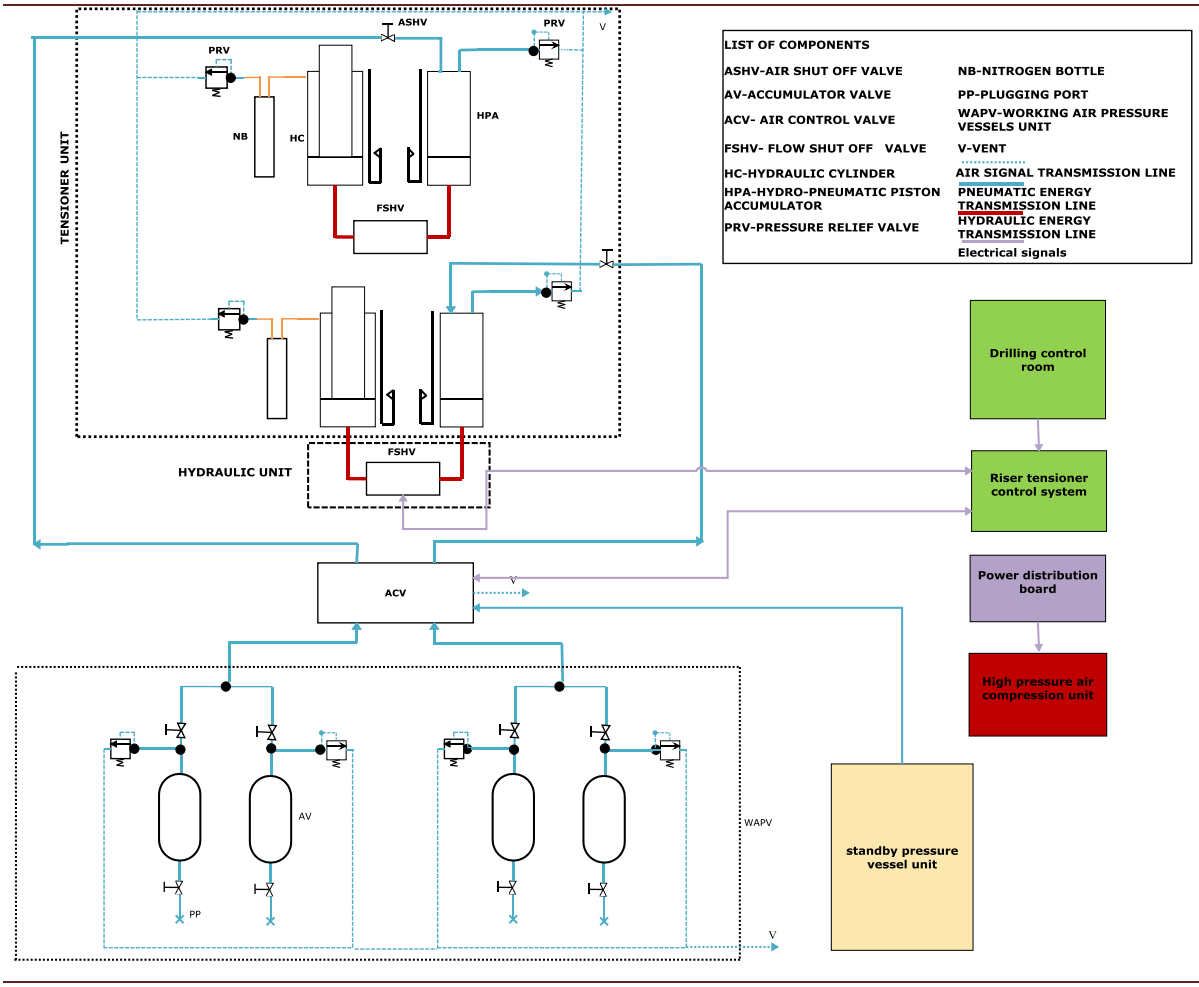

Figure 2: - 2-d diagramming of the system.

Wireline Riser Tensioner (WRT) serves the same function which is to maintain the riser tension approximately constant. This is a passive system that utilizes the potential energy stored in a pre-compressed gas bank transmitted to hydraulic cylinders, however, they utilize different mechanical transformations. The WRT system generates the tension force by transformation via a system of hydraulic cylinders and a plurality of sheaves. The system protection is implemented by incorporating a number of air control valves, air shut off valves and flow shut off valves into a system.

The system is controlled by an operator panel located in the drilling control room. The control system controls several PLCs and serves two purposes; to ensure the system runs within the specified working performances and safety guidelines, and to monitor literally all operations within the system including mud logging system, measurement while drilling, logging while drilling etc.

The pneumatic energy is generated via a high-pressure compression unit, which is supplied through the power distribution system. The accumulated energy is stored through a bank of accumulators. In addition, accumulators are used to serve a variety of system functions such as to maintain the system pressure,

absorb the hydraulic shocks and compensated for pressure losses due to fluid leakage or other causes.

3.1 MECHANICAL SYSTEM

In figure 3 the 2-d layout of the riser tensioner system is shown. Its main function is to ensure a certain tension is maintained in the marine riser, and at the same time avoid that the riser is displaced outside the boundaries of the tensioner system.

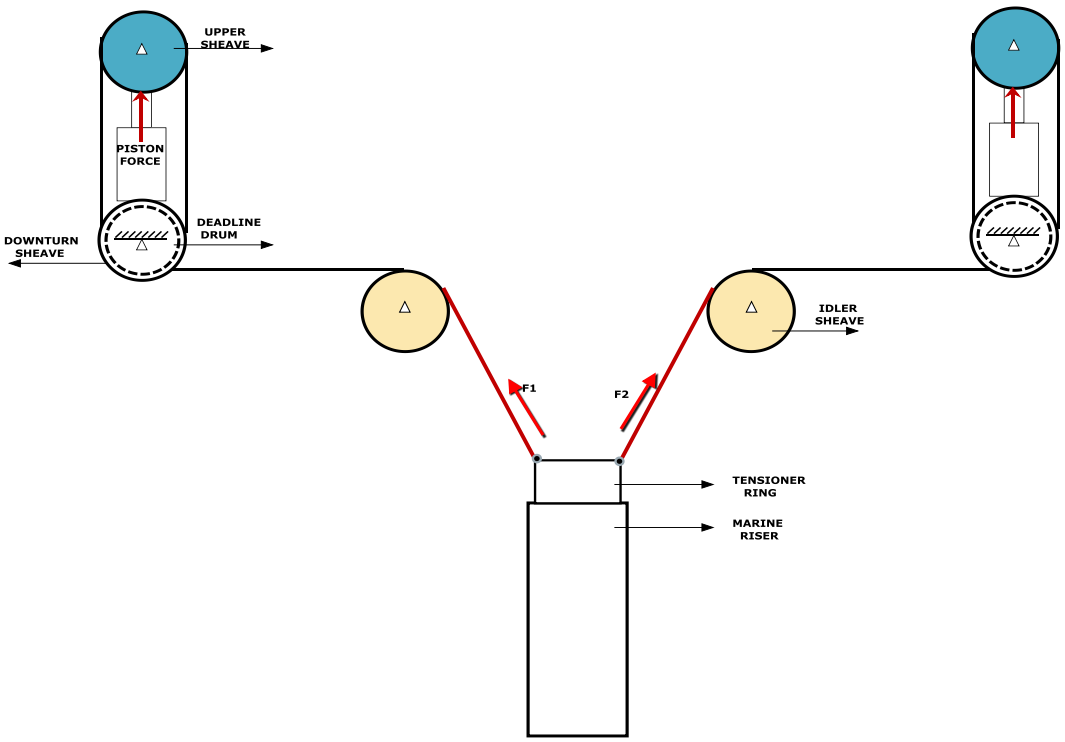

Figure 3: -Simplified construction of the riser tensioner.

According to figure 3, the upward lifting force is transmitted by the plurality of wires (the figure shows only two wires) in contact with sheaves and further coupled to the tensioner assembly. Although two tensioner assemblies are shown, it should be understood that eight dual tensioner assemblies are connected to the riser string in order to maintain the tension.

Lifting forces, F_1 and F_2 are developed in the wire as the high pressure hydraulic chambers in the cylinders are pressurized by a hydro-pneumatic accumulator (see figure 2). The top half of this accumulator is connected through a control valve unit to the working air pressure vessels, which are supplied with pressure valves to maintain the predetermined high pressure in the bottles.

The upper side of the hydro-pneumatic accumulator will maintain the high pressure in the hydraulic cylinder chamber since its volume will change.

When the floating platform heaves down with respect to the riser, the piston of the hydraulic cylinder will move up, increasing the volume of the cylinder chambers, thereby causing additional pressure from the hydro-pneumatic accumulator. When the floating platform moves up with respect to the riser, the cylinder piston will move down and the hydraulic fluid will flow back to the hydro-pneumatic cylinder, contributing to an increase in the air pressure on the top side of accumulator.

To prevent extreme movement of the tensioner piston, a fluid flow shut off valve is inserted between the hydro-pneumatic accumulator and the piston bore chamber of the tensioner. An air shut off valve is inserted between the accumulator and control valve unit.

Under normal working conditions, as the vessel heaves up and down in response to ocean wave movement, the tensioners respond in a passive fashion by taking up a wire cable in phase with the movement of the vessel. As a result, forces F_1 and F_2 will be equal.

However, at times, one or more of the cables will break (according to project problem statement), causing a substantial imbalance in the tension forces F_1 and F_2.

The applied tension force from each tensioner is very large as compared to the gravitational load on the tensioner piston. Therefore, in the case of a wire break, the tensioner piston will tend to move very rapidly in response to the resulting lack of tension.

In order to prevent any damage to the system, an anti-recoil protection system is used. A plurality of sensors, with the purpose of measuring the piston velocities of the tensioners, is mounted on the tensioner. In addition, the heave measurement system measures the velocity of the vessel due to heave motion. Subsequently, the CPU (usually PLC system) processes the measured signals, which are then transmitted to the air control valve in order to restrict the flow volume via flow shut off valve.

3.2 HYDRAULIC-/PNEUMATIC SYSTEM

In figure 4 the tensioner, including associated hydraulic and pneumatic components, is shown.

The lifting force (by one tensioner only) on the riser is developed by means of a hydraulic cylinder having housing and a movable piston, dividing the housing into a high pressure hydraulic chamber and a low pressure hydraulic chamber.

Hydraulic fluid in the high pressure hydraulic chamber is maintained under pressure by a hydraulic accumulator. The accumulator is the air/oil type, and includes a floating piston which separates hydraulic fluid in the bottom half of accumulator from the compressed air in the top half of the accumulator.

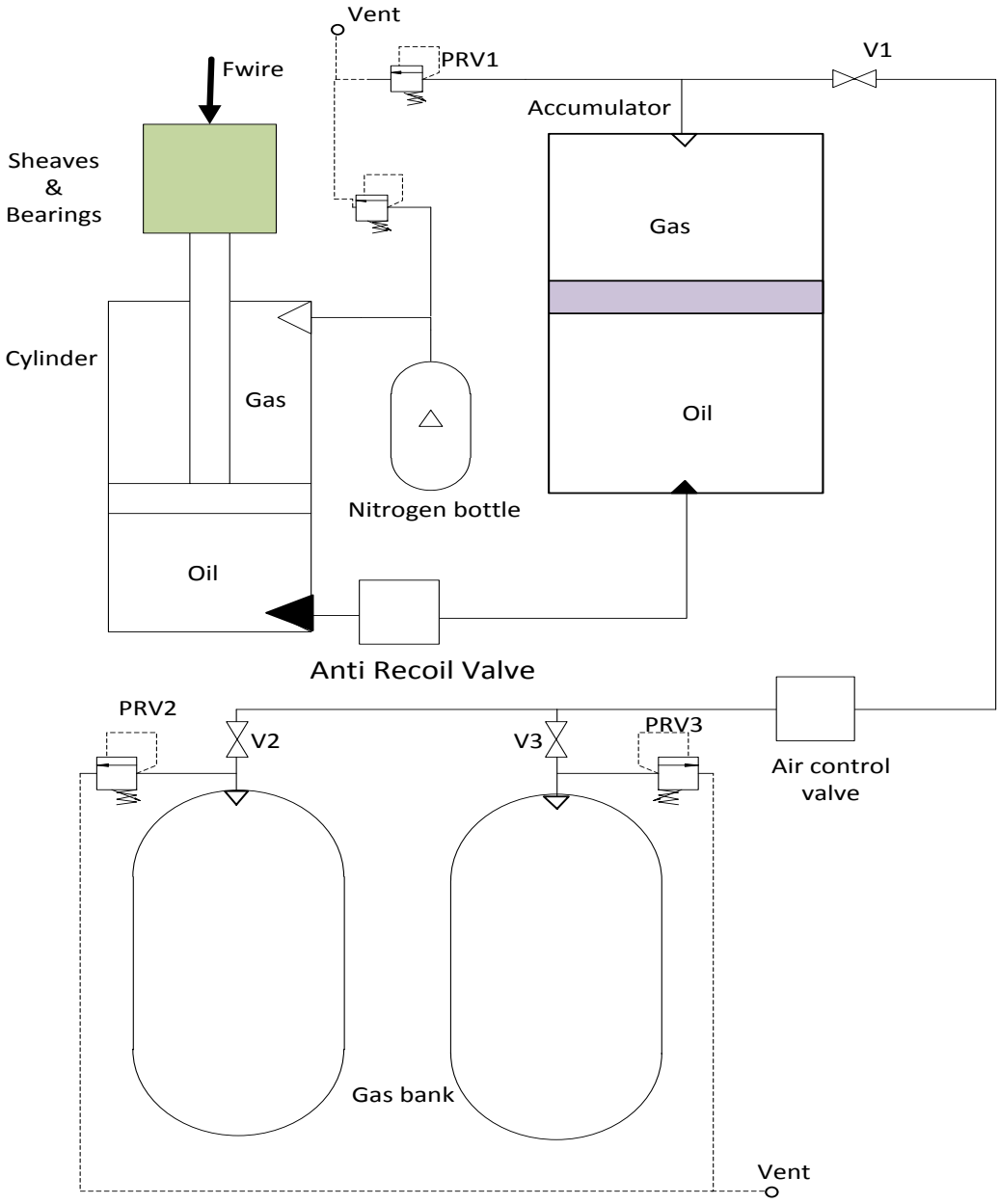

Figure 4: -Simplified layout of the pneumatic-/hydraulic system.

The top half of the accumulator is connected through a pneumatic pressure line to a high pressure gas bank of compressed gas used to maintain a predetermined high pressure level in the accumulator. Hydraulic fluid in the bottom of the accumulator is conveyed through a hydraulic pressure line to the bottom of the cylinder, where it is connected in fluid communication with the high pressure hydraulic chamber.

When the tensioner assembly is being operated in the drilling mode, hydraulic fluid is forced from the accumulator through the pressure line and into the high pressure chamber, where a hydraulic force is exerted to the face of the piston.

The pressure developed on the floating piston in the accumulator maintains the hydraulic fluid in the accumulator and in the high pressure chamber under pressure, as the volume of the hydraulic pressure chamber changes.

When the platform heaves down with respect to the riser, the cylinder housing is displaced down, with respect to the piston, thereby increasing the volume of the high pressure chamber.

4. SIMULATION MODEL-THE RESULTS PRESENTATION IN BRIEF

4.1 THE MODELING STRATEGY-DESCRIPTION OF A SIMULATION MODEL IN SIMX

In figure 5 and 6, both a physical- and a simulation model of the riser tensioner system is shown.

Because the riser tensioner is a rather complex system, the entire modeling and simulation process was a challenging task to accomplish. However, the ultimate goal of the project team was to build a simplified, but yet powerful enough to acquire the most important system parameters. In order to avoid any numerical instability (due to discontinuity points) during the simulation time, we have used quadratic functions at the proximity of disconnection points. By using this strategy, the computation times has been decreased considerably.

The entire system consists of pneumatic/hydraulic and mechanical subsystems. Referring to a nominal model in figure 5, the gas bank is modeled as a pneumatic volume with an initial pressure and a specified size. The flow resistances due to the geometry of a straight pipe (connecting a gas bank and accumulator), as well as flow restrictions because of two manual valves (R2, R3), air pressure control valve (here presented as a variable orifice 2) and a number of bends, are modeled altogether as a pipe, with the note that the restrictions due to fittings are inserted within library element, pipe. The accumulator is modeled as a piston accumulator readily available within hydraulic library elements. This element accepts different input data such as the geometry of the accumulator, as well as initial operating state variables (gas and oil pressure and a temperature) and returns results for a pressure, flow rate, volume and mechanical state variables for a piston.

The anti-recoil valve is modeled as a variable orifice (here orifice 1) defined through pressure drop-flow rate characteristics obtained by a manufacturer catalogue.

Because the tensioner consists of both hydraulic and pneumatic chambers, it has been modeled as a hydraulic accumulator permitting to compute both hydraulic/pneumatic as well as mechanical quantities. The piston and sheave masses are modeled as an inertial mass of a value obtained by TTS energy. The load force consisting of a riser tensioning force and a gravity force is modeled as a force element summing up forces F_2 through F_5. In addition, this element is an interface between the 1D mechanical- and the pneumatic/hydraulic system.

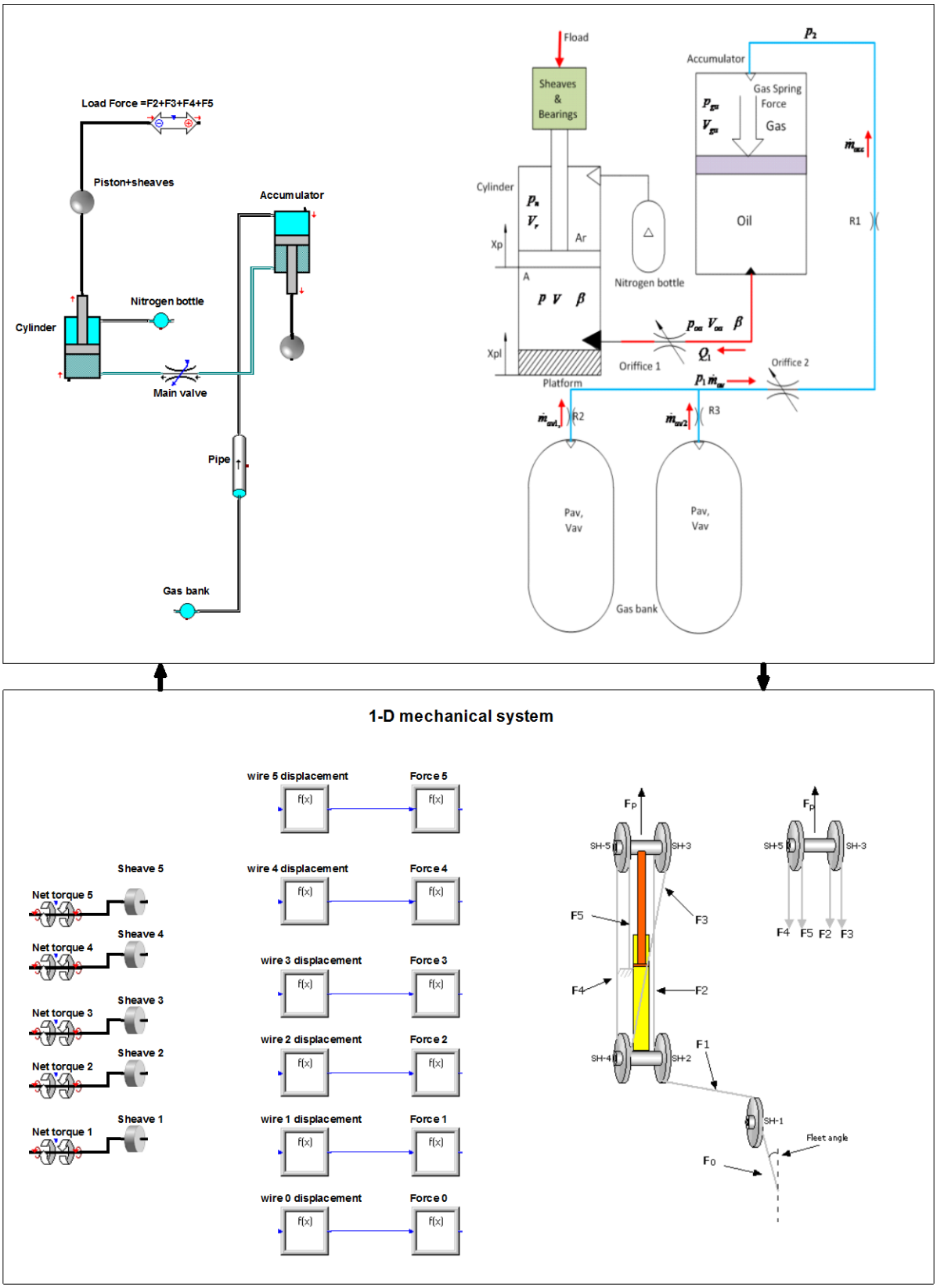

Fig 5: -Physical and simulation model of a mechanical and pneumatic/hydraulic system.

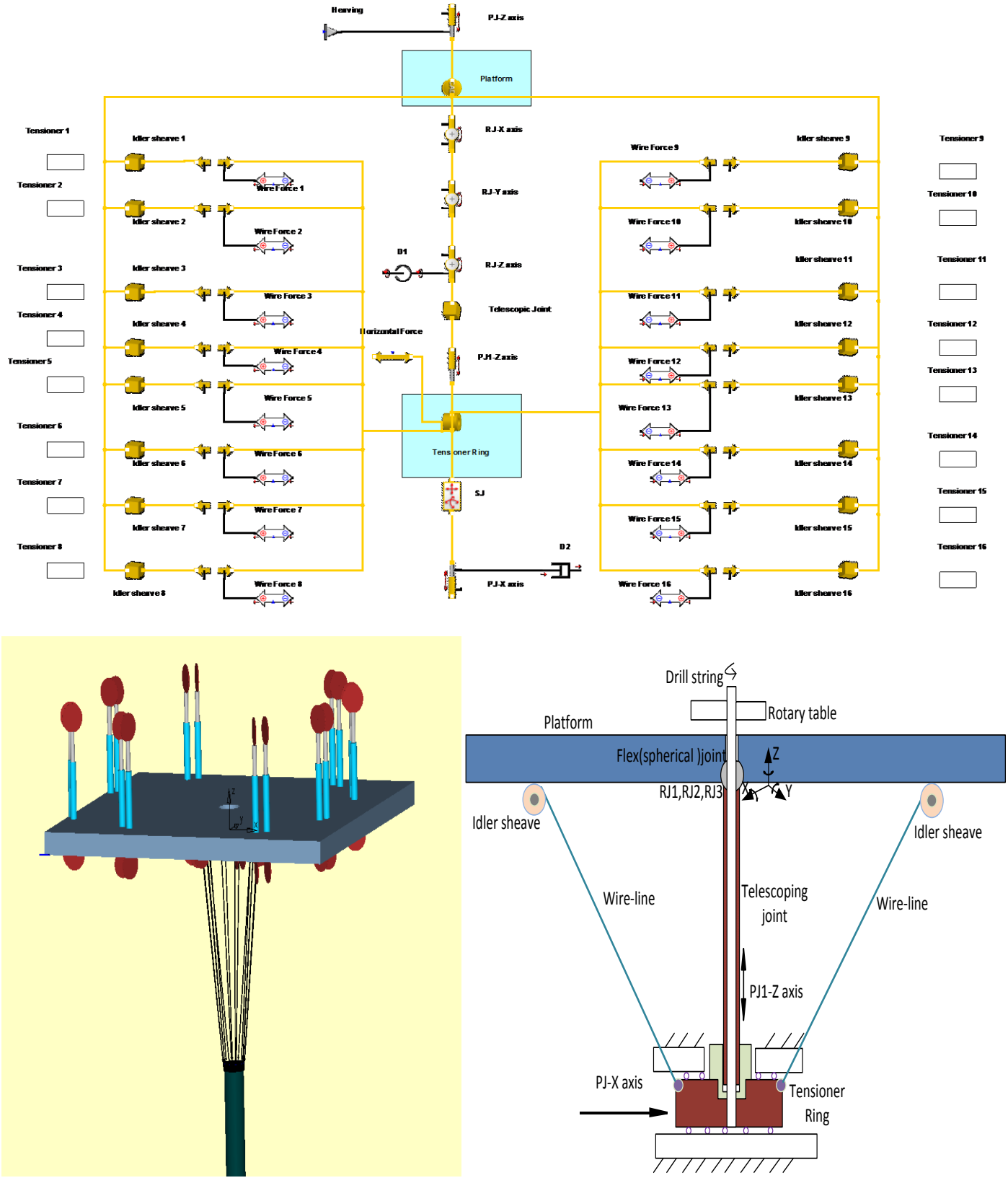

Fig 6: -Multi-body 3-d physical and simulation model.

Because the simulation of a pulley system is not straightforward in simX (such element is inexistent), an alternative approach has been used. Referring to a 1-D model in figure 5, the sheaves (1 through 5) are modeled as a rotational inertia

subjected to a net torque (applied torque minus friction torque) due to tension forces in the wire-line, here denotes as F_1 through F_5. These forces are computed knowing the wire-line stiffness, the initial as well as instantaneous wire elongations in different wire-line sections as shown in figure 5. The wire elongations are computed based on formula derived in chapter 5 (Modeling the riser tensioner system), and then inserted in the function denoted as wireline 0 deflections through wireline 5 deflections. Following this, the wire forces are computed (via functions Force 0 through Force 5) as a product of the wire stiffness and elongations of particular sections. More details are provided in chapter six.

Referring now to the figure 6, the modeling of a multi body 3-D model is based on the CAD drawing provided by TTS Energy. We have utilized dimensions, masses and coordinates of the elements in order to be able to create a realistic and working model.

All 3-D elements are modeled as rigid bodies with a predefined geometrical and material input data as provided by TTS Energy. According to figure 6, the platform heaving is simulated via a preset element named as "heaving", permitting to travel in z-direction due to a prismatic joint, PJ-Z axis. On the other side, the telescoping joint is constrained by the prismatic joint PJ1-Z axis to slide in Z direction. However, in order to decrease the bending moment in riser, the flex joint represented by three revolute joints in x, y, and z direction, will enable the telescoping joint to rotate for a limited angle around these axis. The tensioner ring is allowed to move translationally with respect to x direction (modeled as a roller joint, PJ-X axis) as a consequence of a horizontal force exerted on the riser. The damping effect in the system is added through D1 and D2.

Because the system is composed of as much as 16 tensioners, we had to create 16 blocks (or compounds) denoted as tensioner 1 through 16, each representing an entire tensioner model as given in figure 6. Now, the question is how to relate a 1-D model with 3-D in a way that the system will function properly. The following strategy has been applied:

The output of a tensioner block in figure 5 is a force 0 of the wire connected to a tensioner ring. In 3-D model, the force 0 of each tensioner is denoted as a wire force 1 for tensioner 1 and the same for other tensioners. Then, these forces will be exerted on the tensioner ring. The translative interface element (where a wire force is connected) computes the relative displacement of the tensioner ring with respect to a platform, and then this value is sent back to tensioner as an input, inserted into the expression for calculation of elongation for a last wire segment. As a result, there will be changes in the force 0 which will affect other forces too.

4.2 SIMULATION RESULTS

Nominal input data

At this stage, the most important system parameters will be presented and interpreted in order to show how the actual system behaves under different load case scenarios as described in the problem analysis. The explanations are not associated with providing further details as to how the system was modeled. However, the modeling techniques and the calculation of the initial state variables in an equilibrium state are shown to a great extend in the chapters to come.

The main parameters of the nominal model used in the simulation load case scenarios are summarized in table 1. In this initial phase, we don't consider the friction in the sheaves and tensioners (that will be included later in the sensitivity analysis section). However, some damping is added to the wire-line, assuming a damping coefficient equal to 10 % of the wire-line stiffness.

In addition, both the tensioner piston and the riser displacement are simulated to capture the motion behavior without a control structure which with be included in chapter six.

Table 1: - simulation input parameters.

	Normal operation mode	***A wire breakage mode***	***Emergency disconnection mode***
Heaving amplitude/period [m, s]	*4.8/18*	*4.8/18*	*4.8/18*
Piston mid-stroke [m]	*2*	*2*	*2*
Piston capacity at mid-stroke [kN]	*3280*	*3280*	*3280*
Initial Gas bank pressure [bar]	*190*	*190*	*190*
Initial Back pressure [bar]	*5*	*5*	*5*
Marine riser length [m]	*3000*	*3000*	*3000*
Marine riser mass+ tensioner ring [kg]	*699900*	*699900*	*699900*
Emergency disconnection initialization time [s]	*-*	*-*	*4.5*
Riser elevation observed time [s]	*-*	*-*	*9*
Wire rupture breakage initialization time [s]	*-*	*13.5*	*-*

The calculation of initial state variables in an equilibrium point is discussed in chapter six.

Normal operation mode

The graphs below show how the main system parameters experience changes as a result of heaving energy as the platform heaves up and down for a specified amplitude and frequency.

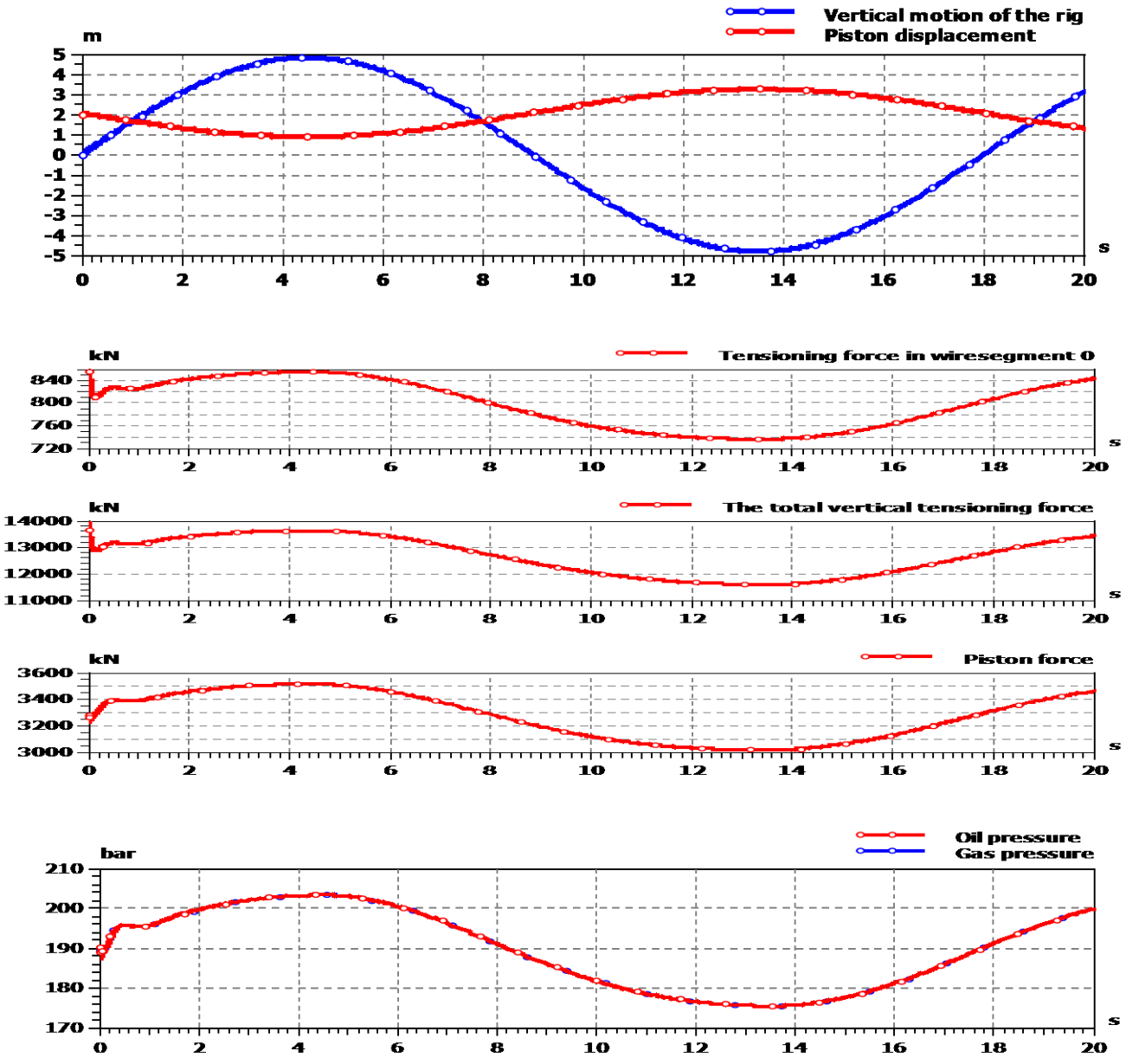

Figure 7: - System parameters due to platform motion.

Referring to the first graph of figure 7, provided that the platform heaves up with respect to a riser, the cylinder housing is displaced up relative to the piston, and

the hydraulic fluid in the pressure chamber is forced from the chamber into the accumulator. As this occurs the volume of air in the accumulator is compressed as the hydraulic fluid is returned. As platform reaches the maximum amplitude (4.8 m), the piston is displaced at its minimum position (0.8 m), corresponding to a mechanical advantage of 1:4 (the same holds true if the ratio of tension force in wire segment 0 versus piston force is considered). During this time period, there is a slight increase of the oil pressure as well until it reaches a peak at just under 205 bars when the maximum heaving amplitude is reached. The tensioning and piston force will experience an increase as well from app. 13000 kN up to just over 13500 kN, and from 3280 kN up to 3450 kN concerning a piston force.

When the platform heaves down with respect to the riser, the cylinder housing is displaced down with respect to the piston, thereby increasing the volume of the high pressure chamber. The pressure exerted by the compressed air in the accumulator causes additional hydraulic fluid to flow from the accumulator to the hydraulic pressure to completely fill the high pressure chamber, and maintains a pressure load on the piston. As platform reaches the pressure exerted by the compressed air in the accumulator, causes additional hydraulic fluid to flow from the accumulator to the hydraulic pressure to completely fill the high pressure chamber, and maintains a pressure load on the piston, reaches its minimum position (-4.8 m), the piston moves up to its maximum position (3.2 m), always maintaining the same mechanical advantage. On the contrary, the piston and tensioning force, as well as oil pressure, will experience a marked decrease. In particular, the tensioning force decreased up to app. 11500 kN and a piston force up to just over 3000 kN. The same pattern is experienced by the oil pressure as well, thereby decreasing up to just over 175 bars.

In summary, the following phenomena were observed:

- The mechanical advantage of 1:4 (velocity ratio defined as the piston over the platform velocity) is preserved throughout the simulation cycle.
- Obviously, the system pressure reacts in a pasive way whenever the system is disturbed by an uncontrolled heaving motion.
- The tensioning, piston, as well as pressures in the cylinder and accumulator, will follow the same pattern of change identical to the heaving.

Wire rupture mode

Figure 8 shows the main variables in the tensioner subjected to a wire rupture. In addition, other parameters such as the riser tensioning force and pressures in the accumulator are observed. At this point, it is important to assess the system response starting at time of a wire rupture until a full heaving period is completed. It is assumed that the tensioner experiences a wire rupture at the worst scenario, that is a maximum piston position (3.2 m) which corresponds with a minimum platform position, 4.8 m (see figure 7).

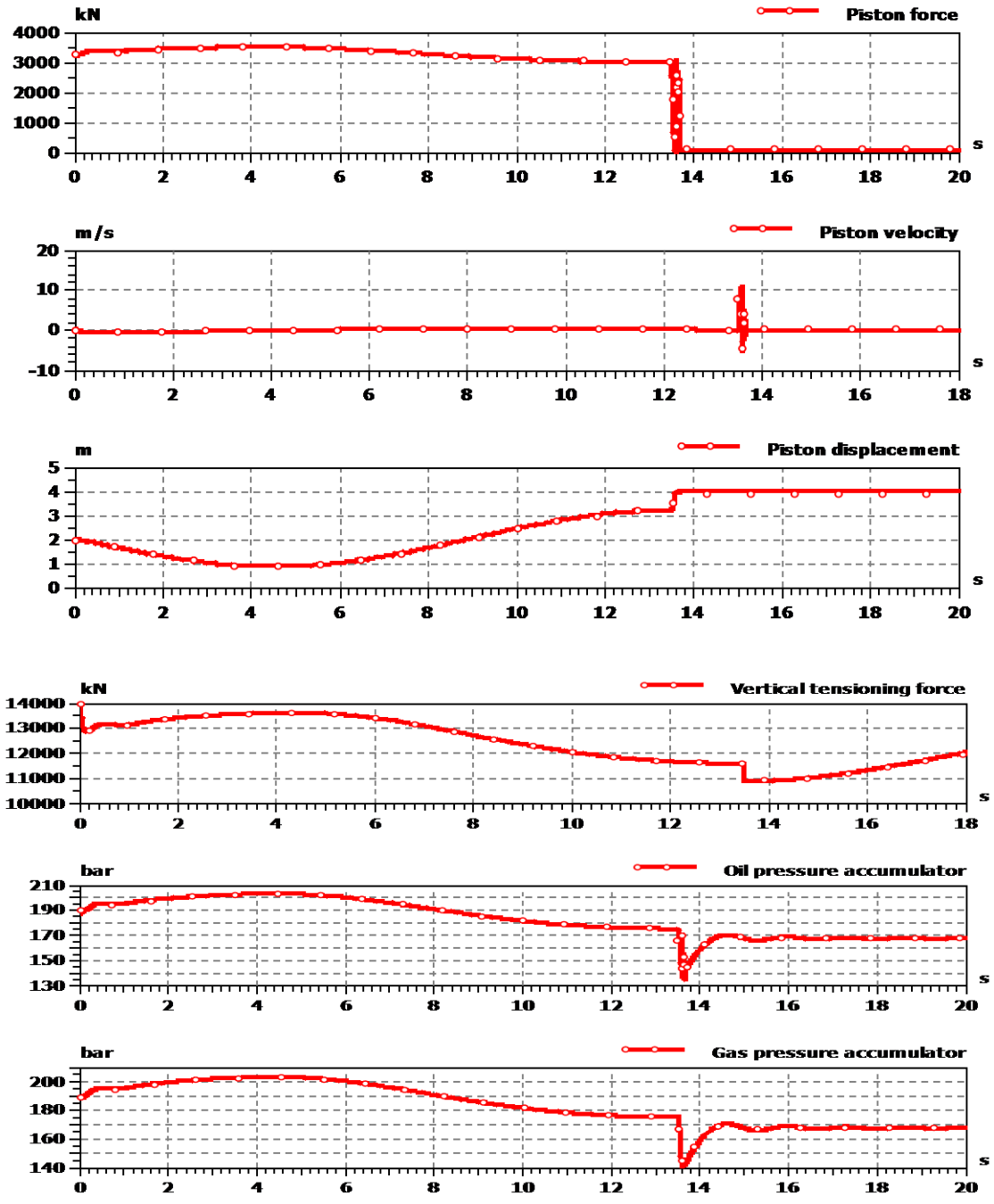

Figure 8: - System variables response due to a wire rupture at t=13.5 [sec].

In a real situation, provided that no control is implemented, this could lead to severe system damage because the piston (due to a large amount of energy accumulated in the gas bank) will quickly reach its end stop at the speed high enough to cause tensioner damage.

According to figure 2, at the moment of the wire rupture, the piston experiences a huge acceleration thereby reaching the cylinder end stop almost instantaneously at the speed of just over 10 m/s. The piston force drops enormously (as much as 3000 kN) to a level necessary to hold the weight of the sheaves (81 kN). Moreover, the tensioning riser force has declined for app. 750 kN, which corresponds with a force in wire 0, subject of a rupture. Likewise, due to a quick volume expansion in the cylinder chamber, the pressure in the piston side drops for as much as 45 bars. However, once the volume is filled with a fluid from the accumulator, the pressure will continue to increase up to a steady level of 167 bars necessary to generate a hydraulic force to be further balanced with the end stop static and pneumatic force as well as the weight of the sheaves.

In conclusion, the system experiencing a wire rupture behaves as follows:

- Due to lack of damping and friction in the cylinder, the piston will move rapidly at a speed much above the maximum speed (1.68 m/s) under the normal operating conditions.
- The gas bank pressure will respond quickly in order to compensate for a sudden pressure decrease in the cylinder due to a fluid volume expansion in the chamber.

In chapter six, further investigations will be performed including the scenario with two wire ruptures in the tensioner system.

Emergency disconnection mode

During this event, several factors are investigated:

- For a different initial system pressure (defined for a piston in its mid-stroke), what is a riser elevation height since initiation of the disconnection process (at t=4.5 sec) during the platform travelling time between a minimum and maximum amplitude.
- Evaluate the riser traveling time.
- Study the piston end stop contact travelling time.

An uncontrolled system response for a system pressure of 180 and 190 bars during an emergency riser disconnection is shown in figures 9 and 10.

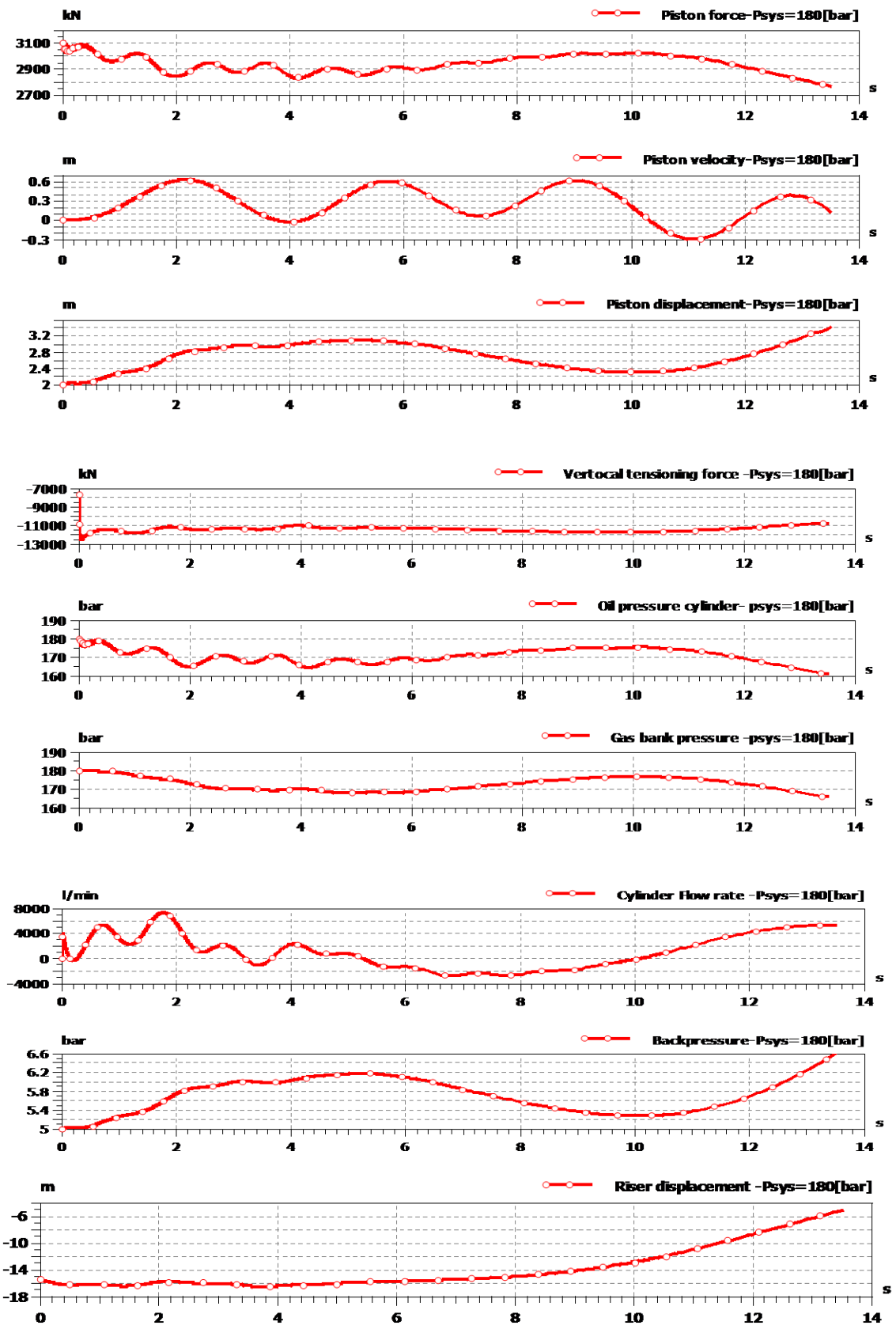

Figure 9: -State and flow variables for an initial system pressure of 180 [bar].

It is worth noting that it is beneficial to make use of the heaving energy, and therefore initiate the disconnection process just after the platform starts heaving up.

According to figure 9, at the moment of the riser disconnection (t=4.5 sec), the system pressure in disposal (just below 170 bars) is not enough to trigger the riser moving up. As the platform moves further up it will cause a very small upward riser displacement because of the piston stroke-in resulting in a decrease of the absolute riser displacement. In contrast, the riser will move up considerably once the piston starts to stroke-out at t=10 sec. Although the piston force and system pressure start to drop, the riser continues to move up because of the heaving energy. As seen from the graphs, during the entire cycle the tensioning riser force has experienced only a slight variation of app. 1000 kN. It is observed that the piston position at the end of the cycle is only 3.4 m, while the riser has moved up for 11 m.

In another development, we have observed the behavior of the system provided the initial system pressure is increased for 10 bars. In contrast with the first case, we notice that the riser starts to move up immediately after a disconnection, because the piston position now remains steady (the piston force is almost constant) as the platform moves up. As seen in figure 10, the piston has reached the end position in 11.63 seconds, and the riser has been elevated for 12.2 m. At the moment of the collision between the piston and end stop, the tensioning riser force drops considerably for an amount of end stop force, but just shortly since the previous value is restored after 2 seconds. Because the piston velocity at instant of contact with end stop (0.34 m/s) is greater than the allowed speed (0.2 m/s), it would be necessary to move the piston in a controlled manner in order to avoid higher impact forces. In chapter six, a control structure has been implemented to serving this purpose.

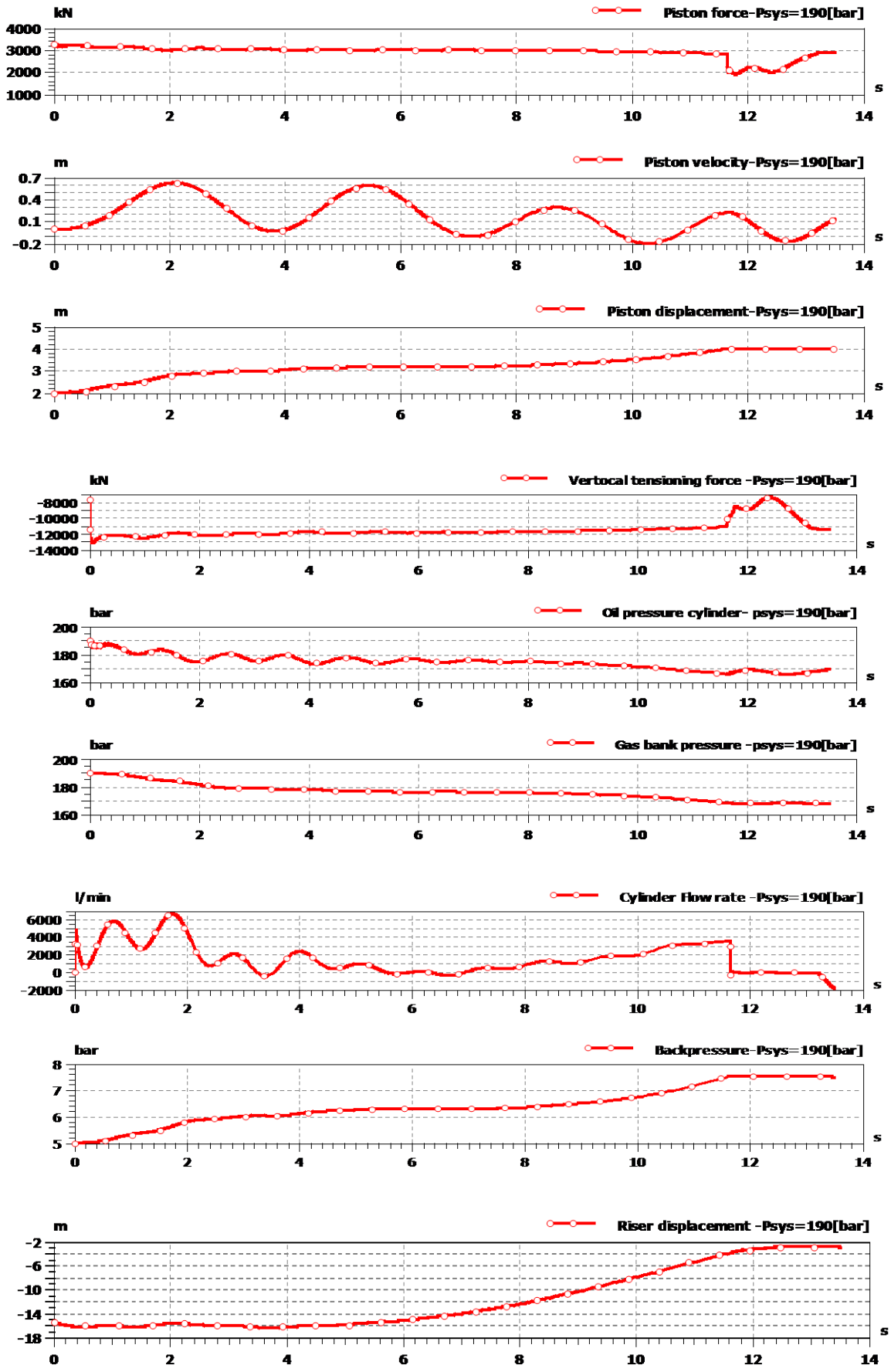

Figure 10: -State and flow variables for an initial system pressure of 190 bars.

Table 2: -Summary of results for different initial system pressure measured at mid-stroke position.

Parameter variations	***Extreme Values***	***Initial System Pressure [bar]***			
		207	***200***	***190***	***180***
Riser displacement [m]	*max/time*	*15.54/4.5sec*	*15.71/4.5sec*	*15.9/4.5sec*	*16.21/4.5sec*
	min/time	*10.02/7.52sec*	*8.5/8.52sec*	*3.7/11.63sec*	*5.2/13.5sec*
	total displacement-[m]	*5.52*	*7.21*	*12.2*	*11.01*
Piston displacement [m]	*piston stroke at instant of a riser disconnection-[m]*	*3.26*	*3.21*	*3.13*	*3.06*
	end stop contact travelling time-[s]	*3.02*	*4.02*	*7.13*	*end stop not reached*
Piston velocity at instant of contact with end stop [m/s]	*-*	*0.45*	*0.31*	*0.34*	*end stop not reached*

Table 2 provides additional information for a simulated system with initial system pressure at 200 and 207 bars.

To recapitulate:

- Before any control algorithm is designed, it is necessary to check whether the system pressure at the moment of emergency disconnection is high enough to move the piston at cylinder end stop, without causing a great impact forces, and elevate the riser higher enough to prevent any collision with BOP as the platform moves down.
- The vertical tensioning force remained nearly constant throughout the heaving period.
- The greater initial system pressure, the faster piston will move, thereby greater piston velocities at instant of contact with end stop. In addition, the riser elevation height will be smaller as we increase the initial system pressure.

5. MODELING OF THE RISER TENSIONER SYSTEM

5.1 MODELLING THE PNEUMATIC-/HYDRAULIC SYSTEM

In figure 11, a 2-d layout of a tensioner unit is shown. Before we derive mathematical expressions for separate pneumatic/hydraulic components, it would be beneficial to observe the work of a tensioner unit as a whole and analyze the interaction between different sub- systems.

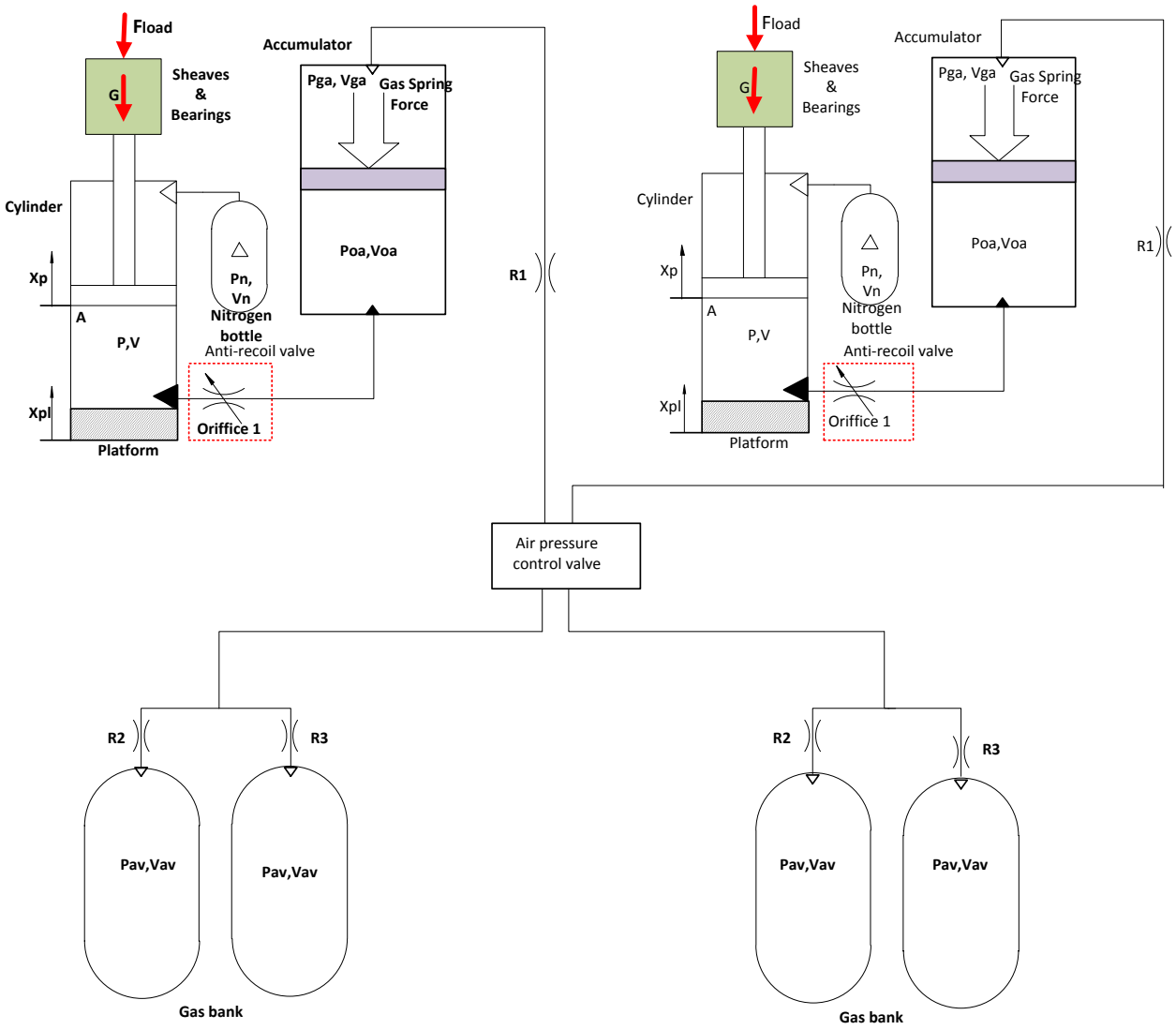

Fig 11: -basic hydraulic-pneumatic diagram of tensioner unit

The lifting force is exerted on the riser by as much as 16 individual tensioners. The force of each tensioner unit is produced by means of a two pressurized hydraulic-pneumatic cylinders with a high pressure hydraulic chamber and a low pressure pneumatic chamber divided by a movable piston, see figure 11. The low pressure penumatic chamber is in communication with a nitrogen gas bottle. The hydraulic fluid is pressurized by a pneumohydraulic accumulator. The accumulator is of the air-oil type and includes a floating piston which separates hydraulic fluid in the bottom half of the accumulator from the compressed air in the top half of the accumulator.

The top half of the accumulator is connected through a pneumatic pressure line to a high pressure gas bank that is used to maintain a predetermined high pressure level in the accumulator and that may be adjusted by the operator. Hydraulic fluid in the bottom of the accumulator is conveyed through a hydraulic pressure line to the bottom of the hydraulic-pneumatic cylinder. Although hydraulic fluid is indeed compressible it may be considered rigid as compared to the gas when describing the principles of the tensioner unit.

When the tensioner assembly is being operated in the drilling mode, hydraulic fluid is forced from the accumulator through the pressure line and into the high pressure chamber, where a hydraulic force is exerted to the face of the piston.
The pressure developed on the floating piston in the accumulator maintains the hydraulic fluid in the accumulator and in the high pressure chamber under pressure as the volume of the hydraulic pressure chamber changes.

When the platform heaves down with respect to the riser, the cylinder housing is displaced down with respect to the piston, thereby increasing the volume of the high pressure chamber.
The pressure exerted by the compressed air in the accumulator causes additional hydraulic fluid to flow from the accumulator to the hydraulic pressure to maintains a pressure load on the piston. On the other side, provided that the platform heaves up with respect to the riser, the cylinder housing is displaced up relative to the piston and the hydraulic fluid in the pressure chamber is forced from the chamber into the accumulator. As this occurs the volume of air in the accumulator is compressed as the hydraulic fluid is returned.

The mathematical modeling of the tensioner unit will be performed after a modeling of particular components in the system is completed.

5.2 MODELING A WORKING AIR PRESSURE VESSEL

In figure 12, simplified schematic of a working air pressure vessel (WAPV) is shown.

The assumption that there is no heat exchange yields an adiabatic relationship given by:

$$p_{av} v_{av}^{\ k} = const$$
$$p_1 v_1^{\ k} = const \qquad (5.1)$$

$$v_{av} = \frac{V_{av}}{m} \qquad (5.2)$$

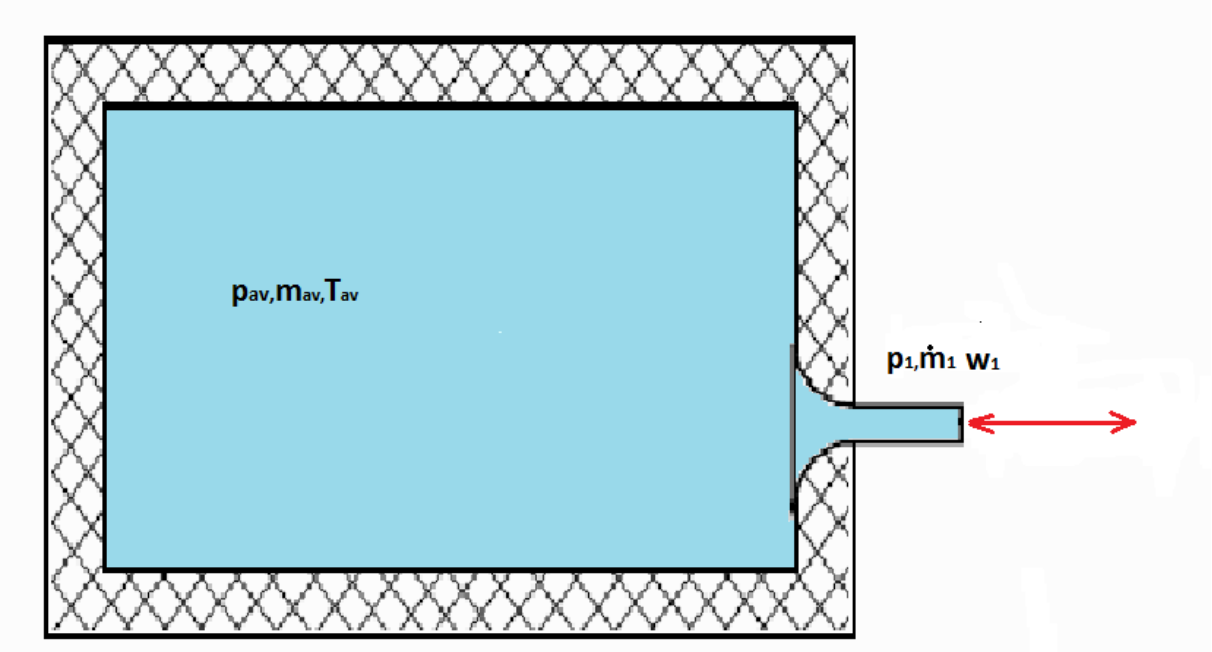

Fig 12: - A simplified schematic of a working air pressure.

Using the ideal gas equation and the general equation of the energy (considering that a mechanical work and heat transfer in the chamber is neglected), the flow velocity leaving the chamber is obtained by the following expression:

$$w_1 = \sqrt{2RT_{av}\left[\frac{k}{k-1}\right]\left[1-\left(\frac{p_1}{p_{av}}\right)^{(k-1)/k}\right]} \qquad (5.3)$$

where R is the gas constant (for air, R=287 $\left[\frac{J}{kg \cdot K}\right]$), T_{av} [K] is the temperature in the wapv.

The mass flow rate, $\dot{m}$ is determined by:

$$\dot{m} = Aw\rho \tag{5.4}$$

where A [m^2] is the flow area, and $\rho \left[\frac{kg}{m^3}\right]$ is the air density.

The mass flow rate is the same along the outlet pipe following the continuity law.

The density in the outlet pipe is found to be [3] as:

$$\rho_1 = \frac{1}{v_1} = \frac{p_{av}}{RT_{av}}\left(\frac{p_1}{p_{av}}\right)^{1/k} \tag{5.5}$$

Combining eqs. (5.5) and (5.3) will give the expression for the mass flow rate

$$\dot{m} = Ap_{av}\sqrt{\frac{2}{RT_{av}}}\sqrt{\frac{k}{k-1}}\sqrt{\left(\frac{p_1}{p_{av}}\right)^{2/k} - \left(\frac{p_1}{p_{av}}\right)^{(k+1)/k}} \tag{5.6}$$

The flow function is defined as

$$\Psi = \sqrt{\frac{k}{k-1}}\sqrt{\left(\frac{p_1}{p_{av}}\right)^{2/k} - \left(\frac{p_1}{p_{av}}\right)^{(k+1)/k}} \tag{5.7}$$

Thus, the air mass flow rate is

$$\dot{m} = Ap_{av}\sqrt{\frac{2}{RT_{av}}}\Psi \tag{5.8}$$

It is interesting to observe the behavior of the gas if the pressure ratio $\frac{p_1}{p_{av}}$ is varied. Indeed, provided that $p_1 = p_{\max} = 0.528p_{av}$ then the air velocity reaches the sonic velocity as it passes through the nozzle. The pressure ratio of 0.528 is also called a critical pressure ratio.

Consequently, the flow function is divided into two piece-wise functions depending on the above pressure ratio

$$\Psi = \begin{Bmatrix} \sqrt{\frac{k}{k-1}}\sqrt{\left(\frac{p_1}{p_{av}}\right)^{2/k} - \left(\frac{p_1}{p_{av}}\right)^{(k+1)/k}} \rightarrow for\left(\frac{p_1}{p_{av}}\right) > 0.528(sonic - flow) \\ \left(\frac{2}{k+1}\right)^{1/(k-1)}\sqrt{\frac{k}{k+1}} \rightarrow for\left(\frac{p_1}{p_{av}}\right) <= 0.528(choke - flow) \end{Bmatrix} \tag{5.9}$$

A further decrease of the pressure ratio below 0.528 will not increase the velocity of the air through the nozzle.

However, we may need to find expressions for a pressure gradient, as well as temperature, in order to completely define the internal pneumatic variables (or state variables), and hence compute all needed variables concerning the air pressure vessel.

The pressure and temperature gradient for an adiabatic law are determined by the following formulae:

$$\dot{p}_{av} = \frac{k}{V_{av}}\left(-\dot{m}RT_{av} - p_{av}\dot{V}_{av}\right) \tag{5.10}$$

$$\dot{T}_{av} = \frac{T_{av}\dot{V}_{av}}{V_{av}} + \frac{T_{av}\dot{p}_{av}}{p_{av}} - \frac{kT_{av}{}^{2}\dot{m}}{p_{av}V_{av}} \tag{5.11}$$

Actually the thermodynamic process in the air vessel has a polytrophic behavior with coefficient "n" varying between 1 and 1.4.

However, in the industry practice, where the temperature difference between the chamber and ambient is small, the heat exchange can be neglected and hence an isothermal process prevail.

Equation (5.10) then takes the form as given below:

$$\dot{p}_{av} = \frac{1}{V_{av}}\left(-\dot{m}RT_{st} - p_{av}\dot{V}_{av}\right) \tag{5.12}$$

where, T_{st} =290.15[K] is the standard ambient temperature.

5.3 MODELING THE FLOW RESISTANCE OF PIPES

6. Because the piping connecting the working air pressure vessels and accumulator is long (as much as 35 m) supplied with a considerable number of fittings(8) in the form of a 90 degree standard elbow, the pressure drops due to flow restrictions imposed because of the piping geometry should not be neglected. It is, however, lumped parameters are considered only, and hence distributed parameters are omitted. According to figure 13, w_1 is an air flow velocity leaving the gas bank nozzle while w_2 is an air flow velocity entering the accumulator. Provided w_1 and w_2 are equal, the following relation holds [3]:

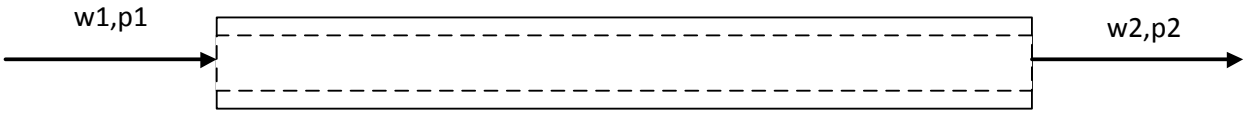

Figure 13: - The pipeline.

$$\frac{p_2^2 - p_1^2}{2p_1} + \frac{\lambda L \rho_1 w_1^2}{2D}\left(\frac{T_1 + T_2}{2T_1}\right) = 0 \qquad (5.13)$$

Where D[m] is the inner pipe diameter, L[m], is the total length of the straight line, T_1[K] and T_2[K] are the temperature entering and leaving the pipe, respectively, and λ is the pipe friction coefficient which depends on the flow conditions. It may be computed according to the following expressions:

$$\lambda = \frac{64}{\mathrm{Re}} \qquad (5.14)$$

where, Re is a Reynolds constant determined by the next expression:

$$\mathrm{Re} = \frac{w_1 D}{\upsilon} \qquad (5.15)$$

$\upsilon\left[\frac{m^2}{s}\right]$ is the air kinematic viscosity. The above expression for the pipe friction coefficient is valid under the assumption that Re<2300 which is true for a laminar flow. If Re>2300,then a turbulent flow will prevail and therefore another expression (for rough pipes) provided by Haaland(1983) should be used as given below:

$$\frac{1}{\sqrt{\lambda}} = -1.8\log_{10}\left[\frac{6.9}{\mathrm{Re}} + \left(\frac{K}{3.7D}\right)^{1.11}\right] \qquad (5.16)$$

Where, K is the pipe inner surface roughness.

The contribution of fittings on the pressure drop is to be calculated using Fleischer (1995) which gives an equivalent length of straight, unrestricted pipe to be summed with a previous pipe length and plugged in expression (5.13).

$$L_{eq} = nFD \qquad (5.17)$$

Where, n is a total nr of fittings along the pipe, F is a multiplying factor (2.5 for a standard 90 degree elbow). Therefore, the computed equivalent length for the nominal model is:

n=8 elbows, D=77.77 [mm] F=2.5

$$L_{eq} = 8 \cdot 77.77 \cdot 2.5 = 1.55\,[\text{m}] \tag{5.18}$$

Therefore, the equivalent length of pipe is 35[m]+1.55[m]=36.55[m]

5.4 MODELING OF A PNEUMOHYDRAULIC ACCUMULATOR

In figure 14, a principle of work of a pneumohydrualic accumulator is shown.

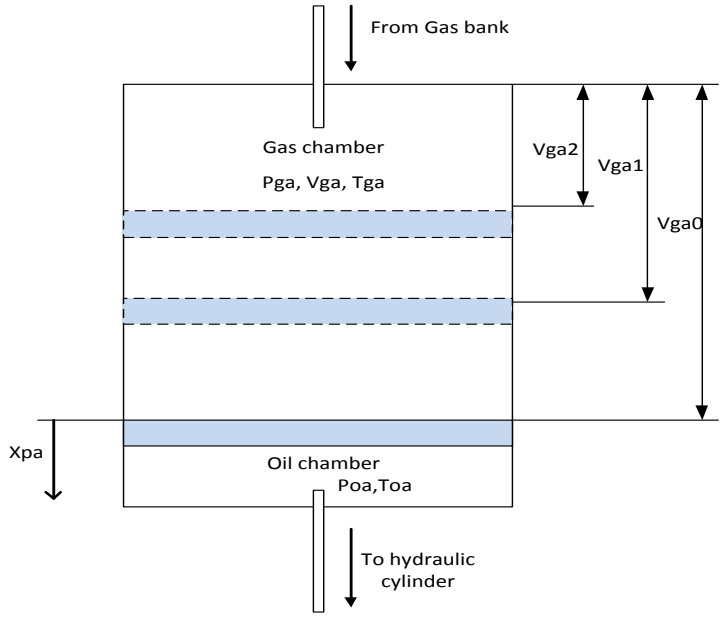

Figure 14: - A pneumohydrualic accumulator.

The following nomenclatures are used as shown in the figure:

p_{ga0} [bar] -accumulator charging pressure, gas pressure,

p_{ga1} [bar]-minimum system pressure,

p_{ga2} [bar]-maximum system pressure,

V_{ga0} [m^3]-accumulator size, volume of charging gas at pressure p_{ga0} ,

V_{ga1} [m^3]-volume of gas at pressure p_{ga0} ,

V_{ga2} [m^3]-volume of gas at pressure p_{ga2} ,

m_{pa} [kg]-mass of the piston accumulator,

A_a [m^2]-piston area,

d_{pa} [m]-accumulator piston diameter,

V_{oa0} [m^3]-dead oil volume,

V_{ga} [m^3]-actual gas volume

Geometric quantities

The piston area side is calculated as:

$$A_a = \frac{\pi d_{pa}^2}{4} \tag{5.19}$$

The accumulator oil side volume:

$$V_{oa} = V_{oa0} + V_{ga0} - V_{ga} \tag{5.20}$$

The minimum oil volume is limited to the dead oil volume, $V_{oa} \geq V_{oa0}$

The volumetric capacity of the accumulator is defined, V_a is defined as volume of oil delivered to/from the accumulator and is defined with the following expression:

$$V_a = V_{ga1} - V_{ga2} = V_{ga0} \left\{ \left(\frac{p_{ga0}}{p_{ga1}} \right)^{\frac{1}{n}} - \left(\frac{p_{ga0}}{p_{ga2}} \right)^{\frac{1}{n}} \right\} \tag{5.21}$$

In order to ensure a proper operations of the accumulator, the charging pressure should be 90 % of the minimum working pressure (hydraulic components and systems), p_{ga1}.

Mechanical quantities

In order to compute different forces in the accumulator, we set up a force balance for the piston motion applying a second's Newton law:

$$F_{hyd} - F_{pneu} + F_f + F_{visc} = m_{pa} \ddot{x}_{pa} \tag{5.22}$$

Where, $F_{hyd} = (p_{oa} + p_{atm}) A_a$ is the hydraulic force, $F_{pneu} = (p_{ga} + p_{atm}) A_a$ the pneumatic force, $F_{visc} = b\dot{x}_{pa}$, the viscous force, and F_{fric} is a friction force based on Stribeck effect, and which will be further explained when modeling a hydraulic cylinder.

Hydraulic quantities

Because the accumulator is connected to the hydraulic cylinder, the accumulator is described with an additional state variable, and volume gradient given by the following expression:

$$\dot{V}_{oa} = \frac{\dot{p}_{oa}}{np_{oa}} V_{ga} \tag{5.23}$$

In addition, the pressure gradient has to be defined in the oil side of the accumulator (the case when the oil is flowing into the cylinder) in accordance with the formula below:

$$\dot{p}_{oa} = \frac{\beta(-Q_{oa} + \dot{V}_{oa})}{V_{oa}} \tag{5.24}$$

where, p_{oa} is the pressure in the oil side of the accumulator, $V_{ga} = \left(\frac{p_{ga0}}{p_{oa}}\right)^{\frac{1}{n}} V_{ga0}$ is an instantaneous gas volume in the accumulator, n is polytrophic coefficient, and Q_{oa} is a discharging oil flow rate.

Pneumatic quantities

Using the same approach as for wapv, the pressure gradient in the gas side is to be determined by the following development:

$$\dot{p}_{ga} = \frac{1}{V_{tg} + A_{ps}\left(0.5x_{stroke} \pm x_{pa}\right)} \left(n_1 \dot{m} R T_1 \mp n p_{ga} A_{ps} \dot{x}_{pa}\right) \tag{5.25}$$

where, V_{tg} [m^3] is the sum of gas volumes in gas bank and the pipe connecting the gas volume and a gas side of the accumulator, x_{stroke} [m] is the piston stroke,

x_{pa} [m] is the piston position, n_1 is the polytrophic coefficients for a state of the gas entering the accumulator, n is the polytrophic coefficient inside the accumulator chamber, A_{ps} [m^2] is the area of the piston side, and T_1 [K] is the gas temperature entering the accumulator chamber.

It would be useful to analyze the role of certain accumulator parameters when the system experiences hydraulic shocks due to a rapid closure of the main valve. In addition, due to its capacitance, the accumulator will smooth the pressure ripples in the system.

5.5 MODELING OF A HYDRAULIC ACTUATOR

In figure 15, the tensioner unit is shown. It consists of a hydraulic cylinder, an anti-recoil valve (only an orifice is shown) and a nitrogen bottle connected to a rod-side of the cylinder.

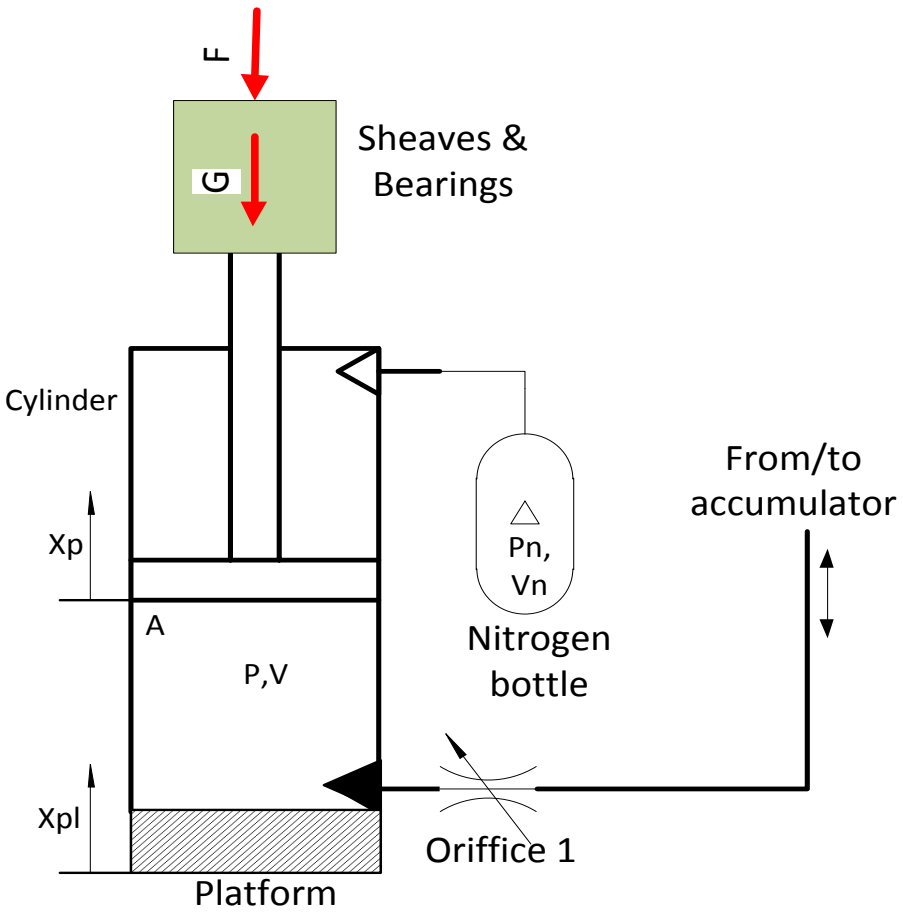

Fig 15: -2D representation of the tensioner.

As illustrated in this figure, the tensioner consists of pneumatic, hydraulic, as well as mechanical components, and hence represents a multi-domain energy system by itself. The hydraulic energy developed in the high pressure cylinder side via oil pressure is converted into a mechanical energy through a force exerted on the piston side of the cylinder. On the other side, the nitrogen gas bottle connected to the rod side of the cylinder serves as a gas spring. The tensioning force exerted on the tensioner ring will be transmitted on the piston through a system of a wireline and sheaves fixed on top of the piston rod. In accordance with the sketch, the following nomenclature has been used:

p = Actual pressure in the high pressure cylinder chamber, Pa (abs)

p_n =Pressure in the low pressure chamber of the hydraulic cylinder, Pa

p_{atm} =Atmospheric pressure, Pa

Q_c =flow rate in high pressure cylinder chamber, $\left[\frac{m^3}{s}\right]$

d_{pc} =the cylinder piston diameter, [mm]

d_{rc} =the cylinder piston rod diameter, [mm]

A = Piston area, [m^2]

Ar = Piston area –rod area, [m^2]

V_o =dead volume of cylinder piston side, [m^3]

V_{r0} =dead volume of cylinder rod side, [m^3]

x_p = Piston displacement, [m]

$x_{\max stroke}$ =piston max stroke, [m]

$x_{midstroke}$ =piston mid stroke, [m]

F_l =load force, [N]

F_f =Friction force, [N]

m_{eff} = mass of the piston including mass of the sheaves, bearings, shaft and a bracket

b=viscous coefficient, $\left[\frac{Ns}{m}\right]$

Geometric quantities

The piston area side is calculated as:

$$A = \frac{\pi d_{pc}^2}{4} \tag{5.26}$$

The piston rod side area is calculated as:

$$A_r = \frac{\pi}{4}\left(d_{pc}^2 - d_{rc}^2\right) \tag{5.27}$$

The cylinder piston side volume is:

$$V = V_0 + x_p A \tag{5.28}$$

The cylinder rod side volume (including the volume of a nitrogen bottle) is given as:

$$V_r = V_{ro} + V_n + (x_{\max stroke} - x_p)A_r \tag{5.29}$$

Mechanical quantities

The hydraulic force F_{hyd} is a force difference on both sides of the piston area generated by a fluid and gas pressure and is written as:

$$F_{hyd} = pA - p_n A_r \tag{5.30}$$

The friction force is to be modeled according to a Stribeck effect.

The Stribeck model enables us to capture a variety of phenomena as follows:

- Coulomb(i.e dry) friction,
- Mixed Friction,
- Hydrodynamic friction, and
- Pressure-dependent friction

The velocity dependent part of the friction force is determined by the formula:

$$F_{fr,v} = F_c + \left(\left(F_s - F_c\right)\exp\left(-\frac{|v_{piston}|}{v_l}\right)\right) + k_v |v_{piston}|^{a_v} \tag{5.31}$$

While, the pressure-dependent part of the friction force is written as:

$$F_{fr,p} = k_p p_{\max} = F_s \tag{5.32}$$

Finally, the total friction force is $F_{fr} = F_{fr,v} + F_{fr,p}$

Where, F_c [N] is the coulomb friction force, F_s [N] is the static friction force, v_{piston} $\left[\frac{m}{s}\right]$ and $v_l\left[\frac{m}{s}\right]$ is the piston and limit velocity respectively. $k_v, a_v,$ k_p are parameters.

The mechanical state variables $x_p, \dot{x}_p$ are to be found by means of a second Newton's law applied for piston equilibrium:

$$pA_p - p_n A_r = m_{eff}\ddot{x}_p + b\dot{x}_p + m_{eff}g + F_f + F_l \tag{5.33}$$

Hydraulic quantities

Pressure builds up equation in the piston side:

- When piston is extracting,

$$\dot{p} = \frac{\beta}{V}\left(Q_1 - Q_{li} - A\dot{x}_p\right) \tag{5.34}$$

- When piston is retracting, then

$$\dot{p} = \frac{\beta}{V}\left(-Q_1 - Q_{li} + A\dot{x}_p\right) \tag{5.35}$$

Flow rate, Q_1 is to be calculated by the following expression:

$$Q_1 = C_d A_d \sqrt{\frac{2}{\rho}\left(p_{mv} - p\right)} \tag{5.36}$$

Here, C_d is discharge coefficient, A_d [mm^2] is discharge area, p_{mv} is a pressure for the fluid volume connecting the outlet of main valve(anti-recoil valve) and the cylinder inlet, $Q_{li}\left[\frac{m^3}{s}\right]$ is the flow leakage rate.

Pneumatic quantities

Pressure builds up equation in the piston rod side:

When cylinder is extracting, $$\dot{p}_n = \frac{k}{V_r}\left(-\dot{m}_r R T_r + p_n \dot{V}_r\right) \quad (5.37)$$

When cylinder is retracting, $$\dot{p}_n = \frac{k}{V_r}\left(\dot{m}_r R T_r - p_n \dot{V}_r\right) \quad (5.38)$$

The mass flow rates and temperatures of the nitrogen gas are to be determined by the same expression we have yielded for air pressure vessels and accumulator.

5.6 MODELING OF AN ANTI-RECOIL VALVE

The proportional anti-recoil valve is used in two distinct modes of operation:

- Conventional flow shut off valve in the event of a wire –breakage, and
- Anti-recoil valve used during an emergency disconnection of the riser from BOP.

In figure 16, a detailed diagram of such valve is shown.

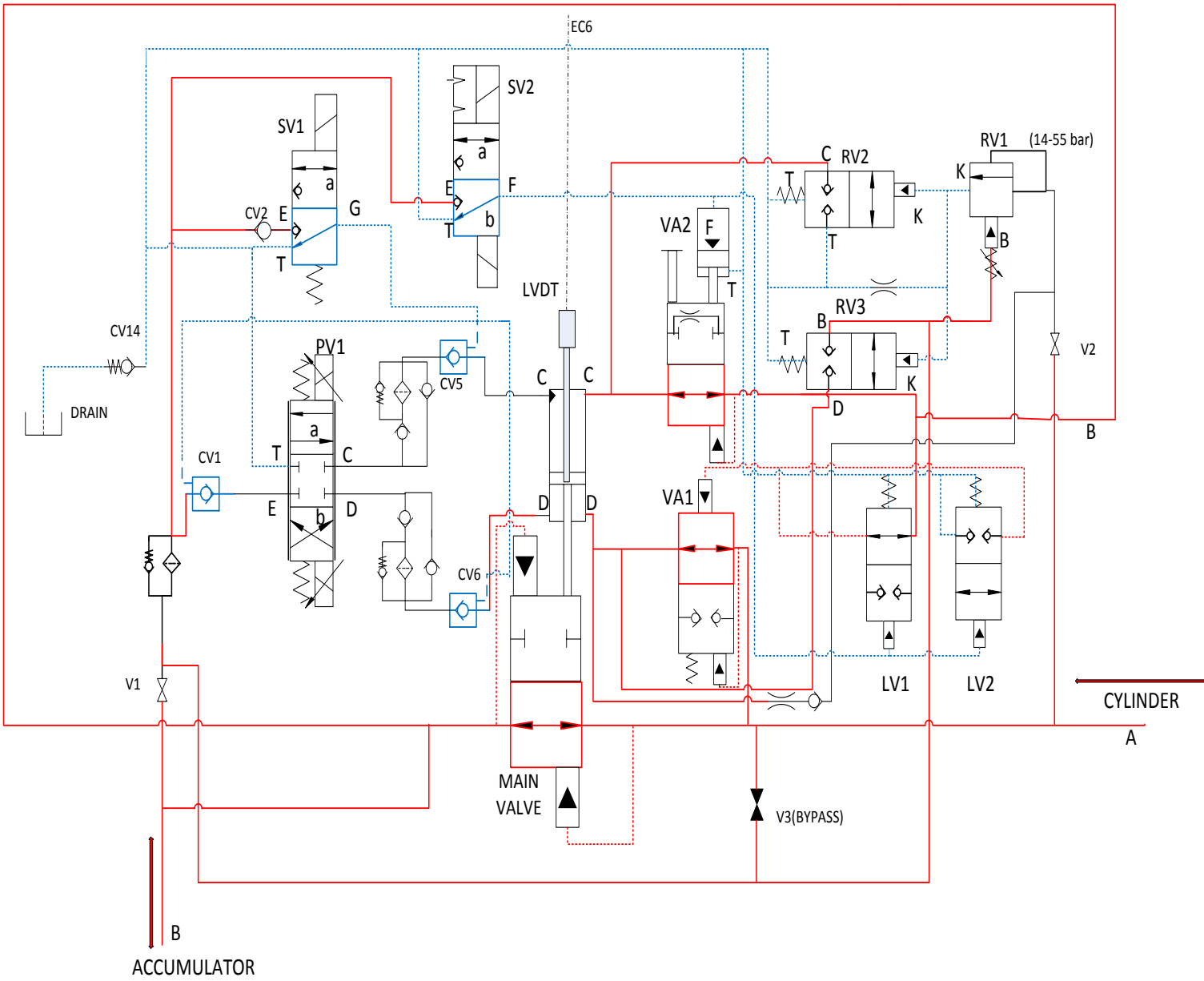

Figure 16: -Anti Recoil Valve-flow of energy and signals during a normal mode of operation.

Normal mode

In the normal mode, SV1 is de-energized which vents the pilot line to CV1, CV5, and CV6. CV1 blocks the pressure supply line of PV1 while CV5 and CV6 prevent standby leakage across PV1. SV2 is in coil 'b' position venting the pilot pressure to the VA1 and VA2 allowing the system pressure to keep them in the open position, as shown in the figure.

Region C, the top side of the control piston, is connected to accumulator pressure through VA2 via region B. Region D, the bottom side of the control piston, is connected to cylinder pressure through VA1 via region A.

When a wire line break occurs on the tensioner, flow will quickly accelerate through the valve due to the stored energy in the gas bank feeding the accumulator. The main valve will close due to internal force generated as a result of a pressure differential on both sides of a spool as flow passes the main valve. The nominal pressure drop needed to actuate the main valve closure was assumed to be a 5 [bar]. Once the cylinder fully extends, the pressures in the regions A and B will be the same, which will cause the valve to reopen.

Emergency disconnection mode

During this phase, solenoid valve, SV1 is energized as well as coil 'a' of SV2. SV1 sends pilot pressure to CV1, CV5 and CV6 making PV1 active. Coil 'a' of SV2 sends pilot pressure to VA1 and VA2, causing them to close. Regions C and D are thus isolated from region B and A. PV1 now control the position of the main poppet. PV1 in conjunction with the LVDT can be programmed to close at a desired rate, hold position or re-open.

For modeling and analysis purposes, the most important data to handle is the throttling of the main valve and its dynamics. As such, the main poppet is modeled as a variable throttling valve, to be controlled by a control structure to be elaborated in the coming sections.

Other components, RV1, RV2, and RV3 are used during a re-opening of the valve. However, because this process is out of the project scope, the principle of work of these components is not further explained.

The pressure drop/flow characteristic for the main valve is shown below. The OLMSTED 80 mm valve is used in the simulation model.

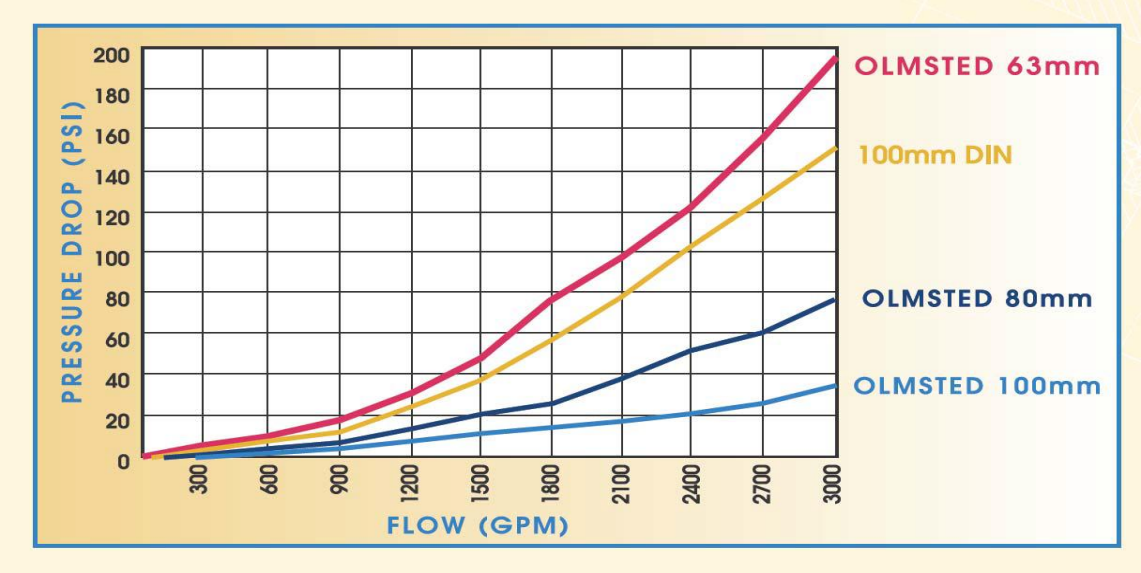

Figure 17: - Characteristics for the OLMSTED 80 mm valve.

5.7 SUMMARY OF CONSTITUTIVE AND CONTINUITY EQUATIONS FOR A TENSIONER UNIT

Because the principle of work of both tensioners within the unit is the same, here the modeling of one tensioner is considered only. According to figure 18, all flow restrictions in the piping are modeled by restrictors R1, R2 and R3 (including both straight pipe length, shut off manual valves as well as 90 degree standard bends), and orifice 2, restrictions due to pressure drop in air pressure control valve.

The pressure drops across the anti-recoil valve is modelled as a variable throttle valve with the note that throttling action will be initiated during a wire break and a riser emergency disconnection only, which means that duringa a normal operation, the valve will be fully open.

The modeling of other constitutive elements in the unit is already discussed in the previous sections.

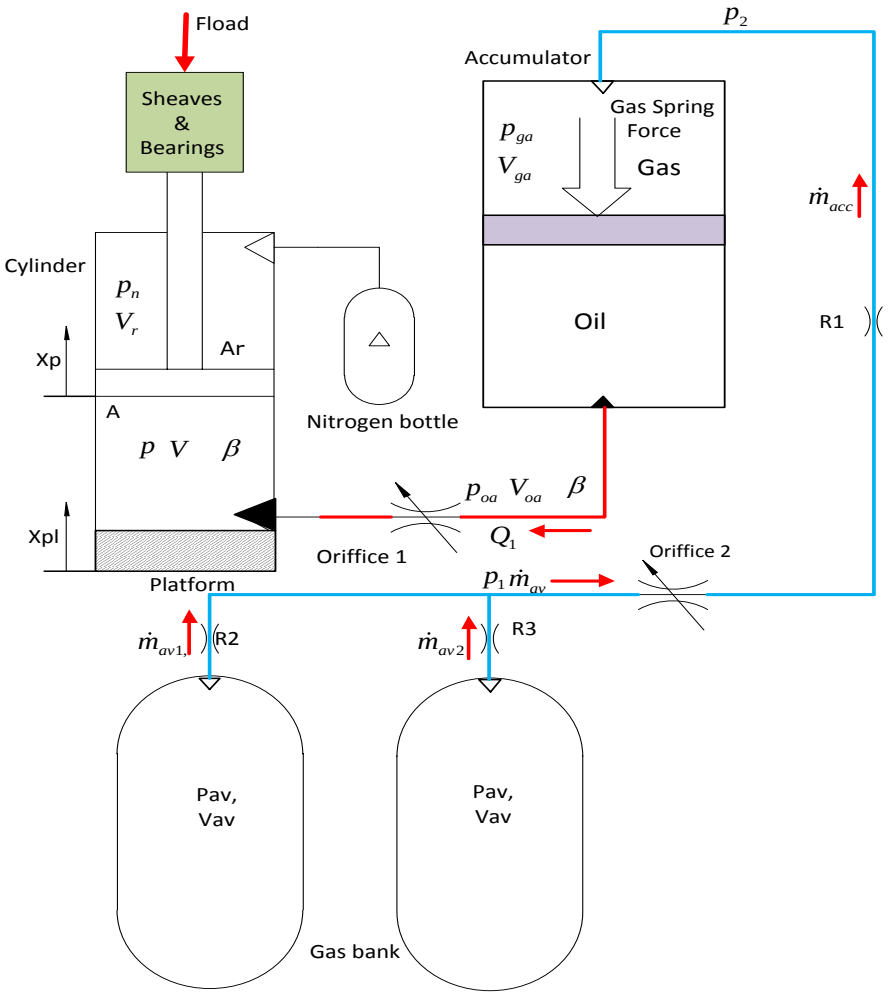

Fig 18: -A 2D layout of a tensioner unit.

For the sake of simplicity, we would denote pressure drop, $dp = p_1 - p_2$, as a sum of pressure drops due to a flow resistance in the manual shut off valves, R2 and R3, pressure drop due to the geometry of the pipe and 90 degree standard bends(8 pcs.) altogether, as well as pressure drop in the air pressure control valve, here indicated by an orifice 2.

The flow continuity equations and pressure build up equations for each pressure node are given as:

p_1:

$$\begin{aligned} \dot{m}_{av1} + \dot{m}_{av2} &= \dot{m}_{av}, \\ \dot{m}_{av1} &= \dot{m}_{av2}, \\ \dot{m}_{av} &= 2\dot{m}_{av2} \end{aligned} \tag{5.39}$$

$$\dot{m}_{av} = 2Ap_{av}\sqrt{\frac{2}{RT_{av}}}\sqrt{\frac{n}{n-1}}\sqrt{\left(\frac{p_1}{p_{av}}\right)^{2/n} - \left(\frac{p_1}{p_{av}}\right)^{(n+1)/n}} \tag{5.40}$$

$$\dot{T}_{av} = \frac{T_{av}\dot{V}_{av}}{V_{av}} + \frac{T_{av}\dot{p}_{av}}{p_{av}} - \frac{nT_{av}{}^2\dot{m}}{p_{av}V_{av}} \tag{5.41}$$

$$\dot{p}_{av} = \frac{1}{V_{av}}\left(-n_1\dot{m}RT_{av} - np_{av}\dot{V}_{av}\right) \tag{5.42}$$

Provided that a polytrophic constants near the nozzle outlet and the chamber are equal to the adiabatic constant, k, then equation (5.41) could be written as:

$$\dot{p}_{av} = \frac{k}{V_{av}}\left(-\dot{m}RT_{av} - p_{av}\dot{V}_{av}\right) \tag{5.43}$$

Note that an expression for a mass flow rate was derived under assumption of sonic flow conditions.

p_2:

$$\dot{m}_{av} = \dot{m}_{acc} \tag{5.44}$$

$$\dot{p}_{ga} = \frac{1}{V_{tg} + A_{ps}\left(0.5x_{stroke} \pm x_{pa}\right)}\left(k\dot{m}RT_1 \mp kp_{ga}A_{ps}\dot{x}_{pa}\right) \tag{5.45}$$

For a small pressure drop in the accumulator nozzle, the following expression is valid:

$$\dot{p}_2 = \dot{p}_{ga} \tag{5.46}$$

The pressure drops due to straight pipe length geometry, and all fittings mounted in the pipe connecting the pressure vessel and accumulator is given as:

$$\frac{p_2^2 - p_1^2}{2p_1} + \frac{\lambda L_{total} \rho_1 w_1^2}{2D}\left(\frac{T_1 + T_2}{2T_1}\right) = 0 \tag{5.47}$$

Where, $L_{total} = L_{straight\_length} + L_{fittings}$. The flow restriction due to the geometry of fittings (bends and manual valves) is given as

$$L_{fittings} = nFD \tag{5.48}$$

Here, n is nr of fittings, F is a multiplying coefficient, and D is the smallest fitting diameter in the pipe.

p_{oa}:

$$\dot{p}_{oa} = \frac{\beta(\mp Q_1 \pm \dot{V}_{oa})}{V_{oa}} \tag{5.49}$$

$$Q_1 = C_d A_d \sqrt{\frac{2}{\rho}\left(p_{oa} - p\right)} \tag{5.50}$$

p:

$$\dot{p} = \frac{\beta}{V}\left(\pm Q_1 - Q_{li} \mp A\dot{x}_p\right) \tag{5.51}$$

p_n:

$$\dot{p}_n = \frac{n}{V_r}\left(-\dot{m}_r R T_r + p_n \dot{V}_r\right) \tag{5.52}$$

Calculation of the air spring stiffness

The variation of the wire force acted upon the riser is determined by the pressure of the compressed air in the gas part of the accumulator. The whole system comprising of the accumulator, gas bank and the high pressure of the cylinder chamber, may be considered as an ideal gas spring whose stiffness needs to be calculated in order to accurately compute wire force magnitude variations due to a heave motion.

An expression for the stiffness of this spring when the platform heaves up is deduced in the following:

Initially, it is assumed that a piston in the cylinder is positioned in its midstroke. As a result, the corresponding gas volume in the accumulator is given by:

$$V_{ga} = V_{ga0} + Ax_p \tag{5.53}$$

Provided that the gas obeys the adiabatic changes (n=1.4), the following expression is yielded:

$$p_{ga}(V_{ga0} + Ax_p)^n = p_{ga0}{V_{ga0}}^n \tag{5.54}$$

In a steady state, the wire force, which is equal to the sum of 4 wire forces, is in equilibrium with the hydraulic and pneumatic pressure forces.

Then, the equation of the piston in the cylinder is expressed (the friction phenomenon is neglected) in the following:

$$\begin{aligned} &F_p = pA - p_n A_r + m_{eff} g \\ &F_p - F_l = m_{eff} \ddot{x}_p = 0 \rightarrow \\ &F_p = F_l \\ &F_l = F_{wire-line} \end{aligned} \tag{5.55}$$

In an equilibrium state, pressure in the gas-chamber of the accumulator, p_{ga} is equal to the hydraulic pressure exerted on the piston

$$p_{ga} = p \tag{5.56}$$

Then, the following expression is valid

$$F_p + p_n A_r - m_{eff} g = p_{ga} A = \frac{p_{ga0}(V_{ga0} + V_{av})^n}{(V_{ga0} + V_{av}) + Ax_p)^n} A \quad (5.57)$$

The equivalent spring stiffness, k is

$$k = \frac{d(F_p)}{dx_p} = \frac{nA^2(V_{ga0} + V_{av})^n}{(V_{ga0} + V_{av} + Ax_p)^{n+1}} p_{ga0} \quad (5.58)$$

Where,

k= Equivalent stiffness, $\left[\frac{N}{m}\right]$

$V_{ga0} + V_{av}$ = Initial gas volume including both accumulator and gas bank volume, [m^3]

F_p =Piston force, [N]

$F_{wire-line}$ =wire line force, [N]

m_{eff} = mass of the piston including mass of the sheaves, bearings, shaft and a bracket, [kg]

The above expressions show that the spring stiffness increases with the piston displacement moving up and vice versa. The smaller size accumulator presents greater stiffness due to the rapid increase of oil volume in the accumulator.

The pressure in the low pressure chamber of the hydraulic cylinder, p_n is regulated to the value which will cause the piston to stroke and reach the equilibrium with the suspended riser load, after retracting the riser to an elevated position above the well head equipment should the emergency disconnection of the riser occur. In addition, this level of the pressure should be enough to prevent any possible collision of the telescoping joint with the rotary table.

The required volume and pressure in the nitrogen bottle may be determined by applying the same adiabatic relation as per above-described approach.

Therefore, by applying the same steps, the stiffness of the gas spring in the nitrogen bottle is described by the following expression:

$$k_n = \frac{A_r^2 * n * p_n}{V_r} \tag{5.59}$$

where,

V_r = total gas volume in the low pressure cylinder chamber including volume of the nitrogen bottle, [m^3]

p_n = pressure in the nitrogen bottle, [Pa] (abs)

n = 1.4 for an adiabatic process

The stiffness of a chamber therefore increases with a larger piston, higher pressure, shorter stroke or a larger value of the polytrophic index, n.

5.8 MODELING OF A MECHANICAL SYSTEM

In figure 19, a mechanical layout for one tensioner unit is shown.

One tensioner unit can be represented as shown, consisting of 5 sheaves and 6 wire-sections. In addition, the cylinder piston will provide a translational motion parallel to four of the wire-forces. The total length of wire in a tensioner unit is 60,471m with a wire diameter of 64 mm. we have assumed a fill factor to be 0, 57 [9]. The following formulas will be implemented into the 1D system for calculating the forces applied to the pistons in the tensioner units.

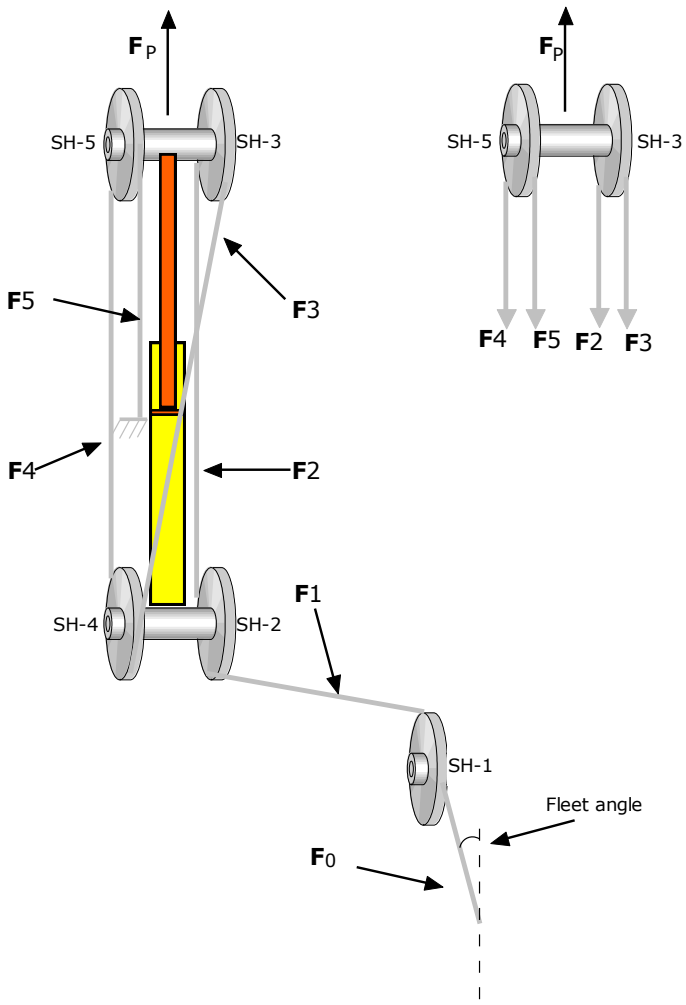

Figure 19: -A mechanical layout for one tensioner.

The wire line tension force due to elongation of a wire is given by the equation:

$$F = kw \cdot x \tag{5.60}$$

However, because the wire line works only in tension, it is assumed that the elongation 'x' will be positive.

The wire line stiffness, kw is derived through the formula:

$$kw = \frac{E \cdot A}{L} \cdot ff \tag{5.61}$$

where,

E = Young's modulus for this steel-wire – $210 \cdot 10^9$ [GPa]

A= Area of the wire [m^2]

L = length of the wire [m]

ff = Fill factor.

If the above parameters are plugged in the equation (5.61), the following value for the wire line stiffness is obtained:

$$kw = \frac{210 \cdot 10^9 \cdot \pi \cdot 0,32^2}{60,471} \cdot 0,57 = 636790871,67 \frac{N}{m} \tag{5.62}$$

The initial static wire line deflection δ_{static} is caused by a riser pulling force applied by a tensioner in its mid-stroke piston position. It is understood, that this force is evenly distributed along a number of wire rope-sections (as much as six wire rope sections). We are assuming that the wire rope length is equally described between the different sections.

$$\delta_{static} = \frac{F_{vertical}}{6 \cdot kw} \tag{5.63}$$

Where, $F_{vertical}$ denotes the tensioning force exerted on the tensioner ring by a wire line for a small fleet angle.

In figure 20, the kinematic relations for all sheaves are shown. For the modeling purposes, the wire rope in a particular section is modeled as a spring and damper (not shown in the figure). The wire elongation is the displacement difference between end points located in two adjacent sheaves.

Elongation of the wire section 5: $\delta_{static} + x_p - \varphi_5 r_{sh}$

Elongation of the wire section 4: $\delta_{static} + x_p + \varphi_5 r_{sh} - \varphi_4 r_{sh}$

Elongation of the wire section 3: $\delta_{static} + x_p + \varphi_4 r_{sh} - \varphi_3 r_{sh}$

Elongation of the wire section 2: $\delta_{static} + x_p + \varphi_3 r_{sh} - \varphi_2 r_{sh}$

Elongation of the wire section 1: $\delta_{static} + \varphi_1 r_{sh} + \varphi_2 r_{sh}$

Elongation of the wire section 0: $\delta_{static} - \varphi_1 r_{sh}$

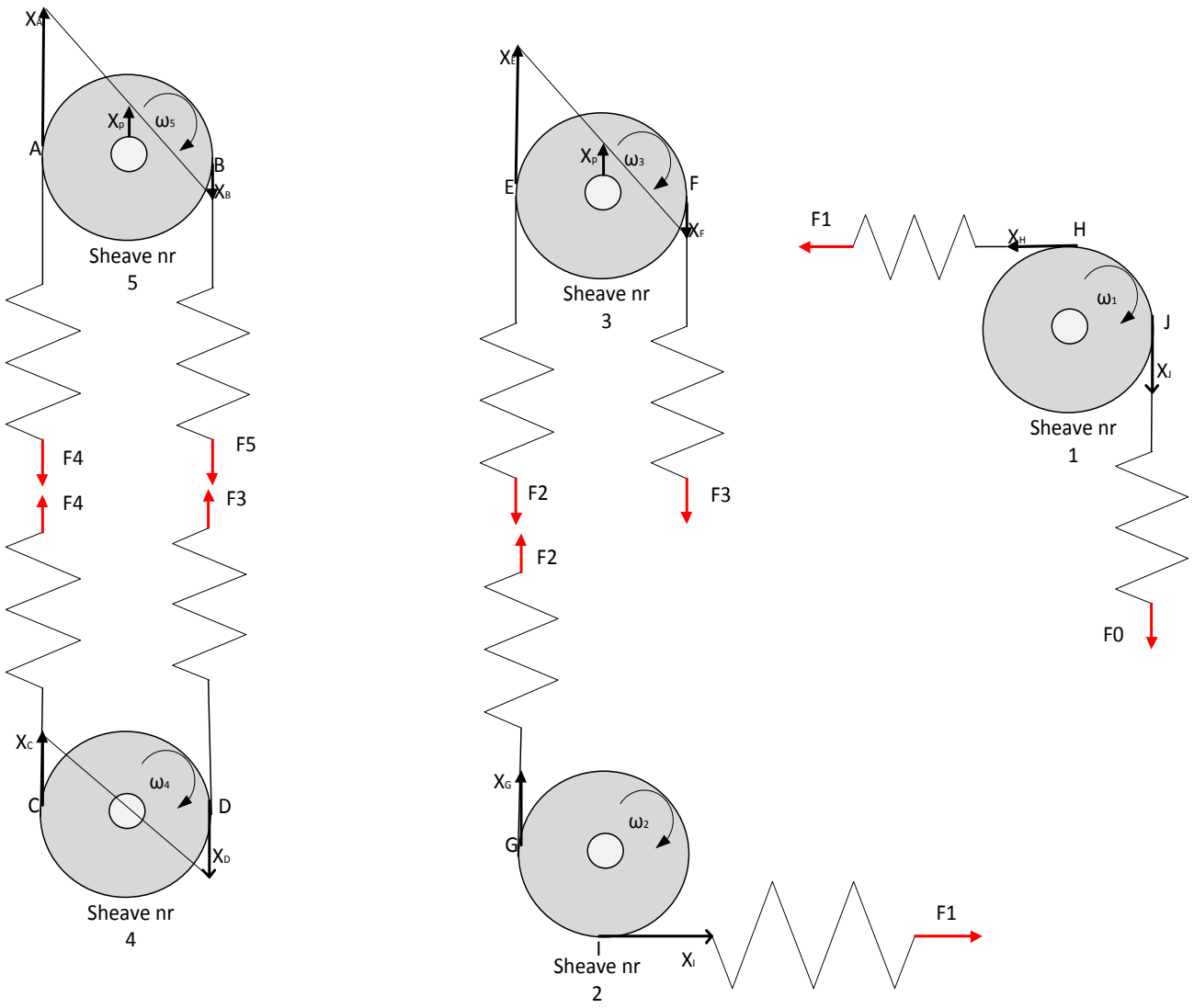

Figure 20: - The kinematic relations for all sheaves.

The forces in the different wire-sections become:

$$F_0 = kw\left(\delta_{\text{static}} - \varphi_1 r_{\text{sh}}\right) + d\left(-\dot{\varphi}_1 r_{\text{sh}}\right) \tag{5.64}$$

$$F_1 = kw\left(\delta_{\text{static}} + \varphi_1 r_{\text{sh}} + \varphi_2 r_{\text{sh}}\right) + d\left(\dot{\varphi}_1 r_{\text{sh}} + \dot{\varphi}_2 r_{\text{sh}}\right) \tag{5.65}$$

$$F_2 = kw\left(\delta_{\text{static}} + \mathrm{x}_{\text{p}} + \varphi_3 r_{\text{sh}} - \varphi_2 r_{\text{sh}}\right) + d\left(\dot{\varphi}_3 r_{\text{sh}} - \dot{\varphi}_2 r_{\text{sh}} + \dot{\mathrm{x}}_{\text{p}}\right) \tag{5.66}$$

$$F_3 = kw\left(\delta_{\text{static}} + \mathrm{x}_{\text{p}} + \varphi_4 r_{\text{sh}} - \varphi_3 r_{\text{sh}}\right) + d\left(\dot{\varphi}_4 r_{\text{sh}} - \dot{\varphi}_3 r_{\text{sh}} + \dot{\mathrm{x}}_{\text{p}}\right) \tag{5.67}$$

$$F_4 = kw\left(\delta_{\text{static}} + \mathrm{x}_{\text{p}} + \varphi_5 r_{\text{sh}} - \varphi_4 r_{\text{sh}}\right) + d\left(\dot{\varphi}_5 r_{\text{sh}} - \dot{\varphi}_4 r_{\text{sh}} + \dot{\mathrm{x}}_{\text{p}}\right) \tag{5.68}$$

$$F_5 = kw\left(\delta_{static} + x_p - \varphi_5 r_{sh}\right) + d\left(-\dot{\varphi}_5 r_{sh} + \dot{x}_p\right) \quad (5.69)$$

Where,

φ = Rotational angle [rad]

r_{sh} = Sheaves outer radius [m]

kw = Wire stiffness $\left[\frac{N}{m}\right]$

$d = 0.1k_w$ Damping factor $\left[\frac{Ns}{m}\right]$

δ_{static} = Initial wire deflection [m]

x_p = Piston travel from initial position [m]

The positive direction for rotation is defined as clockwise.

The torques applied to the different sheaves is given by the following formulas:

$$T_{sh1} = (F_0 - F_1) \cdot r_{sh} \quad (5.70)$$

$$T_{sh2} = (F_2 - F_1) \cdot r_{sh} \quad (5.71)$$

$$T_{sh3} = (F_3 - F_2) \cdot r_{sh} \quad (5.72)$$

$$T_{sh4} = (F_4 - F_3) \cdot r_{sh} \quad (5.73)$$

$$T_{sh5} = (F_5 - F_4) \cdot r_{sh} \quad (5.74)$$

However, the above formula will not hold provided the friction phenomenon is to be considered.

The sheave and a wire system will experience a power loss because of a friction due to a bending resistance as wire passes the outer peripheral surface of the pulley, and a friction caused due to a relative motion of the pulley with respect to bearing pin. The latter friction is insignificant compared to the bending wire resistance. Because it is assumed that friction phenomena will play a greater impact in the behavior of the system parameters, a power loss in the range of 0 to 4 % per sheave is further considered.

Modeling-wise, in order to implement this requirement into the formulas with respect to the torques in the sheaves we can apply the following reasoning. It will be shown for sheave nr. 5:

$$T_{stiction} = \left(F_5 - F_4\right) \cdot \mathrm{r_{sh}} = \mu \cdot F_5 \cdot \mathrm{r_{sh}} = K\left(F_5 + F_4\right) \tag{5.75}$$

Where, $R = F_4 + F_5$ is the normal force in the pin of the sheave, μ is the percent loss due to friction, and K is a constant. For μ=0.02, then:

$$0{,}02 \cdot F_5 \cdot \mathrm{r_{sh}} = K \cdot (F_5 + F_4) \tag{5.76}$$

For $F_5 \approx F_4$, the equation (5.76) becomes

$$\mathrm{k} = 0{,}01 \cdot \mathrm{r_{sh}} \tag{5.77}$$

Hence, the stiction torque in the sheave becomes

$$T_{stiction5} = 0{,}01 \cdot 0{,}91 \cdot (F_5 + F_4) \tag{5.78}$$

The slipping torque is assigned a value at half of $T_{stiction}$.

$$T_{slipping5} = \frac{0{,}01 \cdot 0{,}91}{2} \cdot (F_5 + F_4) \tag{5.79}$$

As a result, the final equations for the torque in the sheaves will depend on the state of the sheave. Consequently, provided that applied torque is less than a sticking torque, the sheave will stand still ($\dot{\varphi}_5 = 0$). In this state, the applied torque will be invested to overcome the initial static friction, only.

However, if the applied torque is greater than a sticking torque, the friction contact is in slipping mode (the sheave rotation is initiated) and the following expressions for a sheaves acceleration torque will become valid:

$$\mathrm{T_{ash1}} = (F_0 - F_1) \cdot \mathrm{r_{sh}} + \mathrm{T_{slipping1}} \tag{5.80}$$

$$\mathrm{T_{ash2}} = (F_2 - F_1) \cdot \mathrm{r_{sh}} + \mathrm{T_{slipping2}} \tag{5.81}$$

$$\mathrm{T_{ash3}} = (F_3 - F_2) \cdot \mathrm{r_{sh}} + \mathrm{T_{slipping3}} \tag{5.82}$$

$$\mathrm{T_{ash4}} = (F_4 - F_3) \cdot \mathrm{r_{sh}} + \mathrm{T_{slipping4}} \tag{5.83}$$

$$\mathrm{T_{ash5}} = (F_5 - F_4) \cdot \mathrm{r_{sh}} + \mathrm{T_{slipping5}} \tag{5.84}$$

The formula for $\mathrm{T_{slipping1}}$ through $\mathrm{T_{slipping4}}$ is computed in the similar manner as provided with equation (5.79).

The acceleration torque in the sheave is given as:

$$T_{ash} = I_{sh}\ddot{\varphi} \tag{5.85}$$

The moment of inertia for a sheave is:

$$I_{sh} = \frac{1}{2} \cdot m \cdot (r^2{}_{sh} - r^2{}_{sh-inner})$$

However, because $r_{sh} \gg r_{sh-inner}$ and the fact that the pin is fitted into the sheave, it is reasonable to consider sheave as a solid body and hence we are permitted to utilize the approximation:

$$I_{sh} \approx \frac{1}{2} \cdot m \cdot r_{sh}{}^2 \tag{5.86}$$

The mass of the sheaves is given as 2920 kg, which gives the inertia of 1221 kgm^2.

5.9 CALCULATION OF THE TENSION FORCE

A minimum tension setting is required to ensure the stability of the riser, and to avoid buckling[8]. The tension setting should be sufficiently high so that the effective tension is always positive in all parts of the riser, even if a tensioner should fail. In most cases the minimum effective tension is encountered at the bottom of the riser.

The minimum top tension, T_{min} **,** is determined by:

$$T_{min} = \frac{T_{TRmin} \cdot N}{R_f(N-n)} \tag{5.87}$$

where,

T_{TRmin} = Minimum tensioner ring tension = $W_b \cdot f_{wt} - B_n \cdot f_{bt} + A_i(d_m \cdot H_m - d_w \cdot H_w)$

and

W_b = Submerged riser weight above the point of consideration.

F_{wt} = Submerged weight tolerance factor (minimum value = 1.05 unless accurately weighed).

B_n = Net lift of buoyancy material above the point of consideration.

F_{bt} = Buoyancy loss and tolerance factor resulting from elastic compression, long term water absorption, and manufacturing tolerance. (Maximum value = 0.96 unless accurately known by submerged weighing under compression at rated depth).

A_i = Internal cross sectional area of riser including choke, kill and auxiliary fluid lines.

d_m= Drilling fluid weight density.

H_m = Drilling fluid column to point of consideration.

D_w = Sea water weight density.

H_w = Sea water column to point of consideration.

N = Number of tensioners supporting the riser

n = Number of tensioners subject to sudden failure

R_f = Reduction factor relating vertical tension at the tensioner ring to tensioner setting to account for fleet angle and mechanical efficiency (usually 0.9 - 0.95) for a DAT system.

We will be using the following parameters in order to exemplify the calculation of a minimum tension setting:

Length of marine riser: 3000 m.

Diameter of marine riser: 0,9 m.

Mass of marine riser: 680000 kg.

Mass of tensioner ring: 19900 kg.

Density of drilling fluid: 1,44 (12 ppg drill fluid).

100 x 15 m sections of joints with buoyancy 4191 kg pr. section.

100 x 15 m sections of joints without buoyancy.

Mass of piston and rod: 2450 kg.

Mass of sheaves, bearings, shafts, sheave brackets etc: 2*2950 kg.

T_{TRmin} can then be calculated as follows:

$$\left(\begin{array}{l} \left(680000kg + 19000kg\right) \cdot 1,05 - 419100kg \cdot 0,96 \\ + \left(\frac{0,9m}{2} \right)^2 \cdot \left(1444 \frac{kg}{m^3} * 3000m - 1030 \frac{kg}{m^3} \cdot 3000m \right) \end{array} \right) \cdot 9,8 \frac{m}{s^2} = 10919,181kN \qquad (5.88)$$

$$T_{min} = \frac{10919,181 \cdot 16}{0,95(16-2)} = 13135,857kN \qquad (5.89)$$

The minimum tension (T_{min}) as calculated and referred to represents the sum of the upward forces exerted on the tensioner ring which should be generated by all 16 tensioners measured parallel to the stroke path of each piston.

$$T_{min} = \left(\frac{1}{4} \cdot F_p \cdot N \right) \qquad (5.90)$$

Rearranging equation (5.90), we get the piston force per tensioner:

$$F_p = \frac{4 \cdot T_{min}}{N} = \frac{4 \cdot 13135,857kN}{16} = 3280,4kN \qquad (5.91)$$

The piston force to be provided is found by the following formula:

$$F_p = pA_p - p_n A_r = m_{eff} \ddot{x}_p + b\dot{x}_p + m_{eff} g + F_f + F_l \qquad (5.92)$$

Therefore, the pressure difference on both sides of piston should create enough force in order to be able to accelerate the piston, overcome both hydrodynamic and a dry friction, as well as the gravity and load force.

Because the capacity of a tensioner is determined by the weight of the marine riser as well as a number of safety factors, it is important design-wise that we don't exceed the maximum allowed capacity of the tensioner as the weight of the riser is increased. However, non-violation of the functional constraints such is the capacity of a tensioner (3500 kN) for different load-case scenarios is not of importance for the analysis to be performed. However, whenever these violations occur an explanation is provided.

6 VALIDATING A SIMULATION X MODEL

Because the validation and verification of a riser tensioner system was not feasible to perform in a real system by means of experiments, we will use the mathematical modeling equations derived in chapter 5 to validate the virtual model in simulationX. If results agree with expected values of the state variables we conclude the simulation model is consistent and sound.

Initially, we have to compute the initial state variables for a system in a steady state under the assumption that the piston is positioned at mid-stroke.

Table 3: -Nominal input data-the main system parameters.

Parameters/components	***Gas bank***	***Hydraulic-pneumatic Cylinder***	***Accumulator***	***Riser***	***Pneumatic piping***
Volume[m^3]	*3.2*	*-Dead volume at oil side-0.005 -Dead volume at gas side -0*	*-Dead volume a oil side-0.01 -Dead volume a gas side -0.035*	*-*	*-*
Maximum stroke [m]	*-*	*4*	*3.626*	*-*	*-*
Piston/rod diameter [m]	*-*	*0.47/0.4*	*0.53/0*	*-*	*-*
Mass of the piston [kg]	*-*	*2450*	*253*	*-*	*-*
Mass of the riser+tensioner ring [kg]	*-*	*-*	*-*	*680000+ 19900*	*-*
Length of the riser [m]	*-*	*-*	*-*	*3000*	*-*
Internal diameter of the riser [m]	*-*	*-*	*-*	*0.49*	*-*
External diameter of the riser [m]	*-*	*-*	*-*	*0.55*	*-*
Piping length [m]	*-*	*-*	*-*	*-*	*35*
Piping diameter [inch]	*-*	*-*	*-*	*-*	*3*
Nr of fittings per pipe [pcs]	*-*	*-*	*-*	*-*	*8*

Table 4: -Computed system parameters.

Parameter	Value	Equation used
Initial static wire elongation [m]	*0.0012*	$\delta_{static} = \frac{F_{pmid-stroke}}{4 \cdot kw}$ *(1.1)*
Wire stiffness [N/m]	636790871,6	$kw = \frac{E \cdot A}{L} \cdot ff$ *(1.2)*
Sheave inertia [kgm^2]	*1221*	$I_{sh} \approx \frac{1}{2} \cdot m \cdot r_{sh}^{\ 2}$ *(1.3)*
Piston side area –hydraulic-pneumatic cylinder [m^2]	*0.173*	$A = \frac{\pi d_{pc}^2}{4}$ *(1.4)*
Rod side area – hydraulic-pneumatic cylinder [m^2]	*0.169*	$A_r = \frac{\pi}{4}\left(d_{pc}^2 - d_{rc}^2\right)$ *(1.5)*
Piston area –accumulator [m^2]	*0.22*	$A_a = \frac{\pi d_{pa}^2}{4}$ (1.6)
Riser tensioning force at mid-stroke piston position [kN]	13135,857	$T_{mid-stroke} = \frac{T_{TRmin} \cdot N}{R_f(N-n)}$ *(5.87)*
Piston tensioner force at mid-stroke piston position [kN]	3280,4	$F_{pmid-stroke} = \frac{4 \cdot T_{mid-stroke}}{N}$ (1.7)

Calculation of the initial state variables at mid-stroke piston position

In order for simX to compute the system state variables at any instant of time, the program requires the initial state variable inputs to be inserted for each component. Some values are assumed, whereas the others need to be computed for a system in equilibrium based on the equations derived in the preceding chapter.

Table 5 shows the initial assumed and those variables that need to be calculated in order to define the initial system operating conditions.

Table 5: - List of state variables that needs to be initialized.

State variables	Accumulator	Gas bank	Hydraulic-pneumatic Cylinder	Sheaves
Pressure [bar]	*For gas side:* p_{ga0} *=190* *For oil side:* p_{oa0} *=190*	p_{av0} *=190*	*For gas side:* $p_{n0}=5$ *For oil side:* $p_0=190$	-
Temperature [K]	$T_{ga0}=293.15$	$T_{av0}=293.15$	$T_{n0}=293.15$	-
Piston displacement [m]	$x_{pa}=0$	-	$x_p=0$	-
Piston velocity [m/s]	$\dot{x}_{pa}=0$	-	$\dot{x}_p=0$	-
Sheave angle of rotation [rad]	-	-	-	$\varphi_1=0$ $\varphi_2=0$ $\varphi_3=0$ $\varphi_4=0$ $\varphi_5=0$
Sheave rotational speed [m/s]	-	-	-	$\dot{\varphi}_1=0$ $\dot{\varphi}_2=0$ $\dot{\varphi}_3=0$ $\dot{\varphi}_4=0$ $\dot{\varphi}_5=0$

We will demonstrate the steps for calculation of the initial system pressure by using equation (5.57) as follows:

$$F_{piston}+p_nA_r-m_{eff}g=\frac{p_{ga0}(V_{ga0}+V_{av})^n}{(V_{ga0}+V_{av}+Ax_p)^n}A\Rightarrow$$

$$p_{ga0}=\frac{(F_{piston}+p_nA_r-m_{eff}g)(V_{ga0}+V_{av}+Ax_p)^n}{(V_{ga0}+V_{av})^nA}=\frac{(3280.4\cdot10^3+5\cdot10^5\cdot0.169-8350\cdot9.81)*(4+0)^{1.4}}{4^{1.4}*0.173}$$

$$=189.78bar\approx190bar$$

In a steady-state, the pressure value in the gas side of the accumulator is equal with a pressure value in the oil side of the hydraulic-pneumatic cylinder, $p_{ga0} = p_0 = 190[bar]$ which has been inserted as an initial value into the simX hydraulic-pneumatic cylinder library element.

In order to verify whether we have a consistent model, we will use equation 5.58 for a gas spring stiffness to compute the variation of the piston force (thereby forces on the wires) in its extreme end positions.

For maximum heave amplitude of ± 4.8 meters, according to a mechanical advantage of 1:4 the piston shall be displaced by as much as ∓ 1.2 meters.

The gas spring stiffness is then,

-for $x_p = +1.2$ [m] and $x_{pl} = -4.8$ [m]

$$k = \frac{nA^2(V_{ga0} + V_{av})^n}{(V_{ga0} + V_{av} - Ax_p)^{n+1}} p_0 = \frac{1.4 \cdot 0.173^2 \cdot 4^{1.4}}{(4 - 0.173 1.2)^{2.4}} 190 \cdot 10^5 = 226185.05 N/m$$

Therefore the piston force due to a piston expansion of 1.2 [m] is:

$$F_p = F_{pmid-stroke} - kx_{piston} = 3280.4 \cdot 1000 - 226185.05 \cdot 1.2$$
$$= 3008.9 kN$$

- for $x_p = -1.2$ [m] and $x_{pl} = +4.8$ [m]

$$k = \frac{nA^2(V_{ga0} + V_{av})^n}{(V_{ga0} + V_{av} + Ax_p)^{n+1}} p_0 = \frac{1.4 \cdot 0.173^2 \cdot 4^{1.4}}{(4 + 0.173 1.2)^{2.4}} 190 \cdot 10^5 = 176268.7 N/m$$

Hence, for a piston retraction of 1.2 [m], the piston force will be

$$F_p = F_{pmid-stroke} + kx_p = 3280.4 \cdot 1000 + 176268.7 \cdot 1.2$$
$$= 3491497.7 N = 3491.92 kN$$

These values have a high degree of consistency with the piston force at two extreme piston positions in the simulation model as shown in the graph below.

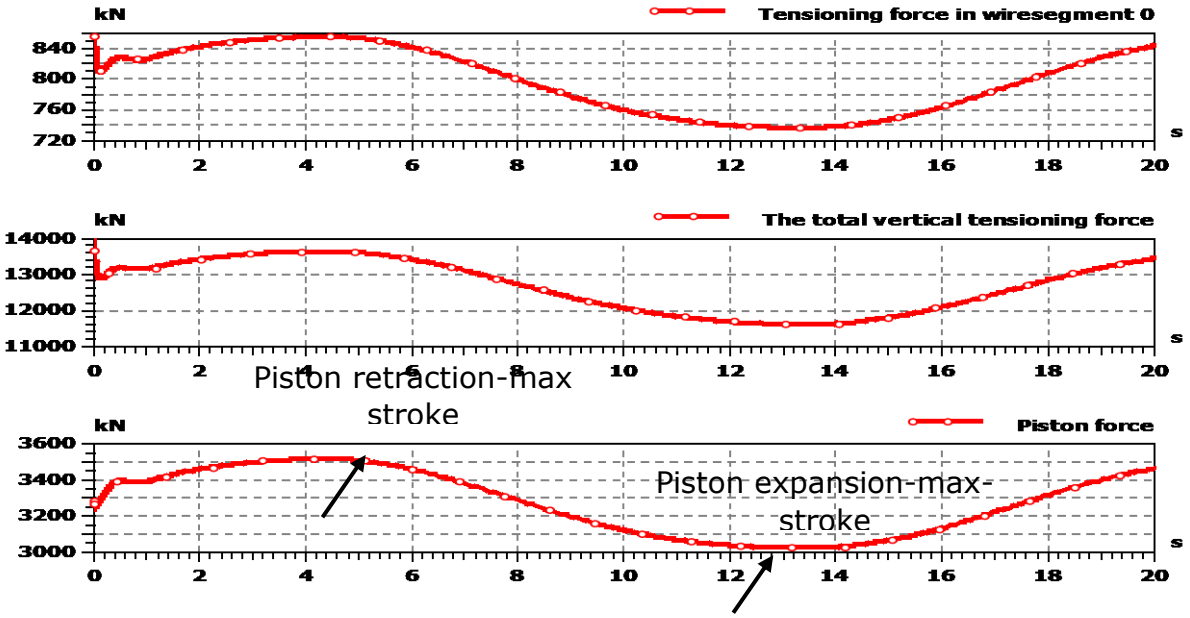

Figure 21: - Piston force variation in the hydraulic-pneumatic cylinder. The upper two graphs show the variation of the wire force in segment 0 and the vertical tensioning force in the riser.

Calculation of the friction force in the hydraulic-pneumatic cylinder

The friction in the sheaves is modeled as explained in chapter 5. For the tensioner cylinders and the accumulators we will be using a Stribeck model when implementing the friction into the model given by equation 5.31 chapter 5:

$$F_{fr,v} = F_c + \left(\left(F_s - F_c \right) \exp\left(-\frac{|v_{piston}|}{v_l} \right) \right) + k_v |v_{piston}|^{a_v}$$

$$F_{fr,p} = k_p p_{\max} = F_s$$

$$F_{fr} = F_{fr,v} + F_{fr,p}$$

The pressure drop due to friction is considered to be 2 bar, which gives a sticking friction of:

$$F_s = p_{drop} \cdot A = 2 \cdot 10^5 \cdot 0{,}173 = 34{,}6kN$$

and a coulomb of $0{,}5 \cdot F_S = 17{,}3\text{kN}$ in a tensioner unit. The respective data for the accumulators are 44,1kN and 22,0kN. The pressure dependency friction is calculated as below:

$$F_{fr,p} = k_p p_{\max} = F_s = 34.6 \cdot 10^3 \Rightarrow$$

$$k_p = \frac{34.6 \cdot 10^3}{190.2 \cdot 10^5} = 0.0018[N/Pa]$$

These values have been inserted in our simulation X model.

Modeling of a riser in SimX- emergency disconnection scenario

In the nominal model, the riser was fixed to a BOP according to a normal operating condition. On the contrary, in an emergency scenario we have to build a model allowing the riser to have a vertical displacement once the riser has been disconnected. In that case, a riser has been modeled according to figure 22.

The model resembles a mass-spring-damper with a two lumped masses, distributed totaling the mass of the riser and the mass of the tensioner ring. Since the mass of the riser is concentrated more on its vertical bottom position, mainly due to a lower marine riser package (as an integral part of the riser), a disproportional distribution of the mass in the ratio 75 % on bottom and 25 % on the upper mass has been applied. It is understood that the more accurate models would require a great number of series connected lump masses.

Applying the second Newton's law for an equilibrium position of two masses, we get:

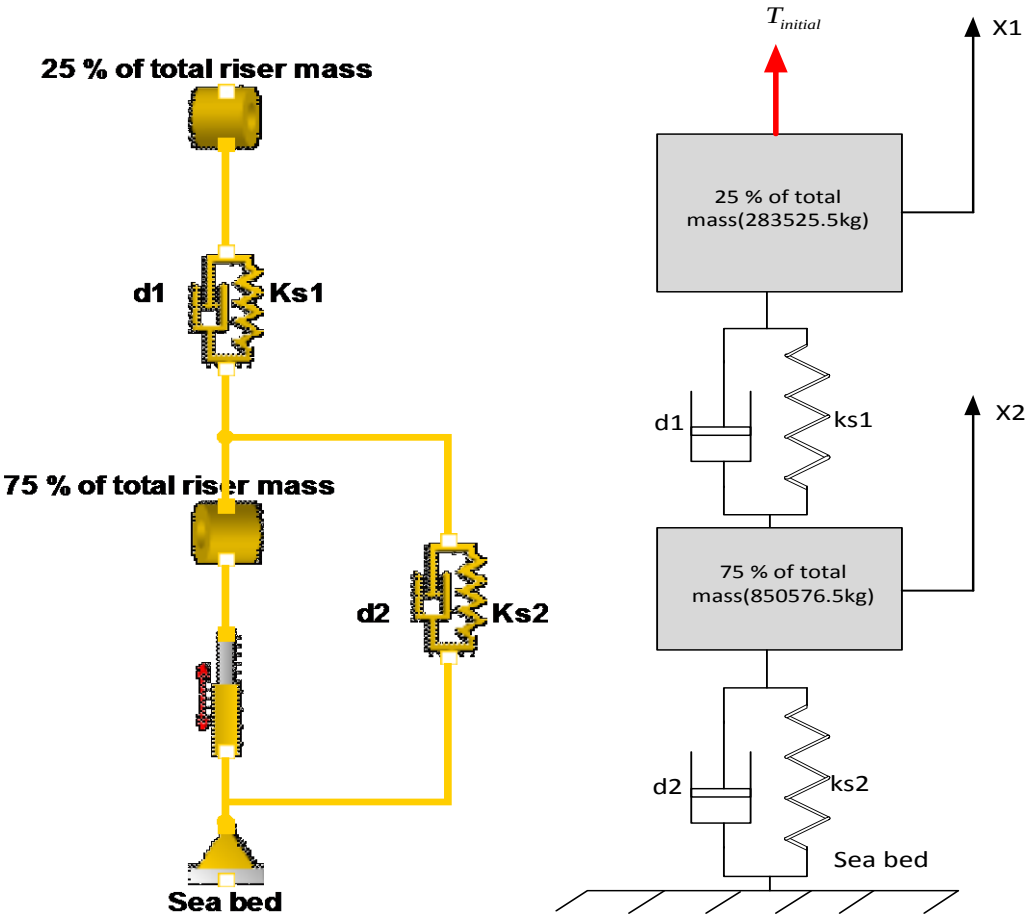

Figure 22: -Modeling a riser as a mass-damper-spring model-emergency disconnection mode.

The equation of equilibrium for the upper mass may be written in scalar form as:

$$T_{initial} - m_1 g - k_{s1}(x_1 - x_2) - d_1(\dot{x}_1 - \dot{x}_2) = 0 \qquad (6.1)$$

where $T_{initial}$ is the initial vertical tensioning force exerted by as much as 16 tensioners (for a midstroke position of the piston cylinder), m_1 is upper lumped mass of the riser and tensioner ring, k_{s1} is the spring stiffness, linearly dependent on modulus of elasticity (E), cross-section area (A), and given by $k_{s1} = \frac{EA}{l_0}$. The displacement of the mass is denoted with x_1, while d_1 is a dampening factor. The equation of the equilibrium for the lower riser mass is given as:

$$d_1\dot{x}_1 - (d_1 + d_2)\dot{x}_2 + k_{s1}x_1 - (k_{s1} + k_{s2})x_2 = m_2 g \tag{6.2}$$

The denotation for factors $d_{2,}k_{s2}$ is the same as described above, and m_2 is the bottom lumped mass of the riser and tensioner ring. In a steady–state, damping factors cancel out and hence we get the following equations:

$$\begin{aligned} k_{s1}(x_1 - x_2) &= T_{initial} - m_1 g \\ k_{s1}x_1 - (k_{s1} + k_{s2})x_2 &= m_2 g \end{aligned} \tag{6.3}$$

Solving this system of equations for initial displacements (and hence initial static elongation of the springs) gives:

$$\begin{aligned} x_1 &= \frac{m_2 g + (k_{s1} + k_{s2})x_2}{k_{s1}} \\ x_2 &= x_1 - \frac{(T_{initial} - m_1 g)}{k_{s1}} \end{aligned} \tag{6.4}$$

- *Spring stiffness,* $k_{s1} = \frac{EA}{l_0} = \frac{210*10^9*0.049}{1500} = 6860000\frac{N}{m}$
- *Spring stiffness,* $k_{s2} = \frac{EA}{l_1} = \frac{210*10^9*0.049}{1500} = 6860000\frac{N}{m}$
- *Cross section area of the riser,* $A = 0.049m^2$
- *Length of the riser,* $l = l_0 + l_1 = 1500 + 1500 = 3000m$
- *The upper mass,*
  m_1 *= (mass of the tensioner ring + mass of the riser)*0.25 = (1134102)*0.25= 283525.5kg*
- *The lower mass,*
  $m_2 = 1134102*0.75=850576.5kg$

Finally, the following values are obtained for the preload displacement of the springs:

$$x_1 = 1.63m, x_2 = 0.21m \tag{6.5}$$

These values are then inserted in the SimX model for the emergency disconnection scenario.

Control structure-wire rupture and emergency disconnection scenario

Figure 23 shows a control structure implemented for both a wire rupture and the disconnection scenario. When a wire breaks, the main valve poppet will start to close after a pressure drop of 5 bars in the main valve is reached.

A block denoted as "triggering pressure drop" presents a function of a poppet stroke signal dependent of a pressure drop in the main valve. The valve dynamics is presented via a transfer function block by using the following equations:

$$\tau^2 \ddot{y}_{rel} + 2D\tau \dot{y}_{rel} + y_{rel} = y_{stroke} \tag{6.6}$$

$$\tau = \frac{1}{2\pi f_0} \tag{6.7}$$

Where, τ is a time constant, f_0 is a natural frequency, D damping ratio (0.8) and y_{stroke} is stroking signal.

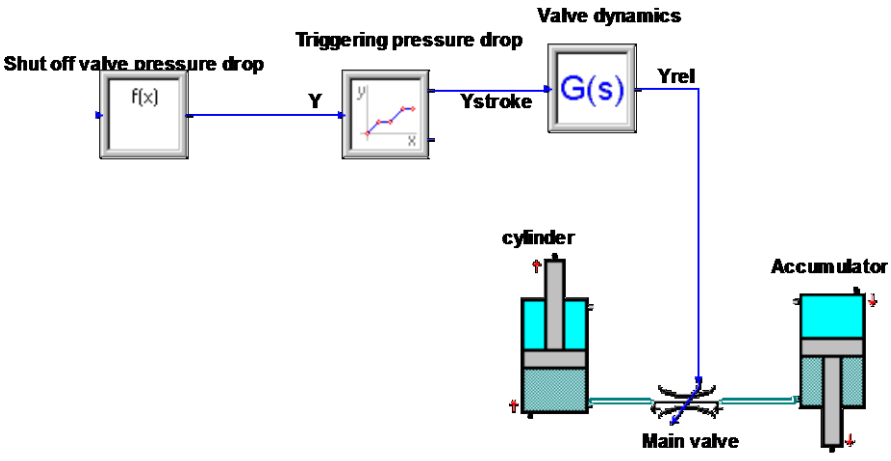

Figure 23: -Block diagram depicting a control structure applied during a wire rupture.

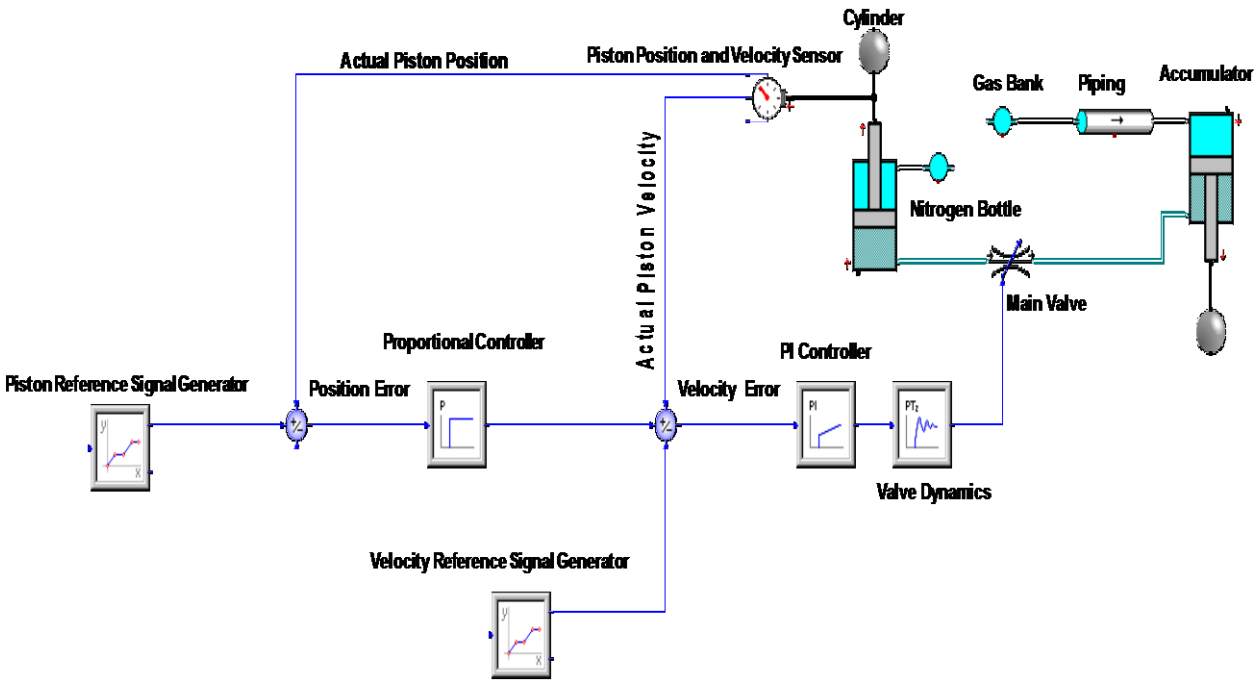

Figure 24: -Block diagram depicting a control structure applied during a disconnection mode.

In the riser disconnection mode, the control objective is to move a hydraulic-pneumatic cylinder piston to an end stop position in a controlled manner, achieving both a desired riser elevation height within a 9 seconds (during this time platform will move up from a minimum to a maximum amplitude), and a zero piston velocity at the instant of contact with end stop.

The control structure consists of an inner loop (velocity loop) and an outer (position loop). The inner loop is controlled by a PI controller, and the outer loop is controlled by a P controller only. The inner loop should have a faster dynamic response compared to the outer loop.

The piston reference position and a velocity signal is designed via a polynomial function, which coefficients are defined by boundary conditions (speed of the piston should be zero at time =9 seconds while the piston has reached the end stop), and are given by the following equation:

Piston position reference signal:

$$REFx_p = \frac{37}{492075}t^5 - \frac{37}{21870}t^4 + \frac{37}{3645}t^3 + 3.26 \qquad (6.8)$$

Piston velocity reference signal:

$$REFv_p = \frac{37t^4}{98415} - \frac{74t^3}{10935} + \frac{37t^2}{1215} \qquad (6.9)$$

The graphs below illustrate the shape of these two signals:

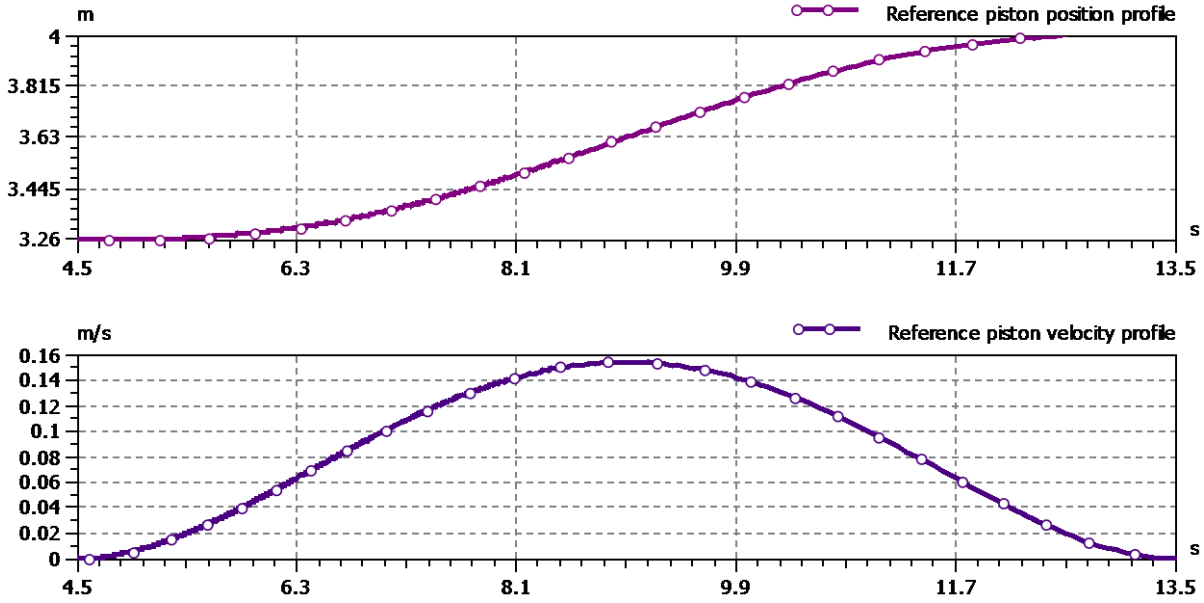

Figure 25: -The profile of a desired piston position and velocity reference signals.

The controller is deactivated until the disconnection is initiated at t=4.5 sec. Note the boundary conditions for a piston position (for t=4.5 sec, $x_p = 3.26m$ and t=13.5 s, $x_p = 4m(\max stroke)$) and a piston velocity (both 0 value at the beginning and completion of a control).

In the next chapter, we will show some simulations in SimX where we have implemented the control algorithm just explained.

7.SENSITIVITY ANALYSIS

In this section, we investigate the impact that the different parameters have on the system. These parameters are mainly:

- Friction loss in the sheaves.
- The volume of the gasbank.
- Impact of the horizontal force.
- Eigenfrequency of the shut-off valve

The aim of this study is to get an understanding of change in system behavior due to variation of parameters, which enables us to draw conclusions regarding which element is of utmost importance for the system performance.

Before we investigate for a variation of different factors, we will show some of results for all load case scenarios when the control is implemented.

Rupture of one wire.

First we will look at the scenario with the rupture of one wire in an arbitrary tensioner unit. Figure 26 show the force in wiresection zero.

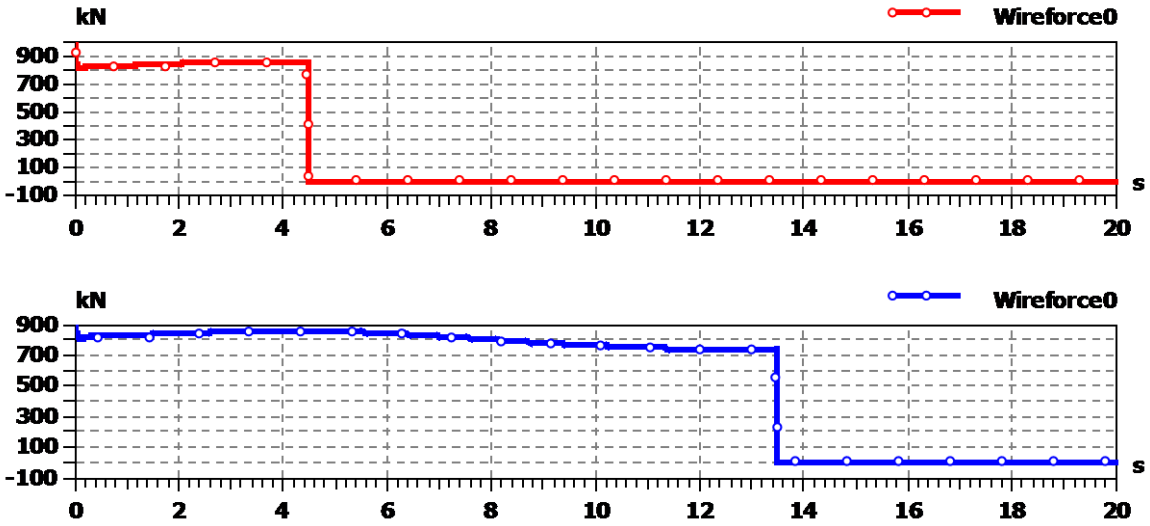

Figure 26: -Wireforces when a rupture occurs after 4,5 sec and 13,5 sec.

The force drops to zero spontaneous when the rupture happens. This again results in drop of tension in the tension ring, shown in figure 27.

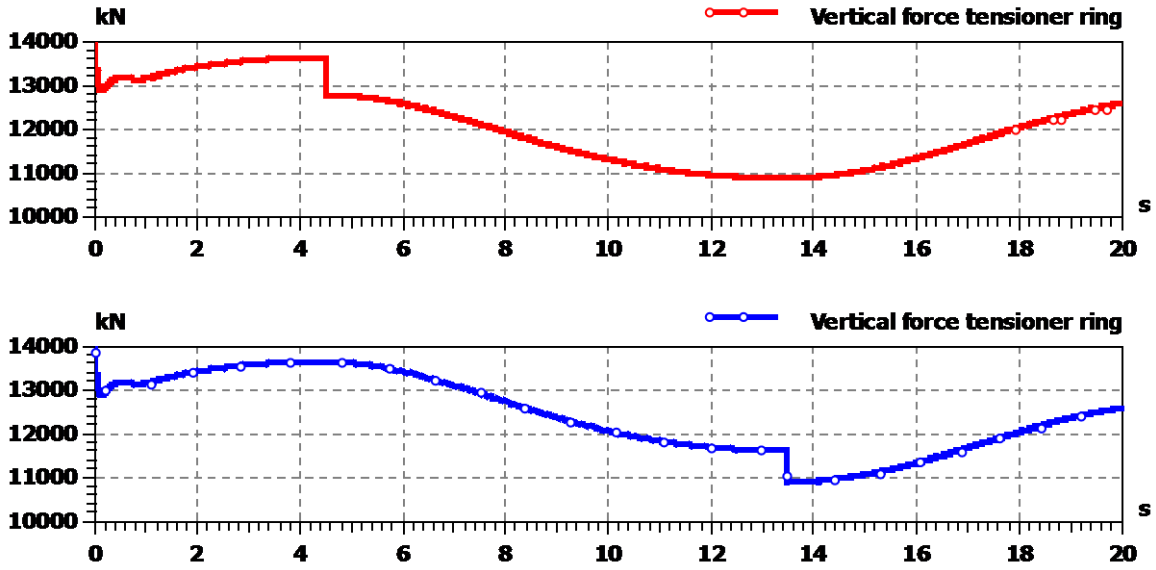

Figure 27: -Forces in the tensioner ring.

These graphs show that the drop of tensioner force is reduced by a factor of approximately 1/16, which corresponds to the number of tensioner units subjected to failure. The reason for why it is not exactly 1/16 is due to the differences of fleet angles for the units.

In chapter five, the layout of the hydraulic and pneumatic system where described. In this simulation we had to control the shut-off valve in order to prevent the piston from reaching its end stop with an unacceptable velocity. This was done by implementing the non-dynamic control. This will give a spontaneous reaction in the shut-off valve, without taking into consideration neither dampening or eigenfrequency. This is parameters which will be subjected for investigation later in this chapter. We will only be showing the graphs during the rupture at maximum piston force. The most important results are as follows:

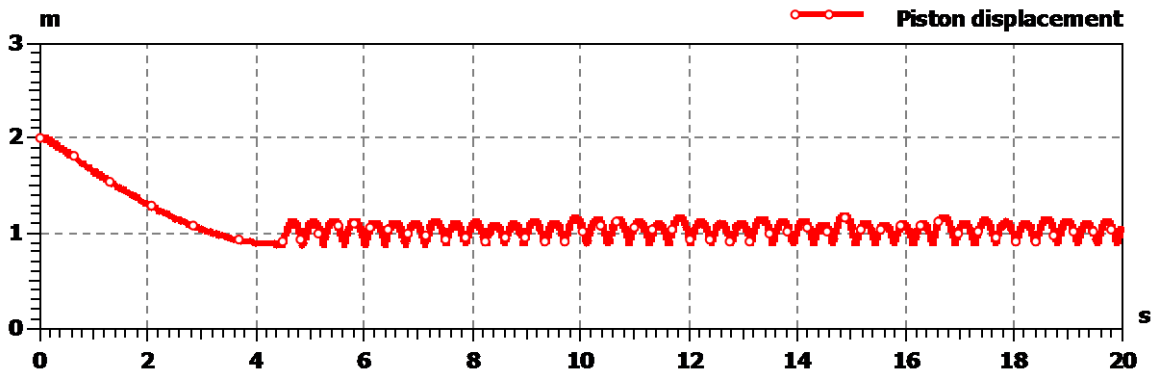

Figure 28: -The displacement of the piston.

The wire rupture takes place at minimum stroke. The energy stored in the gasbank makes the piston move in an upward direction, until the valve shuts of the flow when the pressure drop exceeds 5 bar. Figure 28 shows the displacement of the piston. The reason for the oscillation between 0,91m and 1,16m is the spring effect of the system, and since no friction have yet been implemented into the model, the oscillation will go on for infinity. The same figure shows this phenomenon.

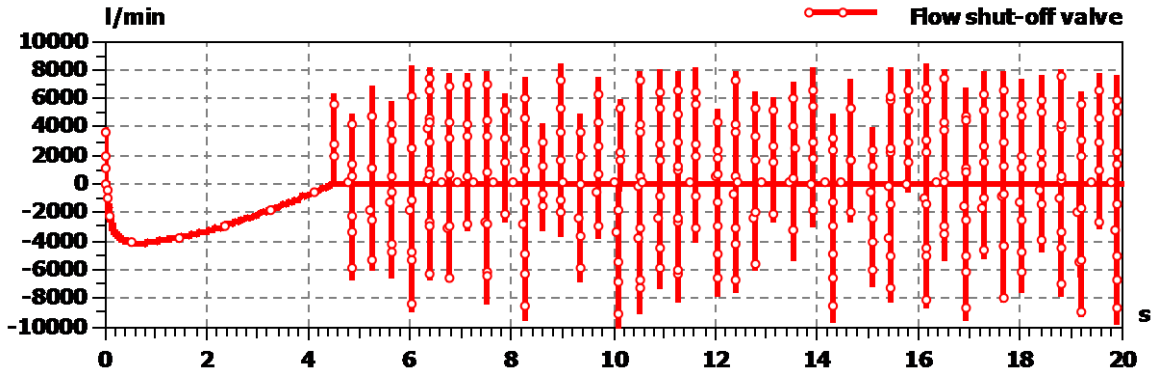

Figure 29: -The flow through the shut-off valve.

The valve closes immediate after the wire rupture takes place. The reason for this good performance is due to that the dynamic is not implemented. The variation of the direction of the flow is due to the fact that every time the pressure gets lower than 5 bar, the valve opens.

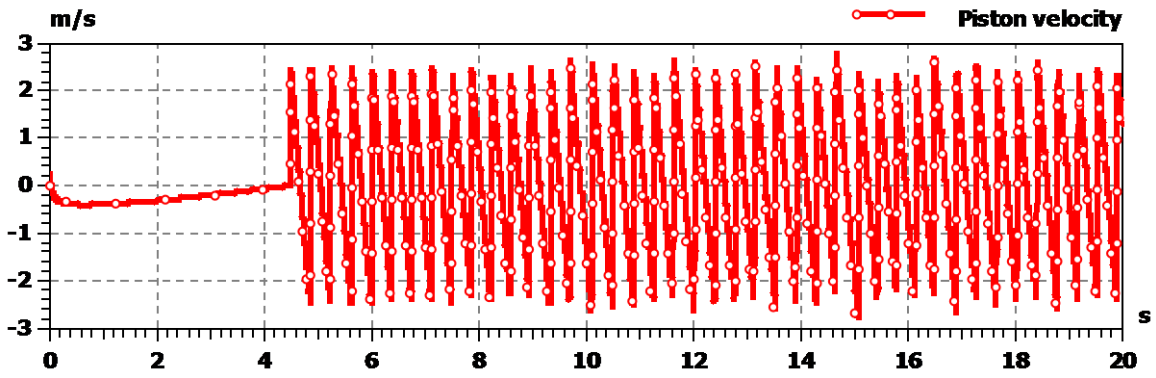

Figure 30: -The velocity of the piston.

After the wire rupture, the piston obtains a positive velocity due to the sudden drop of force acting on it. As the valve closes, the piston velocity is reduced, and becomes negative because of the mass acting on it and the spring stiffness of the hydraulic fluid. The average value of the velocity after the rupture is 0m/s.

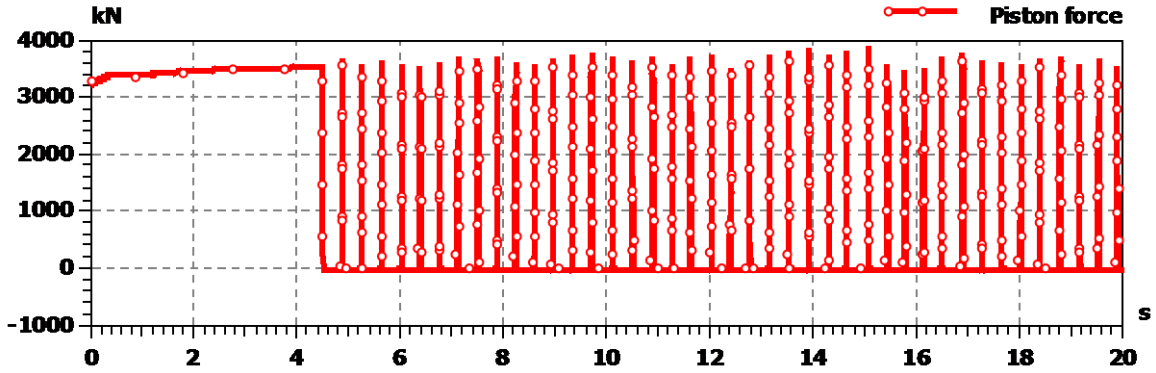

Figure 31: -Piston force.

In figure 31 the piston force is shown, and it drops to zero at the time of rupture. Then, every time the piston experiences a change of direction due to a relative negative acceleration force, it is registered as a spike in the graph.

Figure 32 shows the pressure in the tensioner cylinder, and figure 33 shows the pressures in both sides of the accumulator. The pressure in the tensioner unit is proportional with the piston force. For the accumulator we see the phenomenon of oscillation due to the previous mentioned spring behavior of the undamped system.

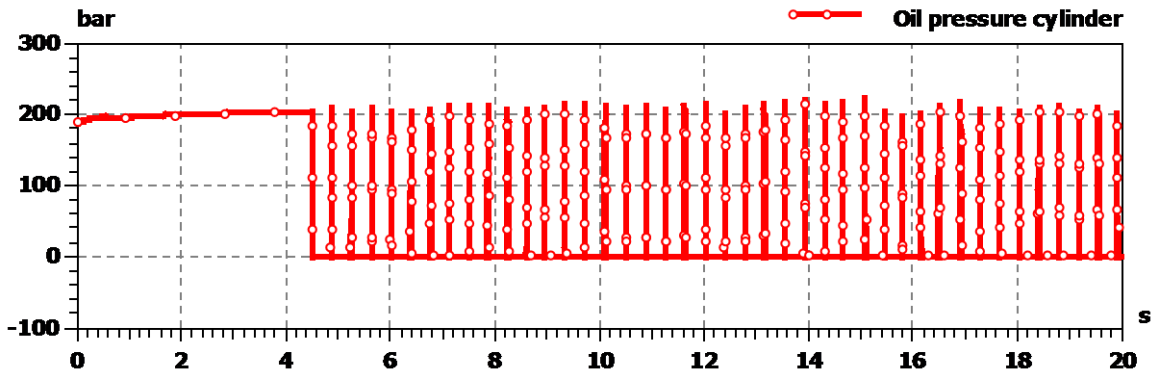

Figure 32: -The oil pressure in the tensioner unit.

.

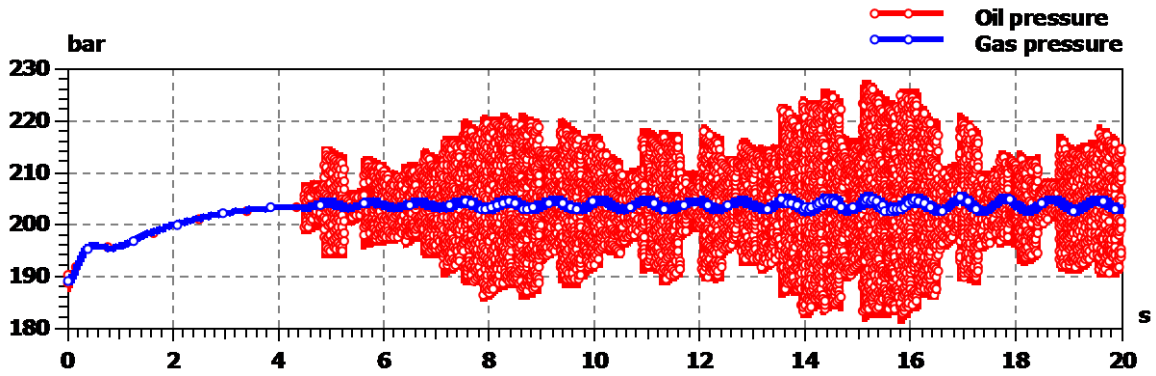

Figure 33: -The pressures in both hydraulic- and pneumatic system of the accumulator.

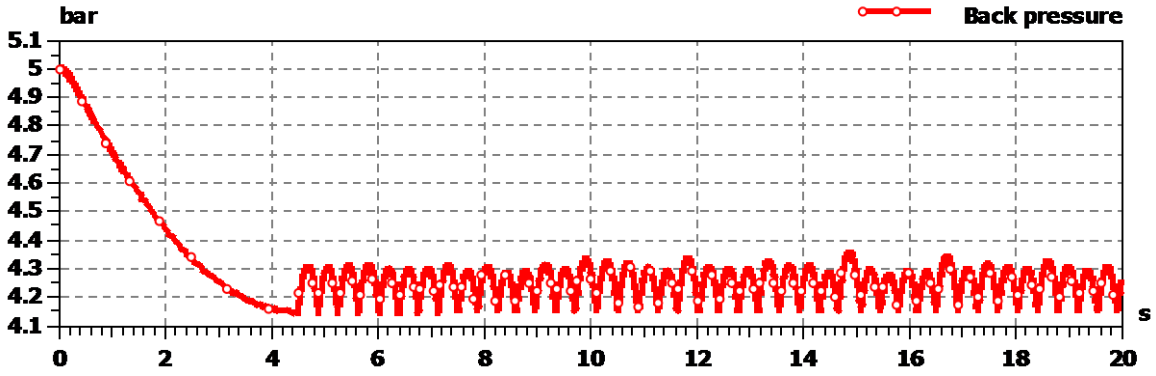

Figure 34: -The back pressure in the nitrogen bottle.

The behavior is as expected. After 4,5 seconds, the pressure drops in the tensioner unit. On the other side of the shut-off valve the pressures oscillates around the value it had before the closure of the valve. Figure 34 shows the back pressure in the nitrogen bottle, and it is proportional to the displacement of the piston.

Rupture of two wires.

The total vertical force in the tensioner ring is shown in figure 35. Results show a sudden drop from 11605kN to 10153kN at the time of rupture, which represent a decrease of approximately 1/8 compared with the system with all units operative. A key parameter in our analysis is to find the minimum vertical tensioning force in the tensioner ring.

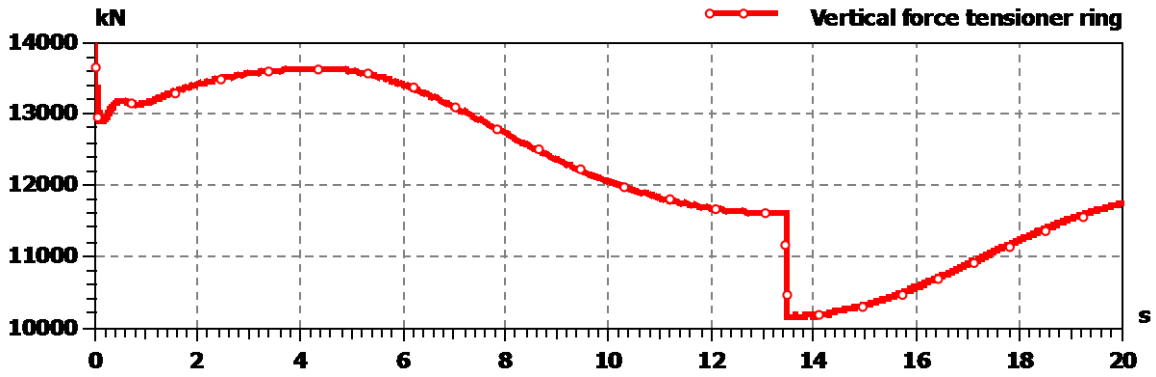

Figure 35: -The total vertical tensioning force.

This force is the one of great importance when designing a system calibrated to withstand undergoing the minimum tensioning force due to a double wire rupture.

The behavior of the rest of the parameters in the model are similar to those analyzed for the previous case, with the exception of the horizontal displacement of the tensioner ring due to the horizontal force of 350kN applied.

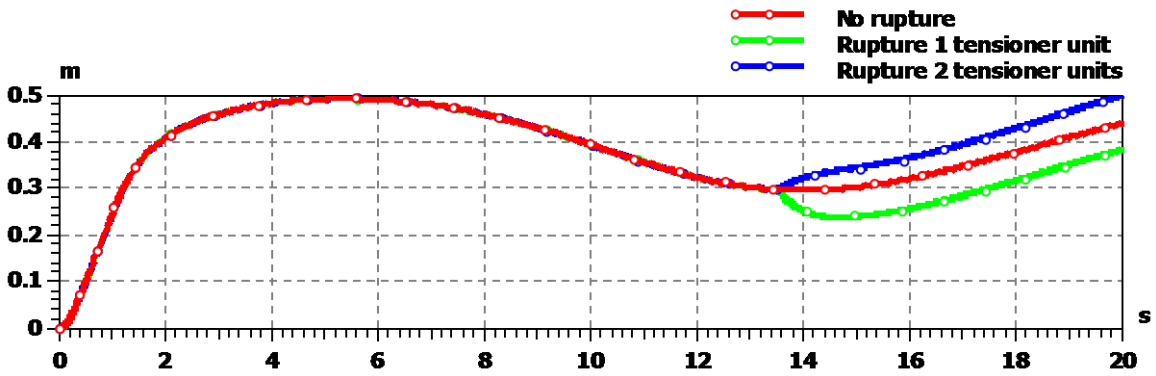

Figure 36: -Horizontal displacement of the tensioner ring.

The displacement of the tensioner ring in this direction is shown in figure 36. The red curve shows the result from the simulation without any wire ruptures, the

blue curve shows the displacement during the one wire rupture scenario and the green one this scenario.

To explain these phenomena we have to look at the geometry of the system. Figure 37 shows the tensioner ring and the wires seen in the direction of the positive z axis.

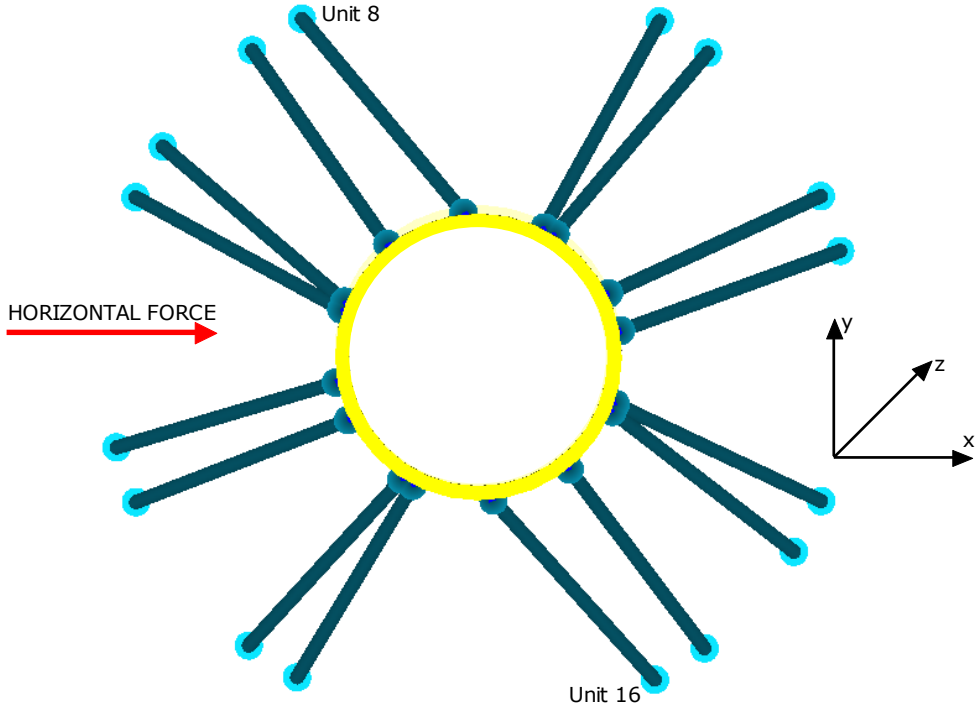

Figure 37: -The geometry of the tensioner ring and the wires.

In our simulation we first cut the wire for tensioner unit 16. The x-component of the wireforce is acting in the same direction as the horizontal force. This explains the reduction of displacement for the tensioner ring for a wire rupture in unit 16, compared with the no-rupture scenario. The fleet angle shown in figure 38 decide the magnitude of this component.

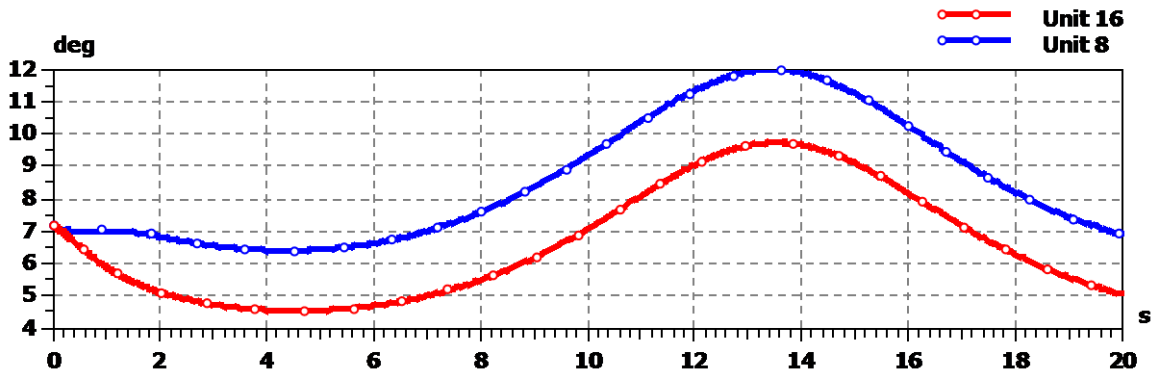

Figure 38: -The fleet angles of unit 16 and unit 8 during heave motion and no wire ruptures.

As the graph shows, the fleet angle for unit 8 is approximately 2,23° greater than for unit 16. The x-component of unit 16 is acting opposite the direction of the horizontal force. When a rupture occurs in this unit the consequence is an increase of horizontal displacement for the tensioner ring, also compared with the no-rupture scenario. Since the two tensioner units are located diametrical opposite, a theoretical similar fleet angles of those two units would have resulted in no change in horizontal displacement for the tensioner ring. But the only situation where this is valid is when the horizontal force is applied perpendicular to the units x-components.

Emergency disconnection

Figure 39 shows a controlled motion of a riser, without implementing the friction in the sheaves and hydraulic-pneumatic cylinder as well. In chapter 6, we have shown more information about the control structure used. For tuned values as seen below, after an iterative process we have obtained satisfactory controller performances.

Tuning values:

Outer loop: proportional gain, P=1.5

Inner loop: proportional gain, P=15, I=1000

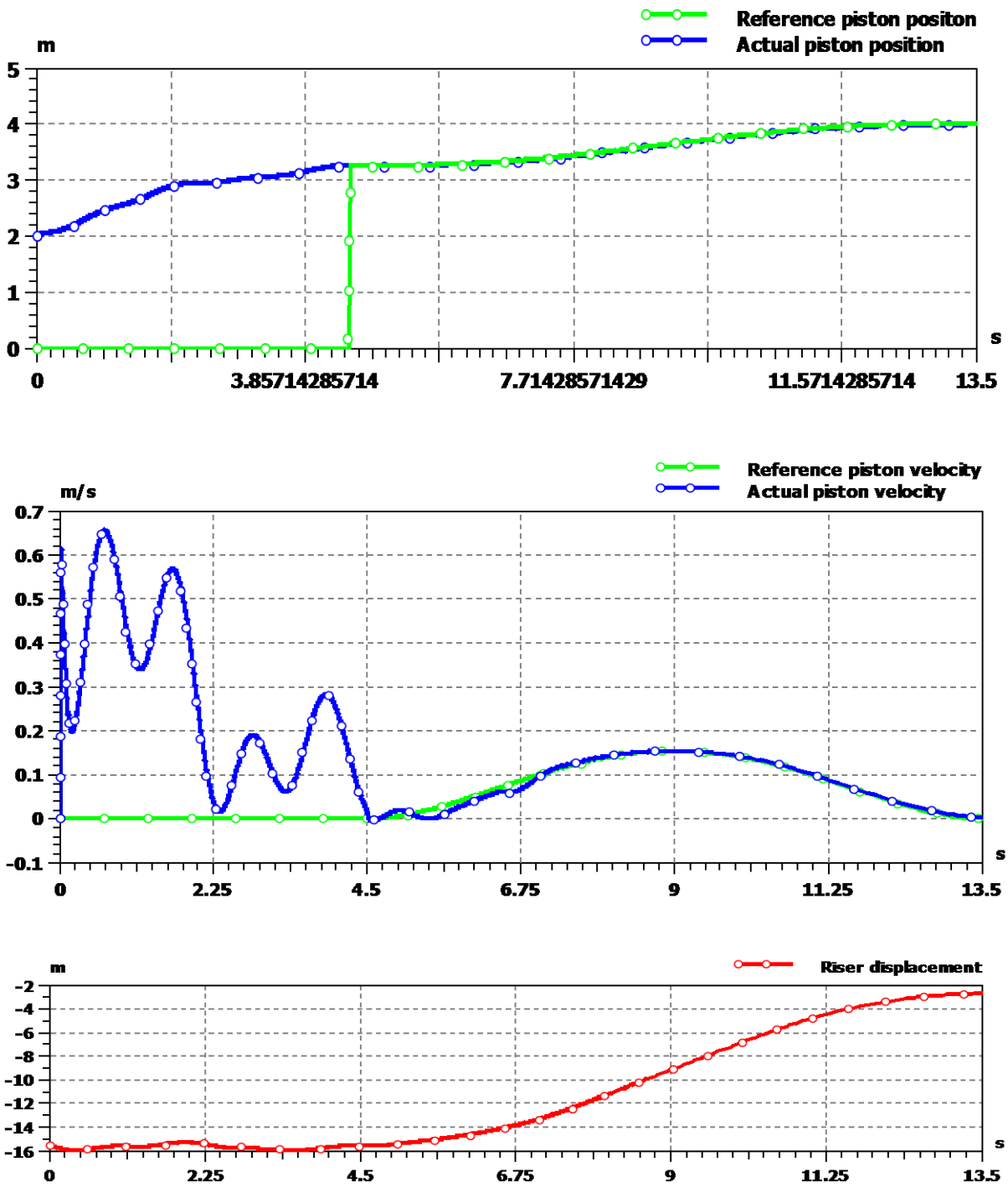

Figure 39: -The motion of the riser in a controlled way without a system friction.

We may compute analytically the riser displacement (difference between a final and initial riser position) using the equation given by:

Calculated riser displacement =

$$x_{platform} + 4x_p - (x_{platform0} + 4x_{p0}) = 4.8 + 4 \cdot 4 - (-4.8 + 4 \cdot 3.26) = 12.56[m]$$

The measured riser displacement is 12.80 m. This discrepancy is because the formula above is used for a non-stretched wire, compared to a SimulationX model that is a flexible wire.

The variation of other parameters (piston force, tensioning riser force and system pressure) will be discussed later in this section.

7.1 PARAMETER VARIATIONS AND THE SYSTEM RESPONSE

The effect of the friction in the hydraulic-pneumatic cylinder is shown in figure 40. The limit velocity between slipping- and sticking friction is set to be 0,02 m/s, and the blue line shows the impact of the slipping friction just before and after the piston reaches minimum and maximum displacement. We also notice that the frictional losses are at maximum when the velocity is at maximum.

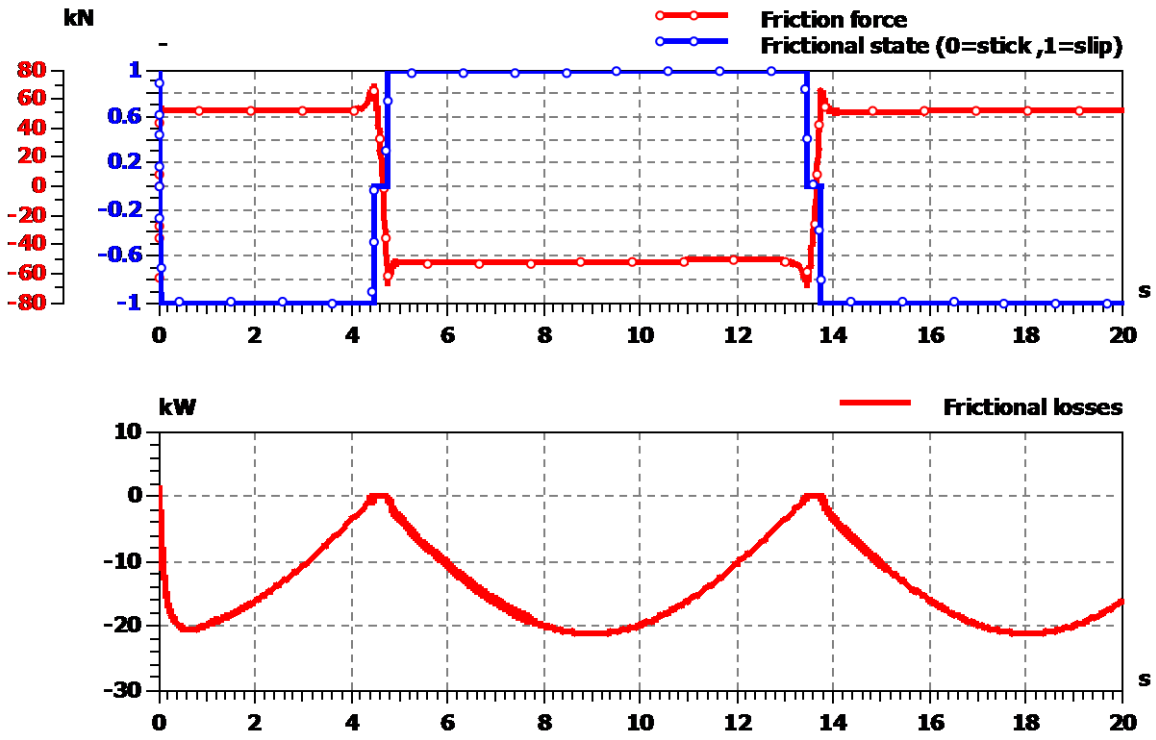

Figure 40: -Cylinder losses due to friction.

In figure 41 we can observe how the friction in the cylinder is impacting the forces in the different wire sections.

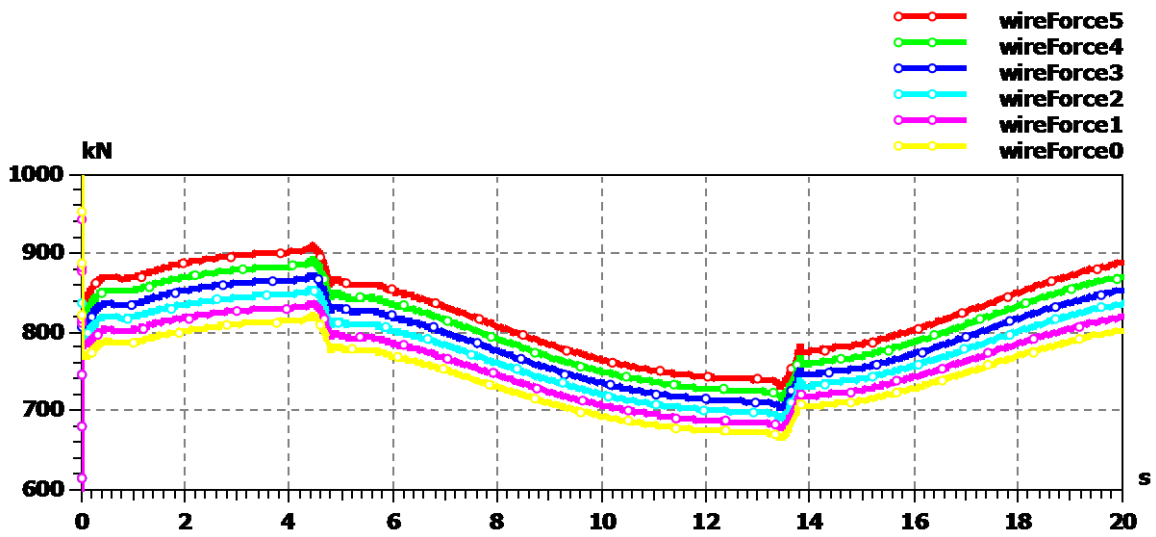

Figure 41: -The force in different wire sections.

Without friction the forces were equal in all sections. With friction implemented in the sheaves we see that the force is reduced by 2 percent for every section. The total vertical tensioning force is shown in figure 42.

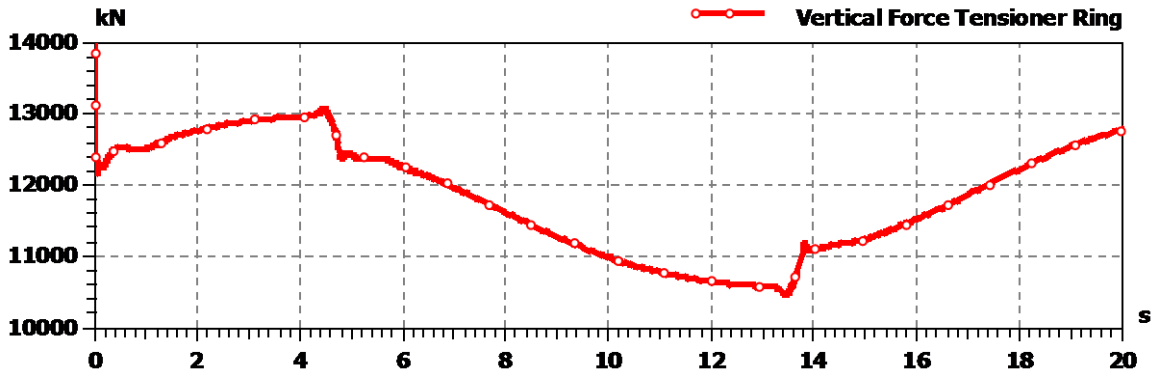

Figure 42: -Vertical tensioning force acting on the tensioner ring.

The maximum force is 13076kN, and the minimum 10460kN. This is a reduction compared to the scenario without friction implemented shown in figure 7 in chapter 4. This result is as expected, since the friction will absorb some energy, generating heat in the cylinders and sheaves. We also see the impact of the slipping friction when the pistons undergoes a change in direction at time 4,5 seconds and 13,5 seconds.The pressures in the hydraulic and pneumatic system remain almost same as before friction was implemented.

We have investigated how the system responds when varying the previous mentioned parameters under different load conditions. The results are shown in tables 6 and 7 below.

Where nothing else is specified, the following parameters have been used for the simulations:

- Initial pressure High Load is set to 190,2 bar.
- Initial pressure Medium Load is set to 67,85 bar.
- Sheave friction loss 2%.
- Piston friction 34,6kN slipping, 17,3kN stiction.
- Accumulator friction 44,1kN slipping, 22kN stiction.
- Pressure dependency friction is $\frac{\text{slipping friction}}{\text{oil pressure}}$.
- Volume gasbank 3,2m^3.
- Eigenfrequency shut-off valve set to 10Hz (100ms).
- Dampening factor shut-off valve set to 0,8.
- Wire-rupture happened at maximum stroke (13,5sec).

Table 6: -Results for normal operation scenario with high load.

Normal operation High Load		No friction	Sheave friction loss				Volume gasbank		No horizontal force
			1%	2%	3%	4%	2,9m³	3„5m³	
Piston Force[*kN*]	max	3511	3613	3614	3614	3615	3636	3594	3615
	min	3018	2919	2919	2919	2919	2900	2936	2921
Piston Displacement[m]	max	3,247	3,233	3,231	3,230	3,229	3,230	3,232	3,222
	min	0,855	0,884	0,882	0,880	0,878	0,883	0,881	0,875
Piston velocity [m/s]	max	0,413	0,412	0,412	0,412	0,413	0,412	0,413	0,419
Pressure oil[bar]	max	203,2	203,9	203,9	204,0	204,0	205,2	202,8	204,0
	min	175,4	175,3	175,3	175,4	175,4	174,2	176,3	175,4
Backpressure[bar]	max	6,369	6,350	6,349	6,347	6,345	6,347	6,350	6,349
	min	4,151	4,150	4,149	4,148	4,147	4,150	4,149	4,145
Pressure gas[bar]	max	203,3	203,9	204,0	204,0	204,0	205,3	202,9	204,1
	min	175,5	175,3	175,3	175,3	175,3	174,2	176,3	175,4
Vertical tensioning force[kN]	max	13623	13541	13076	12622	12188	13161	13004	13080
	min	11605	10831	10460	10100	9751	10390	10521	10464
Vertical tensioning force after rupture of 2 wires[kN]	max	11920	11848	11442	11044	10665	11516	11379	11445
	min	10154	9477	9153	8838	8532	9091	9206	9156
Tensioning variation [% from mean value]	max	8,0	11,1	11,1	11,1	11,1	11,8	10,6	11,1

Table 7: - Results for normal operation scenario with medium load.

Normal operation Medium Load		No friction	Sheave friction loss				Volume gasbank		No horizontal force
			1%	2%	3%	4%	2,9m³	3,„5m³	
Piston Force[*kN*]	max	1237	1338	1338	1338	1338	1346	1330	1339
	min	1050	951	951	951	951	944	957	952
Piston Displacement[m]	max	3,220	3,212	3,212	3,212	3,211	3,212	3,212	3,192
	min	0,836	0,838	0,838	0,837	0,836	0,838	0,837	0,827
Piston velocity[m/s]	max	0,417	0,417	0,417	0,417	0,417	0,417	0,417	0,415
Pressure oil[bar]	max	72,14	72,34	72,34	72,34	72,35	72,83	71,93	72,39
	min	61,98	61,96	61,96	61,96	61,97	61,57	62,30	62,04
Backpressure[bar]	max	6,324	6,323	6,323	6,322	6,322	6,322	6,323	6,296
	min	4,107	4,121	4,120	4,120	4,120	4,121	4,120	4,114
Pressure gas[bar]	max	72,10	72,35	72,36	72,36	72,36	72,85	71,94	72,41
	min	62,03	61,94	61,94	61,95	61,95	61,56	62,28	62,03
Vertical tensioning force[kN]	max	4556	4771	4598	4444	4289	4638	4578	4621
	min	3844	3349	3229	3123	3015	3209	3256	3240
Vertical tensioning force after rupture of 2 wires[kN]	max	3987	4177	4023	3889	3753	4058	4006	4043
	min	3364	2930	2825	2733	2638	2808	2849	2835
Tensioning force variation [% from mean value]	max	8,5	17,5	17,5	17,5	17,4	18,2	16,9	17,6

Table 8: - Results from wire rupture scenarios.

Wire rupture High load		No friction or dynamic valve	Volume gasbank		Shut-off valve		
			2,9m^3	3,5m^3	50ms	100ms	200ms
Piston Force[kN]	max	3512	3634	3590	11689	3610	3610
	min	-	-	-	-	-	-
Piston Displacement[m]	max	3,776	3,435	3,439	3,332	3,347	3,690
	min	0,880	0,882	0,880	0,881	0,881	0,881
Piston velocity[m/s]	max	3,812	6,771	6,846	5,632	6,811	8,086
Pressure oil[bar]	max	203,3	206,5	204,0	205,20	205,20	205,20
	min	-	-	-	-	-	-
Backpressure[bar]	max	7,159	6,633	6,638	6,486	6,636	7,020
	min	4,148	4,150	4,148	4,149	4,149	4,149
Pressure gas[bar]	max	203,3	205,3	202,9	204,00	204,0	204.0
	min	161,1	165,7	167,5	173,20	166,6	155,1
Flow shut-off valve[l/m]	max	8189	49767	50288	28617	50042	72650
	min	-7208	-4539	-4602	-4613	-4613	-4613
Wire rupture Medium load		No friction or dynamic valve	Volume gasbank		Shut-off valve		
			2,9m^3	3,5m^3	50ms	100ms	200ms
Piston Force[kN]	max	1237	1346	1331	3532	1338	1338
	min	-	-	-	-	-	-
Piston Displacement[m]	max	3,334	3,300	3,302	3,259	3,301	3,402
	min	0,834	0,838	0,837	0,837	0,837	0,837
Piston velocity[m/s]	max	1,611	2,587	2,614	2,224	2,602	30,28
Pressure oil[bar]	max	72,16	72,84	71,93	72,34	72,34	72,34
	min	-	-	-	-	-	-
Backpressure[bar]	max	6,489	6,442	6,444	6,386	6,443	6,585
	min	4,118	4,121	4,120	4,121	4,121	4,121
Pressure gas[bar]	max	72,11	72,85	71,94	72,35	72,35	72,35
	min	61,84	60,18	60,89	61,41	60,56	58,79
Flow shut-off valve[l/m]	max	8077	20074	20241	13139	20172	27918
	min	-13606	-4192	-4194	-4193	-4193	-4193

We see from tables 6 and 7 that when we implement friction in the cylinders, and are increasing the friction in the sheaves between 1% and 4%, it has very little impact on piston displacement, piston velocity and the pressures in the system. However, we are experiencing an increase of 2,9% maximum piston force, and a decrease of 3,3% minimum piston force for the high loadcase scenario compared

with the no friction scenario. Reducing the horizontal force to zero seems to have little or no impact on system behavior. The key parameter is the volume of the gas bank. An increased volume results in a reduction of spring stiffness. The change in minimum and maximum tensioning force is proportional to the gasbank volume. The main performance parameter is the variation in the tension force supplied by the wires/cylinders to the tensioner ring.

For the medium loadcase scenario we have the same situation with respect to variance in the system parameters under different simulations. The main different between the two loadcases is the tensioning variation. The reason for the poorer performance of the last scenario is mainly due to the friction in the cylinders and accumulators. Also, the friction in the sheaves will require a greater percentage of the systems energy to overcome when the piston force is reduced.

Table 8 shows the data retrieved from one tensioner when running simulations for the wire rupture scenario. One of the key parameter in this case is the velocity of the piston if it reaches maximum stroke. To have a minimum distance between the piston and the end stop at rupture time, we did it after 13,5 seconds. In the simulations the piston never reached maximum stroke, because the valve managed to shut off the flow after rupture occurred. We see from the table that the piston-travel after rupture is increasing by decreasing eigenfrequency of the shut-off valve. On the other hand, the maximum piston force is significantly increasing as we increase the eigenfrequency. The flow through the valve has relative high values, but this is just for some milliseconds, until the valve closes completely. The volume of the gasbank does not seem to have any significant impact on the system behavior during a wire rupture.

In chapter 5 we refered to a reduction factor R_f which gives the relationship between the minimum tensioning force T_{min} and the minimum tensioner ring tension T_{TRmin}. The literature [8] stated that for a DAT system this factor should be in the area 0,90-0,95. However, this factor has to be increased for the WRT system since we have additional losses in the mechanical system. Data can be taken from table 6 and table 7, and the reduction factor calculated:

Table 9: - Reduction factor for the WRT system.

High load scenario					
Minimum vertical tensioning force after rupture of 2 wires[kN]	No friction	1%	2%	3%	4%
	10154	9477	9153	8838	8532
R_f	0,88	0,82	0,80	0,77	0,74
Medium load scenario					
Minimum vertical tensioning force after rupture of 2 wires[kN]	No friction	1%	2%	3%	4%
	3364	2930	2825	2733	2638
R_f	0,83	0,72	0,70	0,67	0,65

We can conclude that equation (5.87)

$$T_{min} = \frac{T_{TRmin} \cdot N}{R_f(N-n)}$$

is valid with the R_f values given in table 9. This table also reflects the previous explained poorer performance with respect to efficiency of the medium loadcase scenario versus the high loadcase.

We show now how the parameter variations have impact on the system response for the emergency disconnection scenario, including a friction in the sheaves and in the hydraulic-pneumatic cylinder.

Due to changes in the system response, we have to change the initial tuned parameters for the controller in order to meet the projected performances. By iteration, we found the best suitable value for a P-controller value to be 2 and for a PI controller, P=5 and I=2000 respectively. Note that we did not change these values during a sensitivity analysis.

In figure 43 the system parameters are investigated for losses in the sheaves varying between 0 and 4 %.

According to the figure, the levels of losses have a little or no impact on the kinematic quantities and the performances of the controller. In addition, the system pressure experiences very small changes as we vary the lost percentage.

However, a system behaves differently in terms of kinetic quantities such as tensioning, friction and piston force.

For a period before the riser disconnection, the tensioning force curve for a system experiencing the frictional losses will have the same shape as the curve without any losses, but displaced for an amount equal to the friction forces.

The biggest impact has been observed in the variation of the piston force at the moment of the riser disconnection. For a system without friction in the sheaves, the piston force dropped from 3300 kN to 2800kN within t=0.6 sec. On the other hand, the system experiencing a loss of 4 % per sheave dropped from 3300 kN to 3200 kN, only.

The friction force in the hydraulic-cylinder sees slight changes for different friction losses. However, the greater variation is noted between t=3.2 and t=3.6 seconds for a 4% loss and at the time of disconnection. However, a little or no effect is observed in the tensioning and the piston force.

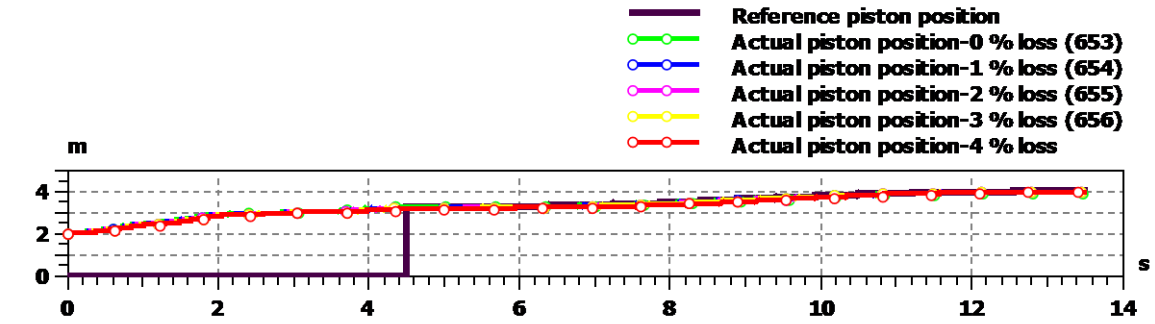
Reference piston position
Actual piston position-0 % loss (653)
Actual piston position-1 % loss (654)
Actual piston position-2 % loss (655)
Actual piston position-3 % loss (656)
Actual piston position-4 % loss
m
4
2
0
0
2
4
6
8
10
12
14
s

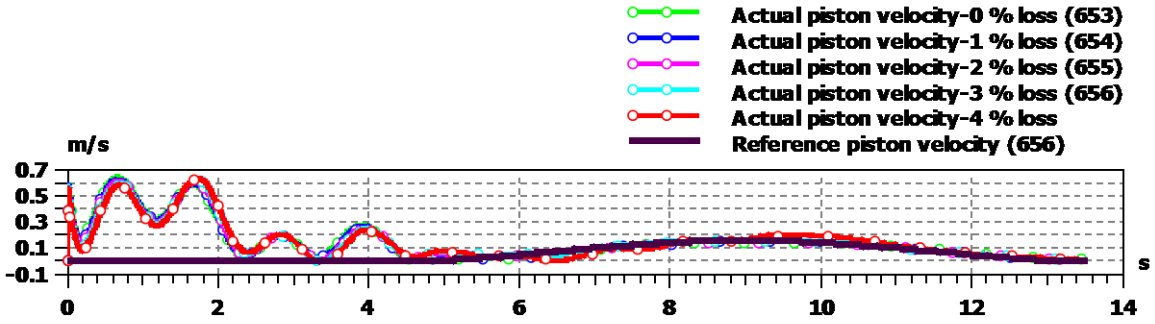
Actual piston velocity-0 % loss (653)
Actual piston velocity-1 % loss (654)
Actual piston velocity-2 % loss (655)
Actual piston velocity-3 % loss (656)
Actual piston velocity-4 % loss
Reference piston velocity (656)
m/s
0.7
0.5
0.3
0.1
-0.1
0
2
4
6
8
10
12
14
s

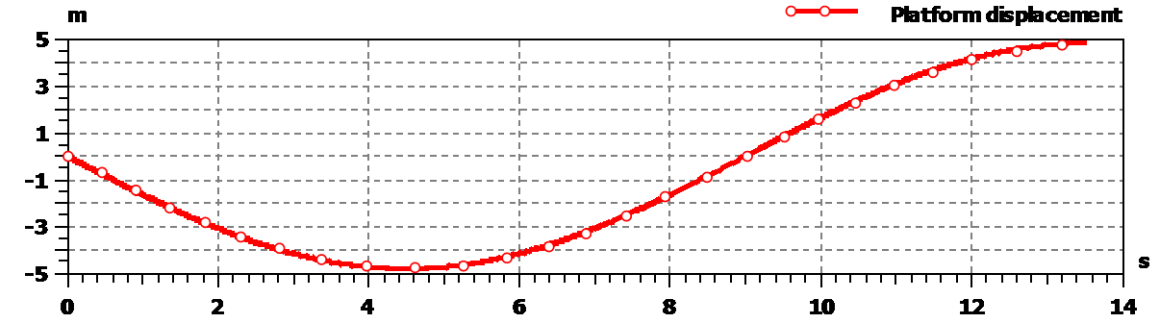
m
Platform displacement
5
3
1
-1
-3
-5
0
2
4
6
8
10
12
14
s

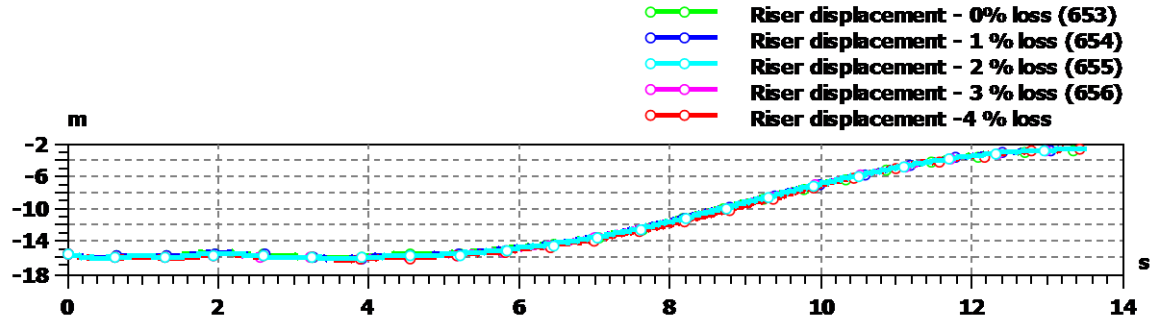
Riser displacement - 0% loss (653)
Riser displacement - 1 % loss (654)
Riser displacement - 2 % loss (655)
Riser displacement - 3 % loss (656)
Riser displacement -4 % loss
m
-2
-6
-10
-14
-18
0
2
4
6
8
10
12
14
s

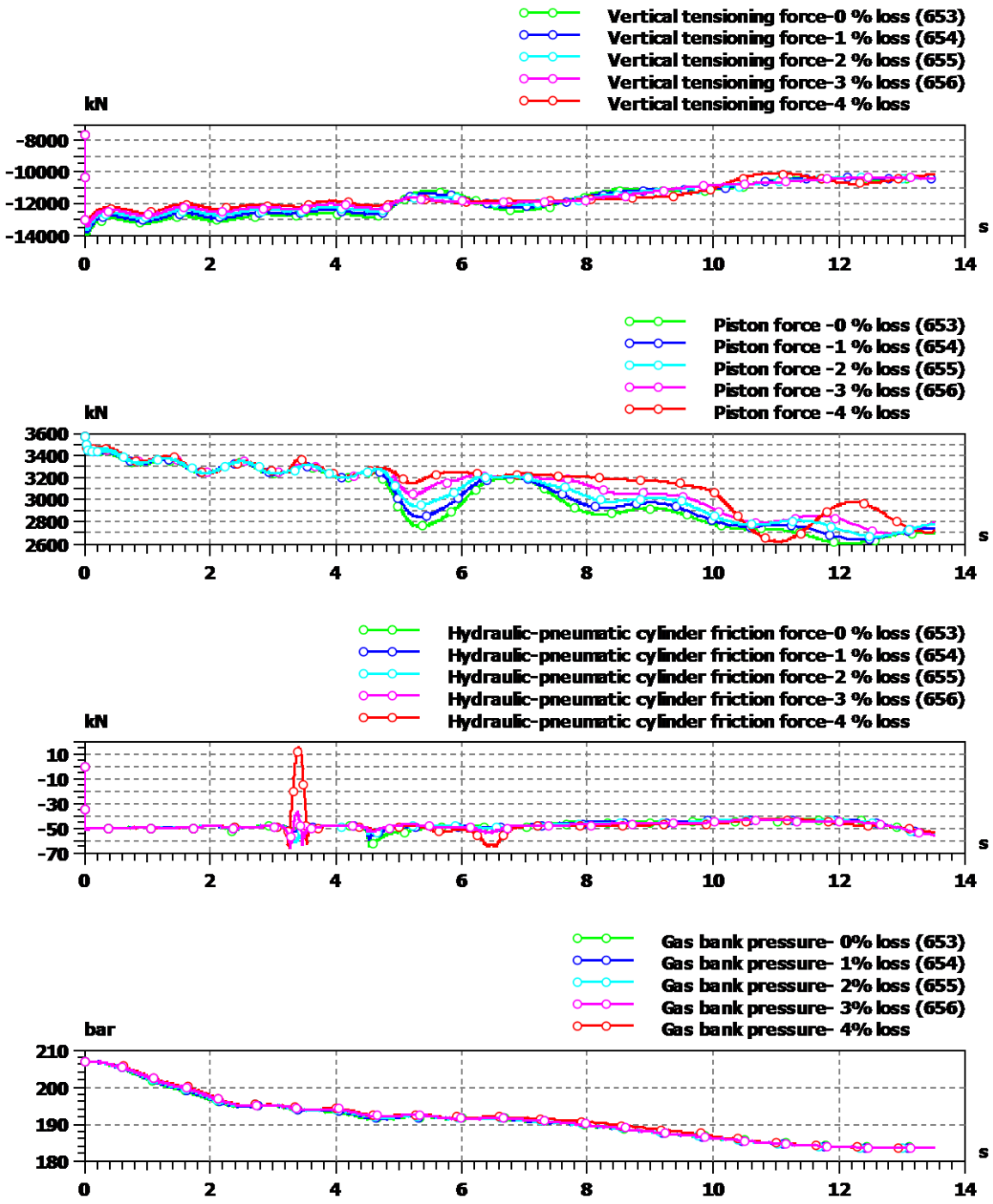

Figure 43: -Data retrieved when varying sheave friction between 0-4%.

We will see now how is the impact of no-horizontal force for a 0 % and 4 % loss and a system with 4 % loss under the influence of a horizontal force.

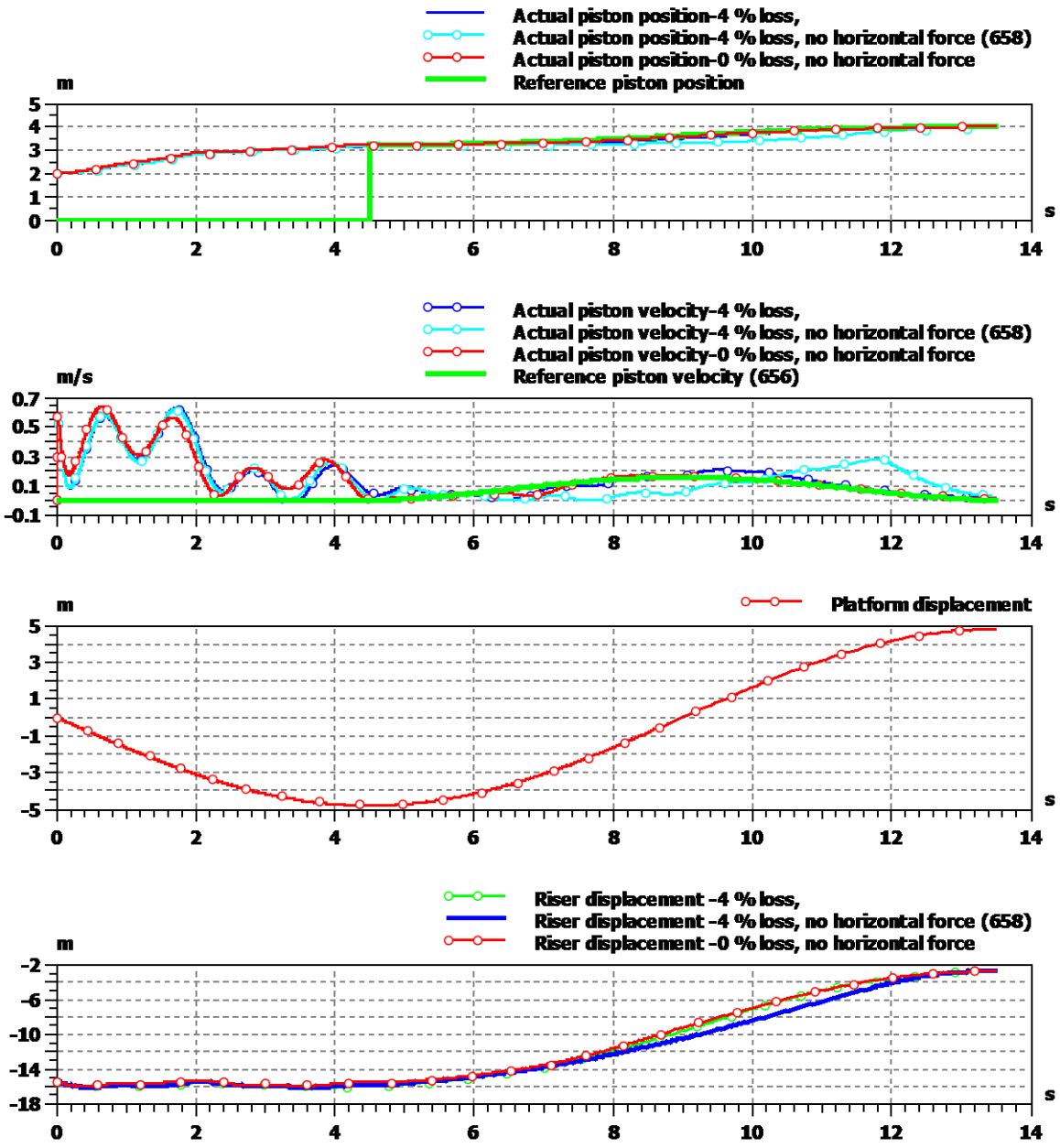

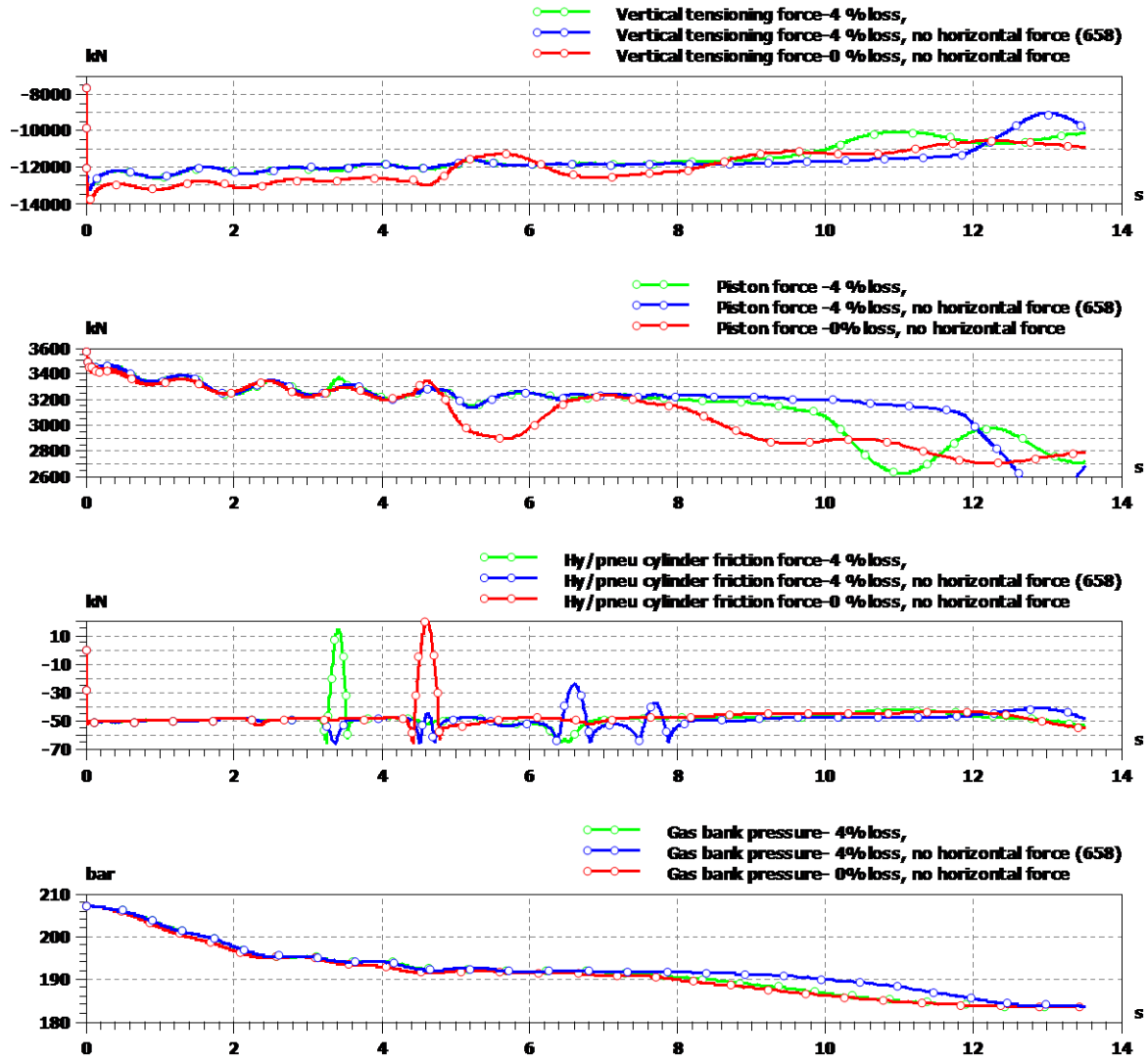

Figure 44: -Parameter variations for a no-horizontal force exerted on the system.

There is no signification impact in the kinematic quantities for a period of a controller deactivation (t=4.5 seconds). On the other side, the actual piston velocity signal does not follow the reference signal after the controller is activated. However, the control objectives are met because the piston is moved in a controlled way at the end stop position, and the riser has been elevated to a predetermined height.

It is interesting the behavior of the friction force in the hydraulic-pneumatic cylinder. Indeed, for a 4 % losses and no horizontal force, the friction force has not experienced (for t=3.2-3.6 sec) a sharp drop compared with a case when a horizontal force was active.

8 CONCLUSION

In this thesis we have developed a mathematical model of the riser tensioner system provided by TTS Energy. The model enabled a project team to calculate for the initial state variables of the system, which have then been inserted into a simulation X model. In addition, by using this software, we were able to cross-check whether our mathematical model provides consistent results compared with results obtained through simulations.

We have focused on building a working and valid model in simulationX, using both 1D and multi-body mechanics. SimulationX offers an option to assembly a large number of components into one component so called "Compound" that has been used to make a tensioner unit appear like a block easy to handle.

Design was outside the project's scope, but by varying system parameters we have been able to conclude which configurations give the best system performance. In addition, by using a simulation model, we were able to observe the behavior of the system when either a few functional constraints are violated (capacity of a hydraulic-pneumatic cylinder, for example), or the system was not able to give the satisfactory performances due to improper state initial values (for instance, when a riser had to be elevated to a certain height).

We have derived the value for the reduction factor which enables users to calculate the minimum top tension force on the marine riser by knowing the load and the friction in the system.

We have also shown that the piston in a tensioner unit will not hit the end stop causing damage when subjected to a sudden wire rupture, even when varying gas bank volume and eigenfrequency of the shut-off valve.

Furthermore, we have investigated the dynamics of an anti-recoil system, and then implemented a control structure to ensure that the cylinder positions are moved in a controlled way to maximum stroke if the marine riser is decoupled from the BOP. More specifically, by making use of polynomial functions, we have designed a piston and velocity loop enabling a safe riser elevation height, and in the same time preventing the pistons to hit the hydraulic-pneumatic cylinders end stop with an unacceptable high velocity, thereby causing a severe damage to the system.

8.1 PROPOSALS FOR FURTHER WORK

Because the riser tensioning system is a rather complex and multidisciplinary system (involving systems like mechanical, hydraulic/pneumatic, and control), it offers a wide range of possible parameter variations, and hence an opportunity for study of the most influential variables in greater detail.

Initially, one of project work objectives was to do some optimization, let say two-three design objectives, mainly reduction of the riser weight and to ensure a constant tensioning force with the least available system resources.

Therefore, one of the identified fields for a further work suggested by a project team is the optimization of the riser system that should be implemented in close cooperation with off-shore oil and gas industry in Agder region.

BIBLIOGRAPHY

[1] Charles P. Sparks, *Fundamentals of Marine Riser Mechanics: Basic Principles and Simplified Analysis*, (2007).

[2] Igor L. Krivts, German V. Krejnin, *Pneumatic Actuating Systems for Automatic Equipment- Structure and Design(2006)*

[3] Peter Beater, *Pneumatic Drives- System Design, Modeling and Control, (2006)*

[4] Peter Chapple, *Principles of Hydraulic System Design, (2003)*

[5] James A. Sullivan, *Fluid Power-Theory and Applications, (1989)*

[6] Michael Rygaard Hansen, *Hydraulic Components and Systems (2009)*

[7] Michael J. Pinches, Brian J. Callear, Power Pneumatics, (1996)

[8] *Recommended Practice for Design, Selection, Operation and Maintenance of Marine Drilling Riser Systems*,
American Petroleum Institute, (1993).

[9] *Product catalogue steelwire,*
Certex, (2010).

APPENDIX

Data sheet – Parameters used in simulationX for one tensioner system.

Gas bank volume	3,2 m^3	Initial pressure: 67,85/190,2 bar	-	-	-	-	-	-
Pipeline	Lenght: 35m	Diameter: 77,6mm	90^0 bends: 8	Roughness hight: 50µm	-	-	-	-
Accumulator	Piston diameter: 530mm	Max stroke: 3626mm	Dead volume (oil side): 10 liters	Dead volume (gas side): 35 liters	Initial pressure: 67,85/190,2 bar	Frictions: Slip: 44,1kN Stick:22kN Pressure dependent: slip/pressure	Limit velocity: 0,02 m/s	Piston mass: 253kg
cylinder	Piston/rod diameter: 470mm/400mm	Max stroke: 4000mm	Dead volume (oil side): 5 liters	Dead volume (gas side): 0 liter	Initial pressure: 67,85/190,2 bar	Frictions: Slip: 34,6kN Stick:17,3kN Pressure dependent: slip/pressure	Limit velocity: 0,02 m/s	Piston mass+2 sheaves: 8350kg
Nitrogen bottle	Volume: 280 liters	Initial pressure: 5 bar	-	-	-	-	-	-
Sheaves	Mass: 2920kg	Diameter: 1829mm	Frictionloss: 0-4%	-	-	-	-	-
Wire	Total length: 60,471m	Diameter: 64mm	Youngs modulus: $210e^9$GPa	-	-	-	-	-